UNIVERSITY OF CALGARY

Myofilament Ca^{2+} Sensitivity of Skinned Rat Cardiac Trabeculae at Physiological $[Mg^{2+}]$ and Osmolality

By

Jun Sun

A THESIS SUBMITTED TO THE FACULTY OF GRADUATE STUDIES IN PARTIAL FULFILLMENT OF THE REQUIREMENTS FOR THE DEGREE OF MASTER OF SCIENCE

DEPARTMENT OF CARDIOVASCULAR/RESPIRATORY SCIENCES

CALGARY, ALBERTA

SEPTEMBER, 2000

Abstract

Force-pCa relationships were studied in Triton skinned rat cardiac trabeculae at physiological [Mg^{2+}] (0.7 mM) and sarcomere lattice spacing by addition of 5% Dextran T500. Force (F) was measured using a silicon strain gauge and sarcomere length (SL) using laser diffraction techniques. The shape of F-SL relationships in 15 trabeculae (7 controls) was identical to that previously published. F_{max} was lower in the controls than that of Dextran treated muscle (79±8 mN/mm^2 vs. 108±6 mN/mm^2). EC_{50} decreased from 1.55±0.09 μM at SL1.90 μm to 1.06±0.10 μM at SL 2.15 μm in controls and from 1.41±0.06 μM to 1.04±0.09 μM over the same SL range in Dextran treated muscle. However, EC_{50} from both groups were still higher than those of intact fibers.

Conclusion: correction of [Mg^{2+}] and osmotic pressure in skinning solutions increase F_{max} development, but it does not increase Ca^{2+} sensitivity to the level of intact trabeculae suggesting the presence of (a) Ca^{2+} sensitizer(s) in the cytosol of cardiac myocytes.

Acknowledgements

There are many people to whom I owe my appreciation and gratitude. This work would never have been completed without their help and encouragement.

Sincere thanks to my supervisor Dr. ter Keurs, who brought me into cardiovascular research. I would never succeed in my graduate study without his kind help and encouragement. His support in every aspect accompanied me through the whole period of my graduate studies. I have not only learned study and research skills from him, but also have been trained to be optimistic in the life. His insightful advice and encouragement will be remembered in my future journey of study.

Special thanks to my committee members: Dr. Tyberg, who trained me well in graduate course work. With his endless help and clear instructions, I enjoyed myself in the study. What I have learned from him is tremendously valuable in my research work.

Much thanks to Dr. Kargacin, who always gives me constructive suggestions and critical ideas in my research. His expert point view on my research work has guided me in finishing the project.

I have to offer my appreciation to Kaoru Saito, for her technical and administrative help in the laboratory. Also, thanks to every body in the laboratory, who have given me support and built a pleasant working environment. Thanks to Dr. Mei Luo Zhang, Dr. Bruno Stuyvers, Dr. Tsuyoshi Shinozaki, Dr. Yuji Wakayama, Al Davidoff, Samer Elkasem, Billie Jean Martin, Donna Allan, for their help and friendship.

As well, I would like to thank my friends and teachers in China for being there for me whenever I need help.

Dedication

This thesis is dedicated to my dear Hong, for her love and companion in my life.

Table of Contents

List of Tables

List of Figures

Abbreviations

ß	F380 (in zero Ca^{2+})/F380 (in saturating Ca^{2+})
λ	Laser wave length
$[Ca^{2+}]_i$	Intracellular Ca^{2+} concentration
$[Ca^{2+}]_o$	Extracellular Ca^{2+} concentration
Å	Angstroms
ADP	Adenosine diphosphate
AP	Action potential
AS	Activating solution
ATP	Adenosine triphosphate
BDM	2,3-Butanedione monoxime
BSA	Bovine serum albumin
CaM	Calmodulin
CaMKII	Ca^{2+}-Calmodulin-dependent protein kinase
cAMP	Cylic adenosine monophosphate
CHF	Congestive heart failure
CICR	Ca^{2+}-induced-Ca^{2+} release
CLSM	Confocal laser-scanning microscope
cTnT	Cardiac troponion T
DCM	Dilated cardiomyopathy
DHPR	Dihydropyridine receptor
DTT	Dithiothreitol
E_{Ca}	Calcium equilibrium current
ECC	Excitation-contraction coupling
EGTA	Ethyleneglycol-bis (ß-aminoethylether)-N,N'-tetraacetic acid
EPMA	Electron microprobe microanalysis
EPR	Electron paramagnetic resonance
ER	Endoplasmic reticulum
F	Force

F340	Fura-2 fluorescence at 340 nm excitation
F380	Fura-2 fluorescence at 380 nm excitation
F_{max}	Maximal force
Force-pCa	Force-free [Ca^{2+}] relation
Force-SL	Force-sarcomere length relation
I_{Ca}	Calcium current
Ie	Ionic equivalence
I_k	Delayed outward potassium current
I_{k1}	Inwardly rectified potassium current
I_{kto}	Transient outward potassium current
Kd	Effective dissociation constant of fura-2 to Ca^{2+}
KH	Krebs-Henseleit solution
LBN	Lewis Brown-Norway
LV	Left ventricle
MI	Myocardial infarction
MLC	Myosin light chain
MLC2	Regulatory light chain
MW	Molecule weight
n_{high}	Hill co-efficient for upper portion
n_{low}	Hill co-efficient for lower portion
PKA	cAMP-dependent protein kinase
PKC	Protein kinase C
PLN	Phospholamban
PMT	Photomulitiplier tube
R	F340/F380
R_{max}	R in saturated Ca^{2+}
R_{min}	R in zero Ca^{2+}
RS	Relaxation solution
RV	Right ventricle
RyRs	Ryanodine receptor
S_1	Subfragment 1

S_2	Subfragment 2
SERCA	Sarco(endo)plasmic reticulum Ca^{2+}-ATPase
SL	Sarcomere length
SR	Sarcoplasmic reticulum
Tn	Troponin
TnC	Troponin C
TnI	Troponin I
T-tubule	Transverse tubule
V1	Myosin isoform V1
V3	Myosin isoform V3

Chapter 1

Excitation contraction--coupling in normal cardiac muscle

1.1 Introduction--basic elements in cardiac ECC

A human heart consists of 50 million myocytes/g and pumps blood out of its chamber by synchronous contractions of each cardiac-working cell. During the cardiac cycle, electrical coupling is a crucial step, during which an electrical stimulus propagates rapidly along the whole heart, depolarizes the cellular membrane and causes synchronous contraction. Thus, study of the cardiac cycle in a single myocyte can give us a clear picture of contraction and relaxation of the whole heart. This coupling of the electrical process to contraction in a single myocyte is named "excitation-contraction coupling" (ECC).

ECC begins when an action potential (AP) depolarizes the plasma membrane, and ends with the binding of Ca^{2+} to Troponin C (TnC), the Ca^{2+} receptor of the cardiac contractile apparatus followed by sarcomere shortening and force (F) development. Recently, the concept of ECC has been modified to add the processes that cause the heart to relax [1]. During the AP, the cell membrane is depolarized and Ca^{2+} enters into the sarcolemma. In the period of repolarization, Ca^{2+} is excluded from cytosol by a cellular Ca^{2+} removal system. Ca^{2+} influx and efflux are balanced during each cardiac cycle.

The sophisticated structure of single myocyte ensures rapid ECC from beat to beat in the cardiac cycle. Figure 1-1 shows a schematic drawing of the structure for ECC in a cardiac myocyte. ECC requires an intact sarcolemma, which propagates an AP as a wave of depolarization and depolarizes the transverse tubules (T-tubule) [2]. The majority of L-type Ca^{2+} channels locate in T-tubule region. T-tubule faces the terminal cisternae of the sarcoplasmic reticulum (SR) at a very narrow distance.

SR has special structures to ensure its important function of release and uptake of Ca^{2+}. The SR membrane can be divided into two different regions, the subsarcolemmal cisternae, which contains Ca^{2+} channels through which Ca^{2+} flow initiates contraction, and the much more extensive sarcotubular network, which contains a densely packed array of Ca^{2+} pumps [1]. In the region of subsarcolemmal cisternae, there are two important proteins: dihydropyridine receptors (DHPRs) and ryanodine receptors (RyRs). The DHPRs are part of the sarcolemma that includes the T-tubular membranes of the heart cells. Recent immunofluorescence evidence has clearly shown that the DHPR and RyR are largely co-localized in the T-tubular region of cardiac cells [3]. The ultrastructural organization of DHPRs and RyRs has not been fully established in mammalian heart, but the chick heart cells have been examined [4]. In the chick heart cells, the ryanodine receptors appear to be located in clusters, space about 30 nm from each other. The SR membrane that contains the RyRs is ~10 nm away from the sarcolemma membrane and the RyRs appear like feet and fill the space between the two membranes. The RyR appears to span the 10 nm gap. The DHPRs seem to be in a matching patch of sarcolemma and overlying the patch of SR membrane that contains the RyRs [4]. This type of unique structure ensures that the RyRs respond to signals from the DHPRs very quickly and specifically.

1.2 Electrophysiological basis of ECC

Na^+, K^+ and Ca^{2+} fluxes through the plasma membrane are the main ionic changes occurring during the AP [5]. At rest, intracellular $[K^+]$ (~150 mM) is much higher than that

Figure 1-1: Schematic drawing of structures mediating cardiac ECC. During the systole, extracellular Ca^{2+} flows into the intracellular space through sarcolemma L-type Ca^{2+} channels, which are mainly located in the T-tubule region. This Ca^{2+} flow is insufficient to activate the cardiac contractile apparatus, but it opens RyRs and results in CICR. The released Ca^{2+} from the SR lumen and a fraction of Ca^{2+} flowing through the sarcolemma activate the contractile system and cause cardiac muscle contraction. During diastole, Ca^{2+} is taken up by the SR pumps or excluded out of the intracellular space through the sarcolemma Ca^{2+} pump or Na^{+}/Ca^{2+} exchanger. The Na^{+}/K^{+} pumps maintain the intracellular high $[K^{+}]$ and extracellular high $[Na^{+}]$ by consuming ATP.

1: sarcolemma, 2: L-type Ca^{2+} channels in the T-tubule, 3: L-type Ca^{2+} channels in the sarcolemma, 4: sarcolemma Ca^{2+} pumps, 5: sarcolemma Na^{+}/Ca^{2+} exchangers, 6: sarcolemma Na^{+}/K^{+} pumps, 7: SR Ca^{2+} pumps, 8: SR RyRs, 9: SR, 10: sarcomere, 11: Regulatory protein

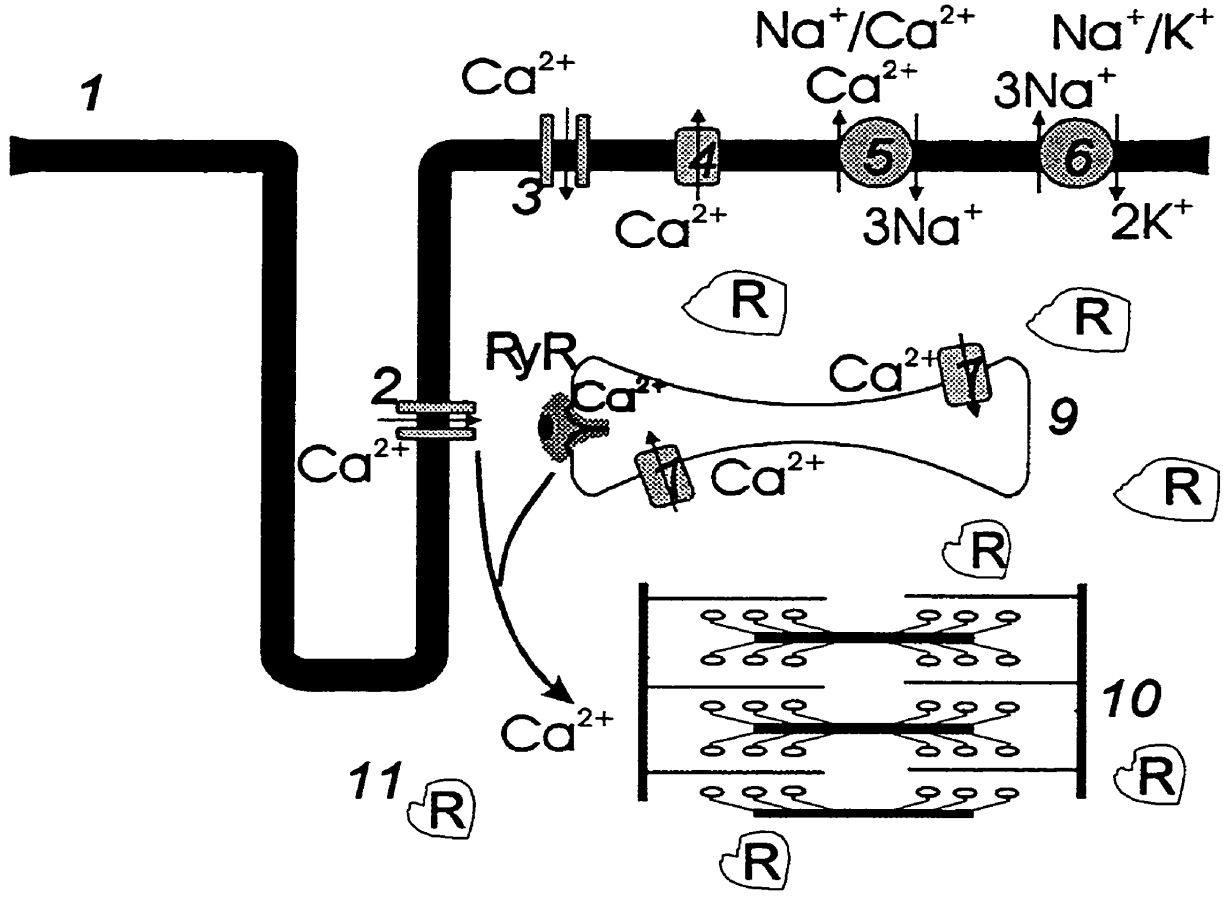
1
Ca2+
Na+/Ca2+
Ca2+
Na+/K+
3Na+
3
4
5
6
Ca2+
3Na+
2K+
R
R
RyR
2
Ca2+
Ca2+
7
9
Ca2+
7
R
R
Ca2+
10
11
R
R
R

of extracellular space (~4.5 mM), whereas the extracellular space has much higher [Na^+] (140 mM) than that of the cytosol (~5mM). [Ca^{2+}] is lower in the cytosol (~100 nM) and higher in the extracellular space (2 mM) at rest. At resting membrane potential, the plasma membrane is highly permeable to K^+, and both Na^+ and Ca^{2+} channels are closed. Therefore, the resting electronegativity of the cell interior is determined largely by the K^+ gradient across the plasma membrane and the resting membrane potential is very close to the K^+ equilibrium potential, ~-90 mv. After activation, the sarcolemma fast Na^+ channels open and Na^+ quickly enters into the cytosol, which initiates an AP. The influx of Na^+ forms phase 0 of an AP in cardiac working cells and increases the potential to ~+25 mV inside of the cardiac cells. The depolarization also turns on a transient outward K^+ current (I_{kto}), resulting in phase 1. The increased membrane potential activates voltage gated L-type Ca^{2+} channels in the sarcolemma. The slow influx of Ca^{2+} balances with outward currents and composes phase 2, which is termed plateau phase in the cardiac AP. A delayed rectifier K^+ current (I_{k+}) increases when the inward Ca^{2+} current decreases at the highest voltage of the membrane potential. The outward delayed rectifier K^+ current forms phase 3. When the cardiac cell repolarizes and the membrane potential drops, the K^+ permeability of cell membrane increases again and causes an inward rectifier K^+ current (I_{kI}), which pulls down the membrane potential to the resting level ~-85 mV and consists of phase 4. At rest, Ca^{2+} is taken up by the SR Ca^{2+} pumps or extruded out of the cardiac cells by sarcolemma Ca^{2+} pumps and Na^+/Ca^{2+} exchangers. Na^+/K^+ pumps maintain the electrical gradient for the Na^+ and K^+ ions [6]. The detailed AP of a cardiac working cell is illustrated in Figure 1-2.

Figure 1-2: Schematic drawing of cardiac action potential. At rest, the intracellular electronegativity is maintained by the outward K^+ current: delayed inwardly rectified K^+ current. This outward current maintains the membrane potential ~-85 mV. The rapid inward Na^+ current depolarizes the cardiac membrane, which increases the membrane potential to ~+25 mV, and forms phase 0. The transient inward K^+ current drops the membrane potential to ~0 mV and causes phase 1. The slow inward Ca^{2+} current balances with the outward currents and forms plateau in the cardiac cycle, which is phase 2. In phase 3, the membrane potential quickly drops to ~-80 mV, which is caused by the activation of delayed outward K^+ current. Then, the membrane potential is brought to resting level (~-85 mV) by the delayed inwardly rectified K^+ current. The resting membrane potential is also maintained by the Na^+/K^+ pump and Na^+/Ca^{2+} exchanger because these two structures are electrogenic.

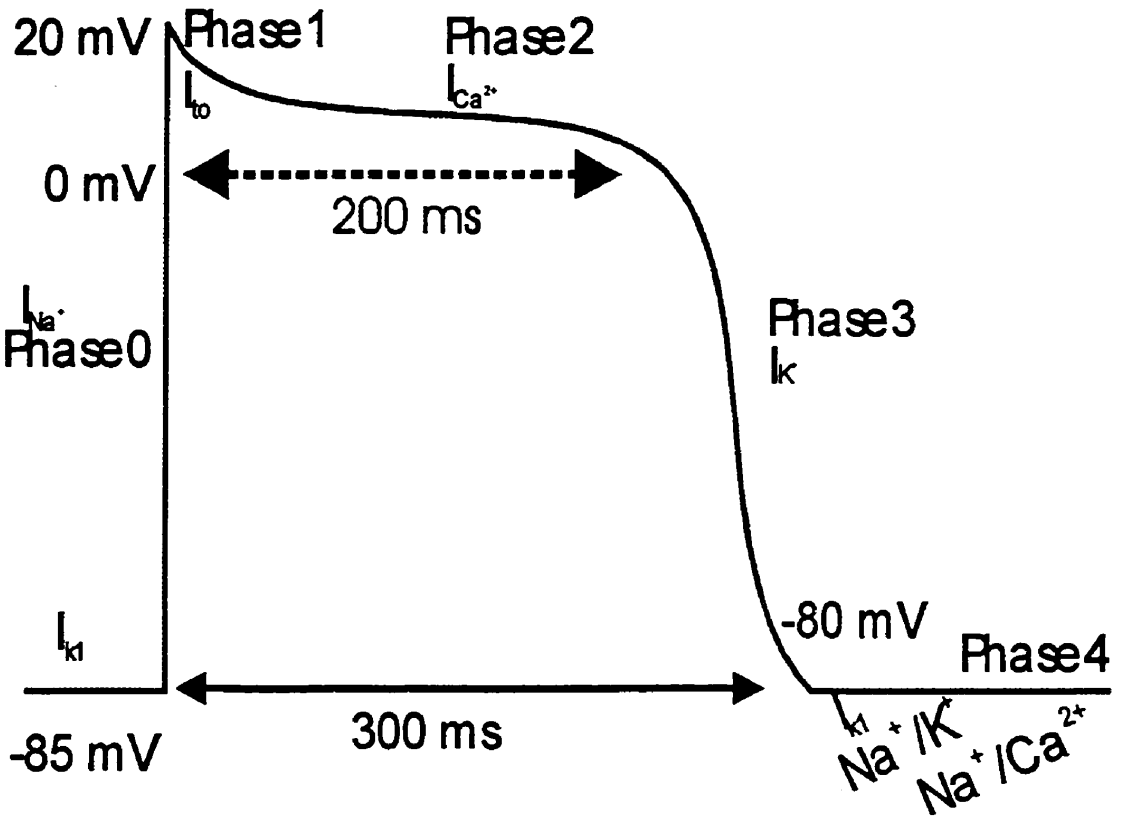
20 mV
Phase1
Phase2
I_{to}
$I_{Ca^{2+}}$
0 mV
200 ms
I_{Na^+}
Phase0
Phase3
I_K
I_{K1}
-80 mV
Phase4
300 ms
-85 mV
I_{K1}
Na^+/K^+
Na^+/Ca^{2+}

1.3 Functions of Ca^{2+} in ECC

Intracellular Ca^{2+} is a key element in ECC. The transport of Ca^{2+} ions among different Ca^{2+} pools during a cardiac cycle is a crucial event in the cardiac ECC. There are five different Ca^{2+} compartments within the heart: the extracellular space, the SR, the cytosol, Troponin (Tn) and the mitochondria. The movements of Ca^{2+} among the extracellular space, the SR, the cytosol and Tn are responsible for the initiation and termination of the contractile event.

In the literature, it has been reported that Ca^{2+} has five important functions during an AP [1]. First, it can carry positive charge into the cell, which contributes to the electrical signal responsible for depolarization. Second, it maintains the plateau phase of depolarization in working cells of atria and ventricles, and the His-Purkinje system. Third, it stimulates K^+ channels to open, which restores the resting electronegativity in cardiac muscle cells. Fourth, this slow inward Ca^{2+} current contributes a small amount of cytosolic Ca^{2+} to bind TnC and activates contractile elements. Fifth, the most important role of Ca^{2+} in the cardiac ECC, the inward Ca^{2+} current can induce SR to release Ca^{2+} stored in the SR lumen [1].

1.4 Intracellular and extracellular Ca^{2+} cycling

Since Ca^{2+} plays important roles in the cardiac ECC, it is crucial to keep Ca^{2+} cycling between the extracellular and intracellular space. Ca^{2+} enters into cells through the L-type Ca^{2+} channel. The amount of Ca^{2+} that enters into the cardiac cells from the extracellular space is insufficient to activate the adult mammalian myocardium. Instead, most of the Ca^{2+} entering from extracellular space binds to the ryanodine receptors (RyRs) on the SR membrane and induces the SR to release a larger amount of Ca^{2+} from

its lumen through Ca^{2+} release channels on the SR membrane. This process is called " Ca^{2+}-induced Ca^{2+} release" (CICR) [7], which is a characteristic of the cardiac ECC. In this way, the $[Ca^{2+}]_i$ is amplified by the Ca^{2+} released from the SR. The released Ca^{2+} from the SR together with a small amount of Ca^{2+} entering through sarcolemma initiates muscle contraction. During relaxation, intracellular Ca^{2+} is extruded by the Ca^{2+} pump and Na^+/Ca^{2+} exchanger in the sarcolemma, or taken up by the SR Ca^{2+} pump. The sarcolemma Ca^{2+} channels, sarcolemma Ca^{2+} pumps, Na^+/Ca^{2+} exchangers, SR Ca^{2+} pumps and SR RyRs allow the Ca^{2+} cycle of from beat to beat in the heart.

1.5 I_{Ca}--trigger of cardiac ECC

Most studies show that Ca^{2+} influx through the L-type Ca^{2+} channel in sarcolemma is the trigger of cardiac ECC.

1.5.1 Properties of Ca^{2+} channels

There are three different types of Ca^{2+} channels: L-type, T-type and N-type [2]. The L-type Ca^{2+} channels are characterized by a large conductance (~25 pS in 110 mM Ba^{2+}), long lasting openings (with Ba^{2+} as the charge carrier), sensitivity to 1,4-dihydropyridines (DHPs) and activation at larger depolarization (i.e. at positive membrane potential). The T-type channels are characterized by a tiny conductance (~8 pS), transient openings, insensitivity to DHPs, and activation at negative membrane potential. The N-type Ca^{2+} channels are neither T- nor L-types, and are predominantly found in neurons. They are intermediate in conductance and voltage dependence. Cardiac muscle has both L-type Ca^{2+} channels and T-type Ca^{2+} channels. The function of T-type channels is not clearly known in cardiac muscle [2].

L-type channels isolated from skeletal muscle are composed of 5 subunits: α_1,α_2, β, γ, and δ. The α_1 subunit appears to bear the main known functional characteristics of these channels. This subunit has the DHP, phenylalkylamine and benzothiazepone receptors [8] and can be phosphorylated by cAMP (Cyclic adenosine monophosphate)- and Ca^{2+}-Calmodulin (CaM) dependent protein kinases [9] and protein kinase C (PKC) [10]. The cardiac α_1 subunit is larger than the skeletal muscle protein α_1 subunit by ~20 or 30 kDa[11].

The activation and inactivation of Ca^{2+} channels are time- and voltage-dependent[5]. Cardiac I_{Ca} is rapidly activated by depolarization, reaching a peak in 2-7 milliseconds. Its inactivation is relatively slow and requires a few hundred milliseconds to be completely inactivated. The Ca^{2+} channels are the most voltage sensitive channels. In patch clamp studies, step-increase of holding potentials from the physiological voltage (-70 to –90 mV) to ~0 mV, I_{Ca} shows stepwise increase with increase of membrane potential. The threshold of activation of I_{Ca} is approximately –40 mV, the current is maximal near 0 mV, and the equilibrium potential (E_{Ca}) is around +100 mV [5].

1.5.2 I_{Ca}—initiating event in cardiac ECC

The Ca^{2+} influx alone through the L-type Ca^{2+} channel is insufficient to activate myofilament contraction. However, it is clear that cardiac contraction depends on extracellular Ca^{2+}, thus it is important to consider the amount of Ca^{2+} that enters via I_{Ca} with respect to the Ca^{2+} requirement for the myofilament activation. The typical peak I_{Ca} is about 1-2 nA in the mammalian ventricular myocyte with a volume about 20 pL [2]. The density of L-type Ca^{2+} channels is 15/μm^2 with an opening probability 0.03 [12]. The total number of L-type Ca^{2+} channels is ~70,000/cell and 2,100 of them open during

depolarization. Based on the above numbers, the intracellular total [Ca^{2+}] will increase by 0.5 M and free [Ca^{2+}] will increase from 100 nM at rest to 200 nM after the myocyte is depolarized. At maximal activation, cytosolic free [Ca^{2+}] is in the micromolar range. There must be other Ca^{2+} source participating in the activation of myofilaments in cardiac muscle.

The Ca^{2+} influx is an initiating event and the primary link of ECC in the heart. The Ca^{2+} entered during an AP links the electrical events to contraction. The Ca^{2+} influx through L-type Ca^{2+} channels provides a trigger for the cardiac SR to initiate the SR to release a larger amount of Ca^{2+} ions stored in the SR lumen, and finally, the myofilament contracts. Based on the numbers from the study of Cheng et al., this amplification of $[Ca^{2+}]_i$ caused by CICR is ~15-20 fold [13].

1.6 CICR--fuel of contraction

1.6.1 General properties of RyRs:

The SR ryanodine receptors release Ca^{2+} from its lumen and amplify the Ca^{2+} influx through the L-type Ca^{2+} channel, to sufficiently activate cardiac myofilaments. The estimation of the number of ryanodine receptors in intact cardiac ventricular myocytes or whole heart homogenates is approximately ~36 nmol/kg wet wt, which is very similar to the number of DHPR. But it is much smaller than that of the SR Ca^{2+} pump, about ~6000 nmol/kg wet wt [2].

The isolated ryanodine receptor molecule weighs ~320—450 kDa for a monomer[14]. The ryanodine receptor complex is a homotetramer, and ~27 nm along each side and ~14 nm tall, which corresponds well with the width and length of the junctional "feet" observed in intact cardiac muscle.

The SR Ca^{2+} release channel is sensitive to ryanodine. Ryanodine is a neutral plant alkaloid, which is found to produce irreversible contracture in skeletal muscle, and a progressive decline in contraction in cardiac muscle. Ryanodine affects the SR Ca^{2+} release in cardiac ECC, thus affects force development. ter Keurs et al. have found that ryanodine causes Ca^{2+} leak to from the SR in a dose-dependent manner [15]. Ryanodine depletes the SR Ca^{2+} content, as a result, it decreases the force development.

The function of RyRs is regulated by Ca^{2+} influx through DHPRs, the cytosolic $[Ca^{2+}]$, and $[Ca^{2+}]$ in the SR. The cardiac muscle SR Ca^{2+} release channel is a ligand-gated channel that is activated by micromolar cytoplasmic $[Ca^{2+}]$ and inactivated by millimolar cytoplasmic $[Ca^{2+}]$. An excessive increase in cytosolic Ca^{2+} can inhibit further Ca^{2+} release. The SR lumen Ca^{2+} also regulates cardiac Ca^{2+} release channel activity perhaps through the open channel and binding to the channel's cytosolic Ca^{2+} activation and inactivation sites [16].

1.6.2 Ca^{2+} release theories

There are four main theories regarding the mechanism of Ca^{2+} release from the SR. The first theory is "Electrical Coupling". Some investigators propose that sarcolemma depolarization causes SR membrane depolarization, which leads to the SR Ca^{2+} release. The second one is "Mechanical Coupling". It is suggested that sarcolemma depolarization causes "unpluging" of Ca^{2+} release channels, which might result in Ca^{2+} release from the SR. The third type is Ca^{2+} release induced by inositol(1,4,5)-trisphosphate (IP_3). IP_3 binds to the IP_3 receptors of the SR membrane and induces Ca^{2+} release. The fourth theory, CICR, is the theory generally accepted in cardiac ECC. It postulates that the entry of a small amount of Ca^{2+} across the sarcolemma, by binding to

Ca^{2+} receptors on the surface of SR, causes a larger amount of Ca^{2+} stored in the SR to release into the cytosol [1].

1.7 Ca^{2+} sparks –elements of SR Ca^{2+} release

The development of the confocal microscope has provided researchers a useful tool to further study SR function, especially Ca^{2+} release from the SR. The confocal technique allows inverstigators to scan a cell along any arbitrarily defined direction. By alternatively taking longitudinal and transverse line-scan images in the same focal plane, the direction-dependent properties of Ca^{2+} sparks can be examined in the same cells. The confocal laser-scanning microscope (CLSM) is widely used in research settings at present since it gives a coherent beam of intense light and short sampling time with high resolution [17]. Fluorescent dyes give clear indication of Ca^{2+} ions in confocal microscope images. Many research works on "Ca^{2+} sparks" have been done with CLSM. Recent studies on Ca^{2+} sparks by confocal microscope have provided exciting new insights into the mechanism of ECC in heart cells.

1.7.1 Ca^{2+} sparks--local event of Ca^{2+} release

The confocal microscope allows imaging local Ca^{2+} release from the T-tubule and the SR membrane junctions. Investigators have observed local Ca^{2+} release and given it the name "Ca^{2+} spark". It has been found that Ca^{2+} sparks are confined to very small areas with radius ~1.5 μm in quiescent cardiac cells. The distance of two longitudinal neighbouring Ca^{2+} sparks is ~ 2 μm, which corresponds well to resting SL 1.86 μm [18]. So, it is reasonable to assume that this Ca^{2+} comes from a point source of Ca^{2+}.

Ca^{2+} sparks are local Ca^{2+} releases from the SR. The intracellular Ca^{2+} could originate either from the extracellular space through L-type Ca^{2+} channels or be released

by the SR from its lumen. The former is ruled out by the observation that Ca^{2+} sparks can be seen when cells are briefly exposed to a bathing medium without Ca^{2+}, or to a medium supplemented with 0.1mM cadmium, which is a blocker of the L-type Ca^{2+} channel [18]. Under this condition, the resting Ca^{2+} sparks could result from the RyR spontaneous Ca^{2+} release from the SR cavity. Further, the effects of ryanodine on the SR Ca^{2+} release channels have supported the hypotheses that Ca^{2+} sparks are generated by the SR. At high concentration of ryanodine, above 1 μM, Ca^{2+} sparks disappeared. When the cardiac cells are exposed to intermediate concentration of ryanodine (100-300 nM), the frequency of Ca^{2+} sparks increased from 1.6±0.22 to 3.53±0.75 [18]. At resting, Ca^{2+} sparks may arise as a result from random opening of L-type Ca^{2+} channels. Mostly likely, the resting cytosolic Ca^{2+} activates spontaneous Ca^{2+} sparks via CICR [18].

Further, a single RyR or a small number of RyR channels may be the functional Ca^{2+} release unit. The biophysical properties of Ca^{2+} sparks are consistent with the functional unit being composed of as few as a single RyR. Cheng et al. have found that the Ca^{2+} flux associated with a spark 2 x 10^{-17} mol/s, which corresponds to an ionic current of ~4 pA [18]. This number is quite consistent with the result from planar lipid bilayer experiments. In the single RyR channel recording of planar lipid bilayer experiments, the current is ~3 pA at 0 mV [19]. So, a Ca^{2+} spark may be explained by the opening and closing of a single SR Ca^{2+}-release channel, or a small number of RyR channels acting in concert.

1.7.2 Local control of SR Ca^{2+} release

"Common pool" and "local control" are two opposite theories regarding to the control of the SR Ca^{2+} release. The former theory proposes that Ca^{2+} releases from a

common pool in cytosol and the Ca^{2+} release is in an all-or-none manner. It fails to explain the graded gain of the Ca^{2+} release from the SR. The local control theory has provided an explanation for how the SR controls Ca^{2+} release. RyRs seem to be extremely insensitive to cytosolic Ca^{2+} in situ. In quiescent cardiac cells, there is an occurrence of 100 sparks/cell/s [18], which indicates an opening rate of 10^{-4}/s for the RyR at ~100 nM [Ca^{2+}], given 10^6 RyRs per rat heart cell [18]. Both evoked and spontaneous Ca^{2+} sparks normally do not activate regenerative CICR activities [20]. The insensitivity of the RyR prevents a single Ca^{2+} spark from triggering its neighboring Ca^{2+} release units despite the large number of RyRs that "see" the Ca^{2+} spark. Further, the DHPRs and RyRs appose to each other with a 10 nm narrow distance between them [21], which provides structural basis for the "local control" theory. The delicacy and tightness of this local control are best exemplified by the evidence that a single DHPR channel can open to elicit a Ca^{2+} spark. Once activated, Ca^{2+} sparks have a short half time of decay, which is not affected by the opening duration of single L-type Ca^{2+} channel flux or the duration of depolarization. The DHPRs are closer to RyRs, with a distance about 10 nm in chick heart cells, which is shorter than a RyR to its neighboring RyRs, with a distance ~30 nm[21]. The average distance between a DHPR to its nearest neighbor RyRS is less than half of the distance between nearest neighboring RyRs. During Ca^{2+} spark diffusion, local $[Ca^{2+}]_i$ decreases sharply with distance, so DHPRs may be in a better position to activate a neighboring RyR than a RyR to activate its neighboring RyR. This tight trigger-release structure provides another support for the local control theory.

1.7.3 Source of the Ca^{2+} spark trigger

There are two different points of views on what the triggering Ca^{2+} comes from. Some researchers propose that the Na^+/Ca^{2+} exchanger operating in a reversed direction can elevate local $[Ca^{2+}]_i$ and causes the SR Ca^{2+} release. Inhibition of both L-type Ca^{2+} current and Na^+/Ca^{2+} exchange decreases more force than inhibition of L-type Ca^{2+} current alone [22]. Lederer et al. showed that under circumstances where the SR was overloaded in sheep Purkinje fibers, SR Ca^{2+} release could be triggered by the Na^+/Ca^{2+} exchanger [23]. Levi et al. also demonstrated that, when the measured Ca^{2+} current was blocked, SR Ca^{2+} release could be evoked by reverse mode of the Na^+/Ca^{2+} exchanger [24]. Further support is from the study of Cannell et al., which demonstrated Na^+/Ca^{2+} exchange-induced SR Ca^{2+} release under abnormal conditions such as "Ca^{2+}-overload" produced by sodium-pump inhibition, and membrane depolarization to +100 mV, as well as at less positive potentials in myocytes perfused internally with high $[Na^+]$ (20 mM) [25]. The wide distribution of the Na^+/Ca^{2+} exchanger also makes it possible for the Na^+/Ca^{2+} exchangers to provide Ca^{2+} to activate RyRs just like the L-type Ca^{2+} channels. However, the significance of the reverse model of the Na^+/Ca^{2+} exchanger under physiological conditions is still uncertain. The extent of this trigger appears to be quite limited in some species [26]; whereas under conditions, such as with pathological or pharmacological modulation of the SR, the role of the Na^+/Ca^{2+} exchanger may become significant [16]. Without the modulation in ECC, the Na^+/Ca^{2+} exchanger can hardly be seen to function in a reversed way in mammalian heart cells.

Other investigators have proposed that the triggering Ca^{2+} enters through L-type Ca^{2+} channels in sarcolemma from the extracellular space. A recent study using

transgenic mice over expressing the Na^+/Ca^{2+} exchanger has shown that even when the Na^+/Ca^{2+} exchanger is over-expressed up to nine-fold, Ca^{2+} entry through the exchanger produces a much smaller systolic rise of $[Ca^{2+}]_i$ than does the L-type current. For a given amount of Ca^{2+} entering the cell, the Na^+/Ca^{2+} exchanger is only 25% as effective as the L-type Ca^{2+} channels in promoting Ca^{2+} release from the SR [27]. The special structure between DHPRs and RyRs is another support for the hypothesis that triggering Ca^{2+} enters through L-type Ca^{2+} channels. The close co-localization between DHPRs and RyRs ensures the small amount of Ca^{2+} entering through L-Ca^{2+} channels acts effectively with RyRs.

Ca^{2+} current is the trigger of CICR, which is further supported by the fact that a single L-type Ca^{2+} channel is sufficient to activate an associated release unit. Cannell et al. [20] and Santana [28] et al. have shown that, at negative membrane potentials (-50 to –30 mV), the voltage-dependent spark occurrence overlaps the activation of the L-type Ca^{2+} channel. The efficacy of I_{Ca} to evoke Ca^{2+} sparks gradually decreased as the magnitude of single L-type Ca^{2+} channel current is decreased. Both of their experiments have provided functional evidence for a single L-type Ca^{2+} channel being the activator of Ca^{2+} sparks.

1.7.4 Ca^{2+} quarks--smaller events than Ca^{2+} sparks in ECC

Most studies have shown that Ca^{2+} sparks are the elementary events in cardiac ECC, however, some investigators have presented "Ca^{2+} quarks" model [29] challenging the idea of a single RyR as the basis of a Ca^{2+} spark. When $[Ca^{2+}]_i$ is elevated homogeneously by photorelease of caged Ca^{2+}, SR Ca^{2+} release by CICR is evident but surprisingly, no Ca^{2+} spark is seen. However, in the same cell, I_{Ca} does elicit discrete local release that looks like Ca^{2+} sparks. These researchers suggest that this phenomenon

occurs because the elementary release units, named "Ca^{2+} quarks" during photolysis are much smaller than Ca^{2+} sparks and are invisible. It has been proposed that RyRs are organized into clusters and RyRs within a cluster are gated independently, and each gives a rise of Ca^{2+}-quark by the global elevation of $[Ca^{2+}]_i$ produced by the photolysis. When I_{Ca} is elicited, the whole group may be activated as a unit, giving a rise of Ca^{2+} spark, due to high local $[Ca^{2+}]_i$ produced by L-type Ca^{2+} current. But this theory does not succeed in explaining the similarities between I_{Ca}-evoked Ca^{2+} sparks and the Ca^{2+} sparks evoked by the resting cytosolic Ca^{2+}, neither can explain the fact that the enormous Ca^{2+} flux from a RyR could not open its clustermates.

1.7.5 Ca^{2+} wave and its propagation

Ca^{2+} waves are the summation of individual Ca^{2+} sparks. Increase of the sensitivity of SR Ca^{2+} release, i.e. the increased SR Ca^{2+} load and under the effects of caffeine and ryanodine, can induce Ca^{2+} waves. Cheng et al. found that the overload of SR Ca^{2+} content by increasing $[Ca^{2+}]_o$ to 10 mM can increase the SR sensitivity to release Ca^{2+} and increase the frequency of Ca^{2+} sparks, resulting in Ca^{2+} wave propagation [18]. Studies have shown that an individual Ca^{2+} spark does not cause muscle contraction [21]. The probable reason is that the Ca^{2+} is buffered by the stronger buffering system in the cardiac cytosol [30]. The macro sparks (summation of several closely spaced individual sparks with a peak around 500 nM) and Ca^{2+} waves can cause muscle contraction and sarcomere length (SL) changes [21].

1.7.6 Summary of Ca^{2+} sparks

The present data from studies of cardiac ECC indicate that: Ca^{2+} sparks are elementary units in the sequence of ECC in heart muscle. However, so far, there is not

enough evidence to exclude the possibility that Ca^{2+} quarks, the events that are smaller than Ca^{2+} sparks, exist in the cardiac ECC. A single RyR or a small number of RyRs acting in concert composes a functional unit to release Ca^{2+} sparks. Functional units of DHPRs and RyRs have delicate and tight local structure to control SR Ca^{2+} release. A single DHPR is sufficient to act on an associated RyR and cause it to release Ca^{2+}. Most likely, Ca^{2+} influxes through the L-type Ca^{2+} channel instead of Na^+/Ca^{2+} exchanger cause the SR to release Ca^{2+}. Further studies are needed to determine the function of the reverse mode of Na^+/Ca^{2+} exchanger in triggering the SR Ca^{2+} release in physiological conditions.

1.8 Na^+/Ca^{2+} exchanger--high capacity for Ca^{2+} removal

Ca^{2+} entering from the extracellular space or released from the SR during contraction must be removed from the cytosole in relaxation. Two mechanisms are responsible for this action: the Na^+/Ca^{2+} exchanger and the Ca^{2+} pumps of sarcolemma and SR. The Na^+/Ca^{2+} exchanger has a high capacity to extrude Ca^{2+} with a low affinity, and the SR Ca^{2+} pump has a high affinity for Ca^{2+} with a low capacity to remove Ca^{2+} from cytosol.

The Na^+/Ca^{2+} exchanger system is one of the primary Ca^{2+} extrusion systems in cardiac myocytes and plays an important role in the termination of cardiac contraction. The Na^+/Ca^{2+} exchanger proteins are distributed over the entire extracellular surface of the membrane, including the T-tubules, so they are well placed to extrude activating Ca^{2+}. It is estimated that the Na^+/Ca^{2+} exchange stoichiometry is 3:1, thus it is electrogenic[31].

The cardiac Na^+/Ca^{2+} exchanger molecule has 970 amino acid with a molecular weight (MW) about 100 kDa. This protein consists of 12 putative transmembrane

domains and one large cytoplasmic hydrophilic domain. The large domain has a CaM binding site and a potential phosphorylation site, which could be a substrate for CaM or cAMP-dependent protein kinase (PKA) [32].

The Na^+/Ca^{2+} exchanger is regulated by many factors. A high concentration of cytosolic Na^+ or the absence of cytosolic Ca^{2+} promote the formation of the inactive states; phosphatidylinositol- (4,5) bisphosphate or other negatively charged phospholipids and cytosolic Ca^{2+} counteract the inactivation process. The exchange function is also dependent upon cytoskeletal interactions and the exchanger's location with respect to intracellular Ca^{2+}-sequestering organelles.

One important function of the Na^+/Ca^{2+} exchanger is to extrude cytosolic Ca^{2+} by using the energy from the Na^+ gradient, but there are still arguments on the reverse model of the Na^+/Ca^{2+} exchanger, which some investigators think it contributes to CICR in cardiac myocytes.

1.9 SR Ca^{2+} pump--the main machinery of Ca^{2+} removal in cardiac ECC

The Ca^{2+} pump is another important cytosolic Ca^{2+} removal system other than the Na^+/Ca^{2+} exchanger. Both the sarcolemma and SR have Ca^{2+} pumps, and they have similar structure and function. The SR Ca^{2+}-pump is the main structure for the cytosolic Ca^{2+} removal.

1.9.1 General properties of SR Ca^{2+} pump

The major protein in the SR membrane is the Ca^{2+}-ATPase, representing 40% of the total protein in the cardiac SR. Recombinant DNA studies have revealed that the SR or endoplasmic reticulum (ER) Ca^{2+}-ATPase family (SERCA) is the product of at least three alternatively spliced genes, which produce a minimum of five different proteins [33].

$SERCA_1$ is expressed in fast skeletal muscle, and $SERCA_2$ has been detected in cardiac muscle and slow skeletal muscle ($SERCA_{2a}$) and in adult smooth muscle and nonmuscle tissue ($SERCA_{2b}$). $SERCA_3$ is expressed in a selective manner, with highest expression in intestine, spleen, lung, uterus, and brain [33].

The structure of cardiac SR Ca^{2+}-pump is similar to that of slow twitch muscle [34]. The protein has 10 membrane-spanning regions (M1-M10). M1-M5 each has an additional α-helical "stalk" region on the cytosolic side. Recently, researchers have found that the important Ca^{2+} binding sites are within the transmembrane domains (M4-M6 and M8) [35]. The transmembrane domains form a cylinder and it acts like an ion channel through the SR membrane [34]. Ca^{2+} can flow into the SR lumen through the channel.

The SR Ca^{2+} pump can take up 60%-70% of Ca^{2+} released into its lumen during systole through its strong internal Ca^{2+} buffering system [5]. Inside the SR lumen, $[Ca^{2+}]$ is in the millimolar range, which is much higher than that in the cytosol, about in the micromolar range. If the myocyte's Ca^{2+} buffering capacity is as high as reported by Isenberg's group, then 99.98% of the Ca^{2+} is bound with the intracellular buffering system, the total $[Ca^{2+}]$ is ~0.5 mM in the cytosol at resting. The total $[Ca^{2+}]$ in the SR lumen is approximately ~5-14mM [2]. Several Ca^{2+}-binding proteins within the SR lumen buffer Ca^{2+} effectively. The most important one is calsequestrin, which traps Ca^{2+} inside the SR. This protein is primarily localized in the terminal cisternae of the SR. Each calsequestrin molecule binds ~35-40 Ca^{2+} ions [36]. Thus, these Ca^{2+} binding sites on clasequestrin can buffer a substantial fraction of the Ca^{2+} ions taken up by the SR with a high capacitance and an appropriately low affinity. Other buffering proteins found in

smaller amount in the SR cavity include calreticulin and histidine-rich Ca^{2+}-binding protein. These proteins also help to retain Ca^{2+} inside the SR lumen.

1.9.2 Regulation of SR Ca^{2+} pump

The function of cardiac SR Ca^{2+} pumps is regulated by the phosphorylation of phospholamban (PLN) [2]. PLN regulation of the SR Ca^{2+} uptake is a characteristic of the cardiac SR Ca^{2+} pumps. This protein binds with the pump and inhibits the SR Ca^{2+} pump function in its dephosphorylated state. Phosphorylation of PLN alters the structure of the cardiac SR Ca^{2+} pump, and allows the pump to transfer Ca^{2+} from cytosol into the SR lumen.

PLN is a pentamer, however, the detailed structure of PLN is not presently known. But based on its amino acid sequence, several models have been proposed. It is generally accepted that there are two major domains: one hydrophilic domain, which contains three phosphorylation sites, and one hydrophobic domain, which is anchored into the cardiac SR membrane. The hydrophilic domain is important in regulating the SR Ca^{2+} pump, which could have a hydrophilic pore through the SR membrane with phosphorylation sites on the cytoplasmic surface [37]. The function of the hydrophobic domain is not clear, although some evidence also have suggested it might have effects on the SR Ca^{2+} pump regulation.

The regulation PLN phosporylation is through PKA and Ca^{2+}-CaM-dependent protein kinase (CaMKII) [38]. PKA can phosphorylate PLN at serine-16 [39], as a result, this phosphorylation increases the rate of Ca^{2+} transport by effects on two steps in the SR Ca^{2+} uptake. First, PKA phosphorylation increases the Ca^{2+} affinity of the SR Ca^{2+} pump. Second, PKA phosphorylation also can accelerate the rate of the overall Ca^{2+} pump cycle.

CaMKII can phosphorylate PLN at threonin-17 and increases the maximal rate of the SR Ca^{2+} uptake [40].

ß-adrenergic agonists can increase the activity of the SR pump by accelerating turnover and increasing Ca^{2+} sensitivity of the SR Ca^{2+} pump through the above regulatory system. Catecholamine binds to the sarcolemmal ß-receptor and activates adenylyl cyclase through stimulator G-protein; as a result, it increases the cytosolic cAMP level, which induces PLN phosphorylation and results in the increase of sensitivity of SR Ca^{2+} pump and its pumping rate. The increase of SR Ca^{2+} uptake by ß-adrenergic agonists has been also considered to be due to Ca^{2+} activated CaM action [40], caused by the increased Ca^{2+} flow through the L-type Ca^{2+} channel.

pH affects the function of SR Ca^{2+} pump. A decrease of pH reduces the SR Ca^{2+} uptake rate [41]. Thus, acidosis and ischemia can depress the SR Ca^{2+} pump and slow the relaxation time.

1.9.3 Active Ca^{2+} transport by SR Ca^{2+} pump

The SR Ca^{2+} pump needs ATP to transport Ca^{2+} uphill: from the lower [Ca^{2+}] in the cytosol to the higher concentration in the SR lumen. The SR Ca^{2+} pump takes up two Ca^{2+} ions into its cavity for each ATP molecule consumed [42].

ATP-induced pump phosphorylation is a key step in SR Ca^{2+} uptake. The Cardiac Ca^{2+}-pump has two ATP binding sites, a high affinity site (Kd~1μM), which is the substrate site and a second low affinity site (Kd ~ 200 μM), which serves a regulatory role [43]. ATP binds to high affinity sites on the cytoplasmic side of the pump. The terminal phosphate of ATP is transferred to aspartate-351 on the pump. It is proposed that the phosphorylation of aspartate-351 causes a series of conformational changes in the

high affinity Ca^{2+} binding site. The access for Ca^{2+} to the sites from cytosol is closed and the pathway to the SR lumen is open, as a result, Ca^{2+} only can be released into SR lumen and not be moved back into the cytosol [44]. During the Ca^{2+} transport cycle, the enzyme undergoes a transition from a high-affinity state to a low-affinity state for Ca^{2+}, and the ions are translocated from the binding sites into the lumen of the SR.

1.10 Summary of cardiac muscle ECC

In summary, cytosolic Ca^{2+} is kept in balance in the heart from beat to beat. Extracellular Ca^{2+} flows into cytoplasm through the L-type Ca^{2+} channel. The amount of Ca^{2+} entering is small and insufficient to activate cardiac myofilaments to contract. Ca^{2+} influx through DHPR binds to RyR and induces Ca^{2+} release. This triggering Ca^{2+} has a fundamental role in cardiac ECC. It causes CICR and the SR release of a larger amount of Ca^{2+} into cytosol from its lumen. CICR increases the $[Ca^{2+}]$ in the cytosol and causes muscle contraction. Equally important is the Ca^{2+} removal from cytosol. Ca^{2+} entering from the extracellular space and released from the SR must be removed from the cytosol during diastole. The Na^{+}/Ca^{2+} exchanger and the SR Ca^{2+} pump are two main systems to extrude Ca^{2+} in cytosol. The sarcolemma Ca^{2+} pump also contributes to removal of a small amount of Ca^{2+}. In normal cardiac cycling, the cytosolic Ca^{2+} cycles and is kept in balance between the extracellular space and the intracellular space.

Chapter 2

Starling's law and possible mechanisms

2.1 Introduction

The effect of stretch to enhance myocardial performance has been known for at least 100 years. In 1895, Frank found that in a frog ventricle, the developed pressure was a function of the end diastolic volume if the contracting volume was kept constant [45]. Later, in 1914, Starling and his colleagues discovered that if the aortic pressure was constant, the cardiac output was a function of venous filling pressure [46]. These two distinct but related discoveries formed Frank-Starling's law of the heart. It describes the relationship between cardiac output and end diastolic volume. This relationship is based on a fixed relationship between end systolic pressure and volume relationship (ESPVR), which is a geometric transform of the force-length relationship of the cardiac sarcomere. So Starling's Law can be explained by the length dependent sensitivity of the myofilaments to Ca^{2+} [47].

The changes in geometry of the whole heart are complex, therefore in recent years many physiologists have chosen to study the effects of muscle length in isolated preparations of cardiac muscle. Studies have show that the isometric length-tension relation of isolated muscle is similar to the isovolumic volume-pressure relation for the whole heart. The studies of the length-tension relation in isolated muscles should be regarded as a way of analyzing the basic mechanism underlying Frank-Starling's relationships in the intact heart. In the working range of SL for mammalian cardiac muscle (1.60 to 2.30 μm), only the ascending limb of the length-tension relation exists [48]. Increased venous pressure stretches the heart during diastole and the improved cardiac

performance is a consequence both of changes in cardiac geometry and of the effect of stretch on cardiac muscle.

2.2 Cellular view of Frank-Starling's law

In cellular view, SL greatly affects the active force development in cardiac muscles, so tremendous work has been done on the force-SL relationship.

In the 1950's, H. Huxley proposed the sliding filament theory. He used the geometry of myofilament overlap to explain the plateau and descending limb of the length-tension relation in frog skeletal muscle. In the descending limb, at SL 2.20 to 3.60 μm in frog skeletal fibers, the decreased force could be due to the decreased overlap of thick and thin filaments, whereas in the plateau range, at SL 2.00 to 2.20 μm, there were no cross-bridges in the central region of the thick and thin filaments, so change of SL did not affect force developed [49]. At SL below 2.00 μm, Gordon et al. suggested that double overlap of thin filaments and restoring forces probably affected the length-tension relationship [50].

Measurement of SL is crucial in study of the force-length relationship. Edman first used diffraction technique to study the force-length relationship in frog skeletal muscle in 1965 [51] and Pollack et al. applied this diffraction technique in measuring cardiac SL in 1972 [52]. In 1975, Fabiato et al. showed length-tension relationship in skinned cardiac muscle fibers. Fabiato's group overcame the difficulties in measuring SL in the studies of length-tension relationship in cardiac muscle, and for the first time, demonstrated that Ca^{2+}-activation in cardiac muscle was length-dependent [53]. In the latter part of 1970's, ter Keurs et al. also confirmed length-dependent tension development in rat cardiac trabeculae using SL feedback control by showing that increase

of SL in cardiac muscle increased force development [54]. Later, in 1980's, the studies of Kentish et al. demonstrated that the force-SL relationship in intact and skinned cardiac muscle was similar [55]. These investigators showed that the Ca^{2+} sensitivity of myofilaments changed over the entire working range of SL in cardiac muscle. The curves of force-SL relationships are convex to the force axis at high [Ca^{2+}] in both intact and skinned cardiac muscles, whereas at low [Ca^{2+}], the curves were convex to the SL axis. Recently, the data from study of skinned cardiac muscle in our laboratory also showed similar pattern for the relationship between force and SL [56]. The concavity and convexity are toward the force axis at low and high Ca^{2+}, respectively.

All the above studies indicate that muscles generate different levels of force at different [Ca^{2+}]. Further, change of SL increases the force developed at the same [Ca^{2+}], which implies that enhanced activation of myofilaments increases the number of cross-bridges during stretch. This is probably caused by the increased Tn affinity for Ca^{2+} since TnC is the only significant Ca^{2+} binding protein during force development [57].

2.3 Mechanisms of the length-dependent force development

The effects of the length-tension relation in cardiac muscle ECC can contribute to both physical and activation factors [58]. Physical factors are the result of changes in myofilament overlap and include changes in: 1) the maximum number of active cross-bridges; 2) the lateral spacing of the thick and thin filaments; 3) the restoring forces associated with deformations in sarcomere geometry. The activation factors result from any effects of muscle length on the activation process, which includes: 1) the AP and Ca^{2+} current; 2) Ca^{2+} transient; 3) TnC binding constant for Ca^{2+} and cross-bridge cycling[58].

2.3.1 Physical factors

The physical factors can be distinguished from activation factors if the internal Ca^{2+} maximally saturates TnC, so that activation is maximal. Under these circumstances, only the physical factors can operate when muscle length or SL is changed [59].

With saturating [Ca^{2+}], the pure effects of physical factors on the Frank-Starling relation are manifested by the well-characterized SL-maximum tension relation. In fully activated heart muscles, a relative flat length-tension relation can be seen. The decrease in tension with the decrease of SL appears to result from an increase of double overlap of thin filaments such that thin filaments from the opposite side of the sarcomere interfere with cross-bridge binding or cross-bridges actually bind to the thin filaments of opposite polarity [50]. Increase of SL can reduce double overlap between actin from opposite sides of the sarcomere, and this allows more cross-bridges to generate active force. Stretch of the muscle also results in reduction of the lattice spacing and cross-bridges are easier to attach with actin, which increases cross-bridge dependent force [59; 60]. At SL less than 1.60 μm, the slope of the F-SL is steeper. This is assumed to be due to a restoring force arising from the compressed thick filaments. In the SL range of 1.70 μm to 2.30 μm, there would be a relatively shallow slope, as seen in fully activated skeletal muscle [59; 61].

2.3.2 Activation factors

Two activation factors can affect the length dependence of cardiac ECC. First, an increase of cytosolic [Ca^{2+}] following excitation results in an increase in the amount of Ca^{2+} supplied to myofilaments during contraction. Previous studies have shown that stretch affects factors such as Ca^{2+} influx during an AP and CICR from the SR [59; 60]. Second, stretch increases myofilament interaction of thick and thin filaments by a given

$[Ca^{2+}]_i$, which means the Ca^{2+} sensitivity of myofilaments increases with an increase of SL [48]. Stretch results in an increase in cross-bridge dependent force by decreasing lattice spacing and increasing cross-bridge attachment, which increases cooperativity of the thin filaments with Ca^{2+} [57].

Effects of length on Ca^{2+} supply

Research results have shown that the effect of change in muscle length or SL on AP, amplitude and duration, is small [62]. There is no apparent correlation between Ca^{2+} entry into the cytoplasm and length-dependent variations in force [63; 64].

However, change of muscle length or SL greatly affects SR Ca^{2+} release. In the later of 1970's and early of 1980's, Fabiato et al. did a series of experiments indicating that SR Ca^{2+} release mechanisms were indeed length dependent by showing that increase of SL resulted in the increased Ca^{2+} release from the SR [61; 65]. These investigators proposed that the possible mechanism is that increase of SL increases the opening possibilities of RyRs. These studies indicate that length change or the degree of stretch acutely affects CICR.

Effects of length on troponin binding to Ca^{2+}

The force-length relationship in cardiac muscle is much steeper than that in skeletal muscle because the degree of activation of the cardiac myofibrils at constant $[Ca^{2+}]$ increases as muscle length is increased. The activation factors are the main cause of the difference, as the change of SL, the cardiac myofilament Ca^{2+} sensitivity is affected more than that in skeletal muscle. Stretch of cardiac muscle to increase the SL over the range of lengths where only double overlap of the actin filaments plays a role leads to an increase of the apparent Ca^{2+} sensitivity of the contractile system.

A number of studies have shown that the Ca^{2+} transient declines more rapidly at longer SL than that at shorter SL while the duration of contraction at long lengths is increased [63; 64]. A quick release during force generation leads to the appearance of "extra" Ca^{2+} in the cytoplasm [66]. Decreased length of isolated papillary muscle produces a slow declined Ca^{2+} transient, relating to a co-responding reduction of force [67]. Allen et al. also showed that rapid shortening of SL could result in a sustained increase in myoplasmic $[Ca^{2+}]$ [68]. Allen et al. proposed that the dominant effect of shortening was a reduction in Ca^{2+} binding to Tn and that Ca^{2+} binding to Tn became more rapidly at long SL.

That the affinity of Tn for Ca^{2+} is length-dependent has been proved in the studies of Hofmann et al.. These investigators showed that TnC is the only significant Ca^{2+} binding bite [57]. Hofmann's group demonstrated that the binding of Ca^{2+} to the Ca^{2+} - specific regulatory site of cardiac TnC in fiber bundles in rigor was length-dependent over the SL range 1.70 μm to 2.40 μm [69]. Hofmann et al. also found that a reduction in SL is correlated with a reduced binding of Ca^{2+} to the regulatory site of TnC. In their studies, these investigators demonstrated directly that Ca^{2+}-sensitivity is associated with changes of SL along the ascending limb of the force-length curve, which could be correlated with changes in the binding of Ca^{2+} to the regulatory site of TnC using radiolabelled Ca^{2+} binding in skinned cardiac muscle fibers [57]. The binding of Ca^{2+} to Tn increases from 0.9 μmole/gm at SL 1.70 μm to 1.15 μmole/gm at SL 2.30 μm at saturated $[Ca^{2+}]$[69].

The results of recent studies have provided further support for length dependent Ca^{2+} sensitivity for cardiac myofilaments. Kentish et al. demonstrated a length-

dependent shift of the force-pCa curves in skinned rat cardiac trabeculae. This sort of curve shift has been interpreted to indicate a change in sensitivity of the myofilaments for Ca^{2+} [55]. With an increase of SL, the maximal force (F_{max}) and myofilament Ca^{2+} sensitivity increased.

Positive force feed-back

Myofilament Ca^{2+} sensitivity is not a function of length per se but of a derivative of length, namely interfilament spacing. Both in skeletal [70] and cardiac muscle [53], the Ca^{2+} sensitivity is increased along the descending limb of the force-length curve where the number of cross-bridge interactions would be expected to decrease with increase in SL. Ca^{2+} sensitivity of myofilament is not a straightforward function of filament overlap since as the SL is increased, the myosin and actin filaments come closer together, consequently, the probability of strong-binding cross-bridge interaction occurring would be increased.

Ca^{2+} binding to Tn depends on the number of cross-bridges attached. Bremel and Weber showed that the Ca^{2+}-TnC affinity in skeletal muscle is enhanced by rigor bridge attachment to actin [71]. In their study, it was shown that the TnC binding constant increased ~20 fold by the attachment of myosin heads to actin. Bremel et al. proposed that the binding of myosin to actin might turn on the neighboring actin and increase myosin ATPase activity. Allen and Kurihara suggested that the TnC binding constant was increased as a function of tension production [63]. Allan et al. also demonstrated in their studies that Ca^{2+} which dissociates from the myofibrils in quick release is correlated with the change in force rather than change in length [68]. The studies of Hofmann and Fuchs et al. further supported this finding by showing that inhibition of the actin-myosin

interaction by the phosphate analog, vanadate, reduced the Ca^{2+}-TnC affinity and eliminated the length-dependence of Ca^{2+} binding [69; 72].

At submaximal [Ca^{2+}], the formation of force-generating complexes-crossbridges, can cooperatively interact within the thin filaments, resulting in increased Ca^{2+} binding to TnC, consequently, forming more force-generating complexes. Since the formation of cross-bridges is length-dependent in the SL range 1.70 μm to 2.40 μm, obviously, increase of SL will augment force generation [57]. Thus, the cardiac force-length relationship is much steeper than that expected purely from the basis of filament geometry.

The effects of mechanical feedback on the Ca^{2+} regulatory complexes of cardiac and skeletal muscle are distinctly different. In skinned fast skeletal muscle fibers, there is no change in Ca^{2+}-Tn affinity associated with changes in either force or length [73]. The length-dependence of Ca^{2+}-Tn affinity appears only in cardiac muscle since in skeletal muscle fibers, Fuchs et al. failed to demonstrate a length or force dependency of Ca^{2+} binding to TnC [74]. In slow skeletal muscle fibers, Ca^{2+} binding to Tn is also independent of SL. Quick release of cardiac muscle results in the "extra" Ca^{2+} seen in cytosol [63], however, this phenomenon is not observed in fast skeletal muscle [75].

In summary, although the length-dependent myofibrillar Ca^{2+} sensitivity is now an established phenomenon, its mechanism remains unclear. The above studies indicate that there is no unique function relating the change in force with a change in average SL. Both physical and activation factors play some role in the cardiac ECC. First, a change of Ca^{2+} affinity to Tn is indeed involved. The effect of SL on force acts through different levels of myofilament Ca^{2+} sensitivity at different SL. It can be concluded that changes in

Ca^{2+} sensitivity as a function of length is one of the major mechanisms underlying the cardiac length-tension relation. Second, at long SL above 2.2 μm where the increase of SL will decrease the number of attached cross-bridge, but still increases Ca^{2+}sensitivity of myofilaments, length-tension relation is mainly determined by SL itself. The increased SL can shrink the lattice space and facilitate the attachment between thick and thin filaments to generate force. Finally, the length-tension relations of striated muscle are altered with different levels of [Ca^{2+}]. Different curvature of the curves of the length-tension relationship indicates different activation levels of thin filaments. Enhanced tension development increases Ca^{2+} affinity for Tn and generates a positive feedback on the thin filament to produce more force.

2.4 Starling's Law in Congestive heart failure (CHF)

Most studies have indicated unaltered myofibrillar Ca^{2+} responsiveness and F_{max} development in either human CHF [76] or animal CHF and ventricular hypertrophy (VH)[77]. Vahl et al. have found a preserved Frank-Starling mechanism in end stage human CHF [78]. This group of investigators showed that an increase of SL leads to a sensitization of contractile proteins of skinned ventricular fiber preparations from failing human hearts. Vahl et al. suggested that the Frank-Starling mechanism was operative in failing human myocardium and there was a clear length dependence of active force in CHF myocardium[79]. Vahl et al. also demonstrated that the length-dependent changes in force were associated with length-dependent modulations of the intracellular Ca^{2+} transient in human myocardium. Diastolic and systolic Ca^{2+} increase significantly with the increase of muscle length. With decreasing muscle lengths, the intracellular Ca^{2+} transient became broader, and the diastolic decay was retarded and the peak of the intracellular Ca^{2+}

transient was flatter. The Frank-Starling mechanism has been also observed by Holubarsch's group in end-stage failing human hearts. In the study, the investigators showed that the myofilament Ca^{2+} sensitivity increases with increase of muscle length [80]. In their studies, this group of researchers demonstrated that both force development and myofilament Ca^{2+} sensitivity increased with the increased SL. In the studies from skinned rat trabeculae, the recent data from our laboratory have shown that the dependence of force on Ca^{2+} and stretch is not changed by CHF following a large MI. Further, force-SL and force-pCa relations in muscles from sham and CHF groups are similar. These studies demonstrated the similar level of maximal force and EC_{50} [56].

Schwinger et al. claimed that the myofilament response to stretch was altered in CHF [81]. In their study, these investigators used papillary muscles. Because of the thickness of papillary muscles, SL measurement would not have been ideal in their study. SL measurement is a crucial point in the study of length-dependent force development. The force-SL relationship can be misleading in experiments without good SL control. Kentish et al. have shown a marked SL dependence of maximum force development, Ca^{2+} responsiveness, and steepness of the developed force-pCa relation in skinned rat cardiac trabeculae [55]. When SL is not measured accurately, ambiguous data may be obtained. This reason can cause the result of Schwinger et al. to be incorrect.

2.5 Cross-bridges in the force development

2.5.1 Structure for the cross-bridge

The first and most crucial observation of cross-bridge links between actin and myosin filaments came from the early electron-microscope studies by H. E. Huxley in 1950's [82]. Huxley showed that the cross-bridges existed in the space where actin

filaments overlapped with myosin filaments as well as on the myosin filaments in the place where no actin filaments lay alongside them. He proposed that the cross-bridges were the only visible mechanical agents by which force could be developed between the thin and thick filaments and they were permanent parts of the heavy-meromyosin subunits. During force development, cross-bridges physically attached with actin filaments and pulled actin to move, then detached from the thin filaments [83]. The cyclical attachment and detachment of cross-bridges caused actin to slide along the thick filament.

H. E. Huxley demonstrated that at a given level of SL, two bridges project out directly opposite each other on either side of the backbone of the thick filament. The next two bridges are rotated relative to the first pair by 120° degree with a distance 143 angstroms (Å). The structure as a whole repeats at 3 intervals in a distance of 429 Å [84] (Figure 2-1). H.E. Huxley proposed that heavy meromyosin acted like a lever and myosin globular head could rotate and attach with actin and pull it to move along with the thick filaments [83]. Later, A.F. Huxley developed this theory and suggested that the "rod" (S2 subfragment) was extensible, which allowed cross-bridges of thick filaments to attach with thin filaments during muscle contraction when the space distance between the thick and thin filaments continuously changed [85]. This hypothesis is further supported by the studies of Spudich et al. [86]. In their swinging neck-lever model, these researchers used mutant myosin with different neck length and proposed that a swinging motion of the neck relative to the catalytic domain was the origin of movement. The force generated was directly related to the length of the myosin neck.

Figure 2-1: Schematic drawing of cross-bridges on the thick filament: two cross-bridges project directly opposite each other in either side of the backbone of the thick filament. The next two bridges are rotated relative to the first pair by 120° degree with a distance 143 Å. The structure as a whole repeats at 3 intervals in a distance of 429 Å (From H.E. Huxley, Journal of Molecular Biology, 1967, (30)).

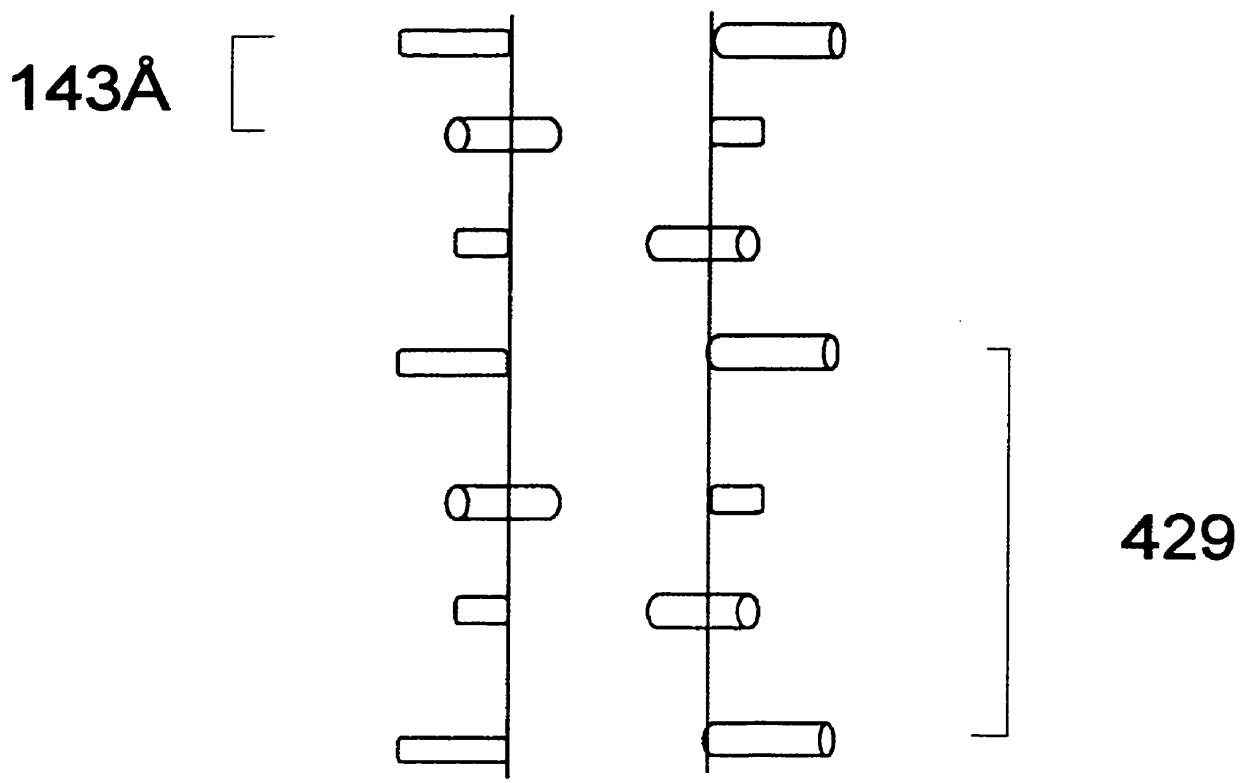
143Å
429

2.5.2 Change of lattice spacing by osmotic compression or stretch of muscle

The interaction between actin and myosin is crucial in the cross-bridge cycle. One of the most important factors affecting the attachment and detachment of actin and myosin is the spatial distance between actin and myosin, which is termed "lattice spacing".

The average center-to-center distance between the myosin and actin filament spacing of relaxed fibers is 28.7 nm [87]. The diameters of actin and myosin are 8 nm and 13 nm, respectively [88]. At optimal state, the center-to-center spacing between myosin and actin filament is 18.7 nm, corresponding to an 8.2 nm interfilament space for the myosin heads [88], which is half of the long axis of myosin S1 16.5 nm [89]. Thus, for the myosin heads, a critical interfilament space of about 8.2 nm could mark the optimal distance necessary for full force generation (Figure 2-2).

The lattice spacing changes with the change of SL. Cecchi et al. demonstrated that ramp releases of isolated muscle fibers decreased the fiber length at constant speed, which resulted in a decreased force with a lattice expansion. After the ramp releases, tension development increased with the lattice compression. On the other hand, ramp stretches caused a compression of the lattice spacing. After the stretch, tension decreased and lattice spacing increased [90]. This finding indicates that there is a radial component of the force generated by cycling cross-bridges.

Skinned muscles are swollen and studies have demonstrated that the lattice spacing could be reduced by treatment with Dextran-containing solutions or by increasing SL.

Addition of polymers in the skinning solution restores physiological lattice spacing. Godt et al. found that Dextran of diameter T-40 and above did not penetrate the lattice [91]. Thus, it is reasonable to assume that addition of the proper amount of Dextran T500 only restores the physiological lattice space without disturbing the interaction between the thick and thin filaments. Ford et al. suggested from their studies that a physiological range of filament spacing might have been achieved at [Dextran T70] of 58 g/liter. The further observation that relative maximum power remained constant up to 76 g/liter of Dextran T70 suggests that the physiological range of lattice spacing might have been achieved over the range of 58-76 g/liter Dextran T70 [92]. The actual amount of a polymer that restores the physiological lattice spacing depends on its molecular weight. Godt et al. demonstrated that 5% Dextran T500 compressed Triton skinned fibers to a width close to that of intact fibers [93].

The reduction of lattice spacing by increase of SL is equivalent to the effect of osmotic compression. Moss et al. found that increasing SL from ~1.85 μm to ~2.25 μm as well as treatment with 2.5% Dextran significantly reduced myocyte width to a similar level. Mean myocyte width decreased by 10.3% when SL was increased by ~0.4 μm and or treated by 6.5% Dextran at short SL [94]. The lattice spacing changes with the muscle shortening and lengthening to keep the lattice spacing volume constant.

2.5.3 Effects of lattice spacing on Ca^{2+} sensitivity from skinned studies

It is known that there is an optimal filament separation for force development. Godt et al. found that addition of 5% Dextran in skinned cardiac fibers maintains force development close to the force development in intact muscle, whereas addition of 10% Dextran decreased force development [93]. Lamont and Miller found that addition of 3%

Figure 2-2: Schematic drawing for lattice spacing in force development. The average center-to-center distance between the myosin and actin filament spacing of relaxed fibers is 28.7 nm. The diameter of actin and myosin are 8 nm and 13 nm, respectively. At the optimal state, the center-to-center spacing between myosin and actin filament is 18.7 nm, which corresponds to an optimal lattice spacing 8.2 nm. This is half the long axis of myosin S_1, which is 16.5 nm.

1: actin, 2: Z-line, 3: myosin, 4: cross-bridges, 5: lattice spacing.

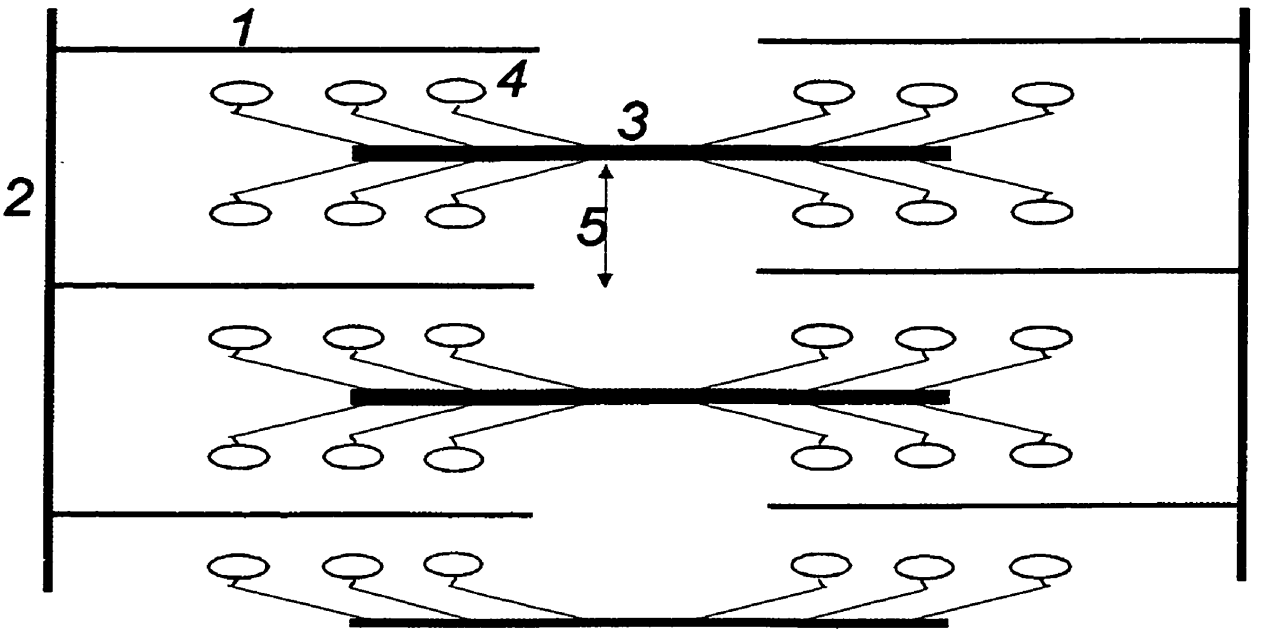
1
2
3
4
5

DextranT-500 in fully activated cardiac skinned muscle increased force development by 15% [95]. With [Dextran T-500] greater than 10%, the active force development decreased[87]. Active force development declines when the lattice separation is either greater or smaller that the optimum.

The lattice spacing change directly affects myofilament Ca^{2+} sensitivity. At short lengths, there is an increase of lateral separation of thick and thin filaments [96], which decreases the cross-bridge interaction in the zone of overlap between thick and thin filaments. Moss et al. found that in single myocyte, treatment with 2.5% Dextran at short SL shifted the tension-pCa relation to a lower EC_{50} and very near to the mean EC_{50} obtained at long SL [94]. This finding is confirmed by the studies from isolated striated muscles that the reduced lattice spacing increases Ca^{2+} sensitivity of tension at optimum SL [93; 97].

Some investigators proposed that the low myofilament Ca^{2+} sensitivity of skinned fibers was attributed to the failure of maintaining constant lattice spacing volume. In intact muscle, an increase of SL from 1.70 μm to 2.30 μm reduces the width of isolated cardiac fibers by 13%, an amount equivalent to that produced by exposure of skinned fibers to 5% Dextran T-500 [98]. In intact skeletal [99] and cardiac muscle [100], the filament lattice maintains a constant-volume with change of SL, however, a skinned fiber not only swells but also loses constant volume behavior. Reedy suggested that there was very little change of lattice space with the change of SL in skinned muscle [101]. The observation from the study of our laboratory showed that the width of saponin skinned trabeculae increased by ~50% when shortened. The increased lattice spacing in skinned muscles increases the distance between actin and myosin. As a result, in skinned muscle fibers,

both skeletal and cardiac muscle, it is quite possible that the altered lattice spacing contributes to the decreased myofilament Ca^{2+} sensitivity.

Lattice spacing and cross-bridge kinetics

Osmotic compression increases myofilament Ca^{2+} sensitivity, which is due to the enhanced cross-bridge formation caused by reduced lattice spacing. Maughan et al. showed that force development increased in fully activated muscles with the increase of cross-bridge attachments due to closer proximity of myosin S1 heads to the thin filament with a decrease of lattice spacing [102]. The greater relative force in Dextran-treated fibers at submaximal [Ca^{2+}] is probably caused by enhanced co-operative activation of the thin filaments resulting from increased cross-bridge attachments [103].

Osmotic compression has a profound effect on cross-bridge dynamics in cardiac ECC. Increase of lattice spacing enhances the muscle shortening velocity. Based on Huxley's cross-bridge theory of contraction, shortening velocity in partial activation of thin filament is determined by the balance between positively and negatively strained cross-bridges [82]. Goldman et al. suggested that the increased lattice spacing by skinning resulted in cross-bridges unable to resist shortening, probably due to an unfavorable angle between bridge and filaments, which reduces the negative strain [104]. Moss et al. demonstrated that V_{max} was substantially decreased with the addition of 5% Dextran [105], which indicated that cross-bridges in the expanded filament lattice of skinned fibers did not bear as great an axial compressive force as in intact fibers. Skinning causes an increase of lattice spacing, resulting in buckling of the myosin subfragment S2 associated with a cross-bridge. Dextran radially compresses fibers and increases the ability of

myosin S2 to bear an axially compressive load to decrease velocity [105]. Cross-bridges are better able to bear an axial compressive force as the filament lattice spacing is reduced.

The lattice spacing affects the position of myosin head for force generation. Adhikari and Fajer et al. reported that both the myosin head orientations and dynamics showed a biphasic change as a function of radial compression with varying [Dextran T-500]. The two phases were separated by a critical lattice spacing. Compression up to the critical spacing resulted in small but significant changes in mobility and orientation without a loss of tension, whereas dramatic changes of lattice spacing at higher compression caused a sharp decline in tension [88]. By using electron paramagnetic resonance (EPR), Fajer et al. successfully showed increased attachment of cross-bridges with a 3 fold decrease of mobility if the muscle was highly compressed with 20% Dextran T-500 without affecting cross-bridge stiffness and tension development. The force generation involved transform from a random state to regular state by the rotation of the strongly attached heads, leading the cycle to its end, where the heads are strongly attached, rigid, and oriented [106]. The results suggest that a minimum mobility, which is determined by a critical lattice spacing, is necessary for force generation.

Length dependence of osmotic compression effects

The effect of lattice spacing on myofilament Ca^{2+} sensitivity is SL dependent. First, at different SL, osmotic compression increases myofilament Ca^{2+} sensitivity to a different level. Harrison et al. demonstrated that 5% Dextran T-500 caused an increase in Ca^{2+} sensitivity of 0.15 pCa units at SL 2.0 μm and 0.08 pCa units at SL 2.20 μm in skinned cardiac fibers [97]. In skinned skeletal muscle, the effect of osmotic compression on myofilament Ca^{2+} sensitivity disappeared at SL 2.70 μm to 2.80 μm [107]. Wang et al.

demonstrated in their studies that at SL 1.70 μm, 5% Dextran T-500 exposure increased myofilament Ca^{2+} sensitivity of about pCa_{50} 0.25 unit; whereas at SL 2.30 μm, the same [Dextran] caused only a slight shift of pCa_{50} (<0.1 pCa units) [98]. Thus, at longer SL, the effects of lattice spacing on Ca^{2+} sensitivity may be masked by the augmented Tn binding affinity to Ca^{2+}.

On the other hand, the effects of reduced lattice spacing by osmotic compression on myofilament Ca^{2+} sensitivity is similar to that induced by increase of SL. Moss et al. showed that at SL ~1.85 μm, 2.5% Dextran increased pCa_{50} from 5.54 to 5.65. Increase of SL from 1.85 μm to ~2.25 μm also enhanced myofilament Ca^{2+} sensitivity to a similar degree, and pCa_{50} increased from 5.54 to 5.68 [94]. The authors found that osmotic compression of myocytes at short SL resulted in shrinkage to 93% of the width before compression, which was similar to that induced by an increase of SL to ~2.25 μm with a decreased width to 90% of the pre-stretched value. The shift in Ca^{2+} sensitivity was similar under both conditions [94]. These results support the idea that the length dependence of Ca^{2+} sensitivity of myofilament in cardiac muscle is due to the changes in interfilament lattice spacing that changes with the increased SL.

Chapter 3

Abnormalities of ECC in Congestive Heart Failure

3.1 Introduction

Congestive heart failure (CHF) and ischemic heart disease are the important causes of death in the world. Although much effort has been put into the study of the mechanisms of CHF, the exact causes of CHF are still unknown. Recently, based on molecular studies of CHF, some investigators have proposed quite a few potential mechanisms involved in the heart failure. First, it is suggested that the failing heart is accompanied by a change in ventricular shape and dimension, a process called cardiac remodeling [108]. The second possible mechanism is called apoptosis [109], which is characterized by the loss of myocytes. The third one is extracellular matrix hyperplasia[110;111]. The increased amount of collagen among myocytes makes the heart stiffer. Thus, alterations in the extracellular matrix may have a potentially large impact on ventricular function. This non-myocyte remodeling process may play a significant role in the decline of cardiac pump function in CHF. The last, but the most important mechanism is decreased myocyte function [112]. Studies from both experimental animal models and human tissues have demonstrated depressed contractile function in CHF. Now, more and more research has been focused on the dysfunction of myocytes in CHF.

The mechanism of the decreased contractile function in CHF myocytes is uncertain at present. The most likely abnormalities involve alterations in Ca^{2+} handling, myofilament function, and the cytoskeleton.

3.2 Ca^{2+} handling in CHF

From recent studies in CHF, it has been suggested that altered myocyte Ca^{2+} handling plays an important role in the development of CHF. It has been found that CHF exhibits abnormalities in ECC, either in the form of depressed contractile function or impaired relaxation. The former is called inotropic failure and it may be caused by a decrease in cardiac myofilament Ca^{2+} sensitivity and in SR Ca^{2+} release. The latter is called lusitropic failure, and it is mainly caused by dysfunction of the SR Ca^{2+} pump, which results in inadequate removal of Ca^{2+} from the myofibrillar space [47]. These abnormalities have been viewed as a compensatory mechanism for myocytes to preserve energy consumption and allow better maintenance of basal cellular homeostasis by down regulating its function and metabolic activity. The end point of myocyte dysfunction is reduced contraction and impaired relaxation, which, in turn, might cause a reduced cardiac output and subsequent heart failure.

3.2.1 Ca^{2+} influx (I_{Ca}) through sarcolemma L-type Ca^{2+} channels

In general, the influx of Ca^{2+} through the L-type Ca^{2+} channels is a trigger in ECC of cardiac muscle. The alteration of Ca^{2+} influx might be the result from the prolongation of APD or change of the number of DHPRs in the sarcolemma.

CHF is usually accompanied by an increase of APD [113]. This is probably explained by a reduction of inwardly rectified K^+ current I_{k1} and transient outward K^+ current I_{to} [113; 114], where the latter is heart rate dependent. The prolongation of APD results in an increase in Ca^{2+} influx through L-type Ca^{2+} channels and therefore increases the SR Ca^{2+} load.

A potential role for mechanosensitive Ca^{2+} channels also has to be considered. Vahl et al. suggested that the extraordinary afterload dependence of the Ca^{2+} transient in end-stage heart failure might be attributed to an increased Ca^{2+} inflow due to altered permeability of Ca^{2+} channels during shortening and the reduction in afterload increased shortening in isolated working human myocardium was associated with extraordinary alterations in the shape, amplitude and time to peak of the Ca^{2+} transients [78].

On the other hand, studies of gene expression of L-type Ca^{2+} channels have shown conflicting results. Some investigators reported that the alteration of gene expression is related to the abnormalities of Ca^{2+} inflow through the sarcolemma in CHF. Takahashi et al. studied the expression of genes encoding the cardiac DHPR in human heart failure and the abundance of DHP binding sites was assessed by ligand binding techniques [115]. In their study, the level of mRNA encoding the DHP receptor was decreased by 47% in the LV myocardium from CHF compared to the normal controls. The number of DHP binding sites was also decreased by 35-48%. These researchers concluded that the altered expression of these genes might be related to the decreased Ca^{2+} inflow in the failing myocardium. In contrast, Rasmussen et al. reported that DHP Ca^{2+} antagonist binding sites were not reduced significantly in the failing heart [116], indicating that the number of DHP receptors were not reduced in CHF. Thus whether the function of L-type Ca^{2+} channels is altered in the failing heart is still questionable.

3.2.2 Alterations of Ca^{2+} transient and SR Ca^{2+} release channels (RyRs)

Some investigators have claimed that there is a reduction in the amplitude of the Ca^{2+} transient in failing hearts. It could arise from any of the following steps involved in ECC: (i) a reduction of I_{Ca} (which supplies the trigger for RyR activation); (ii) a reduced

sensitivity of the RyR to the triggering Ca^{2+} influx; (iii) a change in the number of RyRs; (iv) altered properties of the elementary SR Ca^{2+}-release events or Ca^{2+} sparks (because summation of these events leads to the cell-wide Ca^{2+} transient); and (v) a decrease of the amount of releasable SR Ca^{2+} [117; 118].

Alterations of the SR Ca^{2+} release channel may contribute to a change in the Ca^{2+} transient. One abnormality of Ca^{2+} handling in the SR of failing hearts is due to the altered expression of the genes encoding Ca^{2+} release channel-ryanodine receptor, RyR_2. RyR down-regulation could contribute to the alteration of Ca^{2+} transient. The RyR mRNA level has been found to be decreased by 31% in the failing human heart [119], which could result in the decreased density of RyR. However, western blot analysis in non-failing and failing hearts has shown that protein levels of RyR and calsequestrin are similar in control and CHF myocardium [120]. On the other hand, Nimer et al. have demonstrated that increased efflux of Ca^{2+} current from the SR may contribute to the abnormal Ca^{2+} homeostasis described in failing human myocardium without a change in receptor density [121]. These investigators have proposed that the differences of RyRs in response to ryanodine between failing and non-failing human myocardium are due to an altered gating mechanism in human CHF.

In contrast, other investigators showed that the properties of RyRs and DHPRs are unaltered in animal CHF models caused by hypertension. The reduction in the ability of the DHPR to activate Ca^{2+} release may be simply because the probability of RyR activation is very sensitive to the geometric rearrangement of RyRs and DHPRs in the dyads [122]. The local increase in $[Ca^{2+}]_i$ by the RyR Ca^{2+} release depends on the average distance of the DHPR to the RyR. Therefore, if the mean distance between the RyR and

the DHPR is increased, the RyR will be less effectively activated by the local Ca^{2+} influx produced by a DHPR opening. The slowing of I_{Ca} inactivation in hypertrophied cells would be consistent with the idea that the physical location of DHPRs with respect to their neighboring RyRs may be altered in hypertrophied cells. The ability of I_{Ca} to trigger Ca^{2+} release from the SR in failing hearts is reduced. Because I_{Ca} density and SR Ca^{2+}-release channels are normal, the defect appears to reside in a change in the interaction between the SR Ca^{2+}-release channels and the sarcolemmal Ca^{2+} channels.

Recent data from our lab have indicated that there are other abnormalities of RyRs in CHF. In experiments with intact trabeculae, the CHF trabeculae exhibit substantial spontaneous activity, whereas control and sham trabeculae are very quiet. In the CHF trabeculae, the opening probability of RyRs is apparently increased; as a consequence, RyRs simultaneous release Ca^{2+} from the SR lumen even at rest. A possible mechanism underlying the increased opening probability of RyRs is that the oxidative stress and the products of nitrosyl groups augment the opening probability of RyRs in CHF. Both the oxygen free radical scavenger MPG and angiotensin II receptor Losartan are approved to significantly inhibit the spontaneous activity in failing heart trabeculae in animal studies.

3.2.3 The SR Ca^{2+} pump

The reduced capacity of failing human myocardium to restore low resting Ca^{2+} levels during diastole has been explained by the impairment of Ca^{2+} uptake into the SR via the SR Ca^{2+} pump.

Flesch et al. found that the activity of the SR Ca^{2+}ATPase was significantly reduced in failing myocardium [123]. The investigators observed that mRNA levels for the

SR Ca^{2+} ATPase and PLN were significantly lower comparing to nonfailing myocardium. However, there were no significant changes observed at the level of proteins. Since the alterations of mRNA did not cause changes of SR Ca^{2+}-ATPase and PLN protein levels, these investigators proposed that the above mRNA alterations were not the underlying cause of the end-stage heart failure [123].

On the other hand, Schillinger et al. proposed that altered systolic and diastolic function in failing human hearts might result from altered expression of Ca^{2+} cycling proteins [124], and the crucial one was the SR Ca^{2+}-ATPase. In their experiment, the decreased systolic force production and inversion of the force-frequency relation seem to be related to reduced protein levels of the SR Ca^{2+}-ATPase and/or to the increased protein levels of the Na^{+}/Ca^{2+} exchanger resulting in an increased ratio of Na^{+}/Ca^{2+} exchanger to the SR Ca^{2+}-ATPase. Impaired diastolic function might result from reduced SR Ca^{2+}-ATPase and was most pronounced in failing hearts with lack of upregulation of Na^{+}/Ca^{2+} exchanger. Thus, failing hearts with reduced SR Ca^{2+}-ATPase protein level and unchanged Na^{+}/Ca^{2+} exchanger protein level exhibit severe impairment of both systolic and diastolic function. Some other evidence also has suggested that the under-expression of mRNA Ca^{2+}ATPase and PLN is related to the depressed function of the SR Ca^{2+} pump. In the animal models of pressure overload-induced cardiac failure, the rate of SR Ca^{2+}-uptake and the affinity of SR Ca^{2+}ATPase for Ca^{2+} are significantly decreased, which is associated with depressed protein expression of the SR Ca^{2+}-ATPase and PLN[125].

One should remain aware that although mRNA levels have been consistently reported to be down regulated in human and animal CHF, measurements of the protein

levels of SR Ca^{2+}-ATPase and PLN have been inconsistent in human CHF. The enhanced diastolic Ca^{2+} levels observed in cardiac myocytes from CHF may be either a consequence of functional impairment of SR Ca^{2+}-ATPase (SERCA 2) and its regulator protein PLN or due to a reduction in the number of SERCA 2 proteins. Schwingger et al. suggested that the altered Ca^{2+} handling in dilated cardiomyopathy (DCM) might be a consequence of reduced SERCA 2 enzyme activity, but not the result of differences in protein expression of the Ca^{2+} regulating proteins SERCA 2, PLN, and calsequestrin in human myocardium [126].

The SR-Ca^{2+} pump function is impaired in CHF. Bridge et al. found the maximal uptake rate of Ca^{2+} by the SR-Ca^{2+} pump is not reduced in CHF rats 5 months after MI. The results suggest that the slower rate of relaxation of cardiac muscle in CHF rats may be explained by a lower SR-Ca^{2+} pump rate in the intact myocytes as a result of a lower Ca^{2+} sensitivity of the SR-Ca^{2+} pump [127]. This result is also confirmed by experiments in our laboratory. The maximal SR Ca^{2+} uptake rate are the same in both sham and CHF rat hearts, but EC_{50} is higher in the failing group than in the sham controlled group. The depressed SR Ca^{2+} pump causes prolonged relaxation and decreased SR Ca^{2+} load, resulting in the depressed myocyte contractile function [56].

3.2.4 The Na^+/Ca^{2+} exchanger

It has been proposed that the function of Na^+/Ca^{2+} exchangers be enhanced because of the depressed activity of the SR Ca^{2+} pump in CHF.

Flesch et al. investigated the expression of the Na^+/Ca^{2+} exchanger and its functional role in human failing myocardium [123]. The Na^+/Ca^{2+} exchanger mRNA and protein levels were significantly increased in failing myocardium due to dysfunction of

the SR Ca^{2+} pump. The increased expression of Na^{+}/Ca^{2+} exchanger was a possible explanation for the increased Na^{+} channel activity in failing human myocardium. The increase in the exchanger molecules could be of functional relevance for the modulation of cardiac contractility and might be a powerful mechanism for increasing cardiac contractility in CHF.

Lehnart et al. found that the levels of the proteins involved in Ca^{2+} removal were significantly altered in the failing human heart: (1) SR Ca^{2+}-ATPase levels and the ratio of SR Ca^{2+}-ATPase to its inhibitory protein PLN were significantly decreased, and (2) Na^{+}/Ca^{2+} exchanger levels and the ratio of Na^{+}/Ca^{2+} exchanger to SR Ca^{2+}-ATPase were significantly increased [128]. SR Ca^{2+}-ATPase levels were closely correlated to systolic function as evaluated by frequency potentiation of contractile force. The frequency-dependent rise of diastolic force was inversely correlated with protein levels of the Na^{+}/Ca^{2+} exchanger. These findings indicate that altered expression of SR Ca^{2+}-ATPase and Na^{+}/Ca^{2+} exchanger is relevant for altered systolic and diastolic function in human heart failure.

3.3 Myofilament function in CHF

In advanced heart failure, several molecular abnormalities, which affect in particular contractile protein function and ECC, have been identified. The contractile dysfunction that is seen in CHF and VH may cause a decrease in the force that is generated by the contractile proteins for any given level of $[Ca^{2+}]_i$.

3.3.1 Shift of myosin isoforms in CHF Hearts

Heart failure is associated with changes in the distribution and content of myocardial contractile proteins both in human failing heart models and animal failing

models [129; 130]. In failing hearts, the myofibrillar ATPase activity decreases [131]. This abnormality is associated with a marked shift in the myosin isoform expression from the V1 to V3 [129; 132]. The V3 isoform is a "slow" myosin isoform and has a lower ATPase activity [133]. The expression of myosin isoform V3 is correlated with a reduction in the maximum velocity of sarcomere shortening. However, in human and other large mammals, the shift from myosin isoform V1 to V3 in diseased myocardium is not seen, and the possible reason is that the main form of cardiac myosin is V3 in these species [129].

3.3.2 MLC alteration

Changes in myosin light chain (MLC) in heart failure may affect contractile activation. MLC2 demonstrated the importance in modulating contraction and cross-bridge interaction. Morano et al. has recently shown that the change of the interaction between the MLC and actin can have a profound effect on force development and Ca^{2+} responsiveness [134]. Moss et al. have shown that in skinned myocardium, MLC2 extraction resulted in decreased velocity of shortening and decreased Ca^{2+} responsiveness[135]. The changes in myosin structure and function link to a protease-mediated cleavage of the reduced regulatory light chain (MLC2) in myosin [136]. The protease exhibited a significant degree of specificity: it was present at a very low level or was inactive in the control heart tissue. The length of the control myosin synthetic thick filament and turbidity were twice as large as those of myopathic heart myosin. These effects induced by myopathy could be reversed upon reassociation of diseased myosin with normal MLC2 [136].

The alteration of MLC in CHF is controversial. Margossian et al. reported a marked decrease in the MLC content in dilated cardiomyopathy [136], apparently due to

increased levels of neutral protease in the CHF hearts, while Sutsch et al. have demonstrated an increase in the atrial form of MLC1in CHF caused by valve diseases [137]. The difference is probably caused by different disease process and the cause of disease.

3.3.3 Abnormalities of Tn in CHF

Tn subunits are important in modulating Ca^{2+} sensitivity of the contractile filaments.

The expression of cardiac TnT (cTnT) isoform, a protein essential for Ca^{2+}-regulated myofibrillar ATPase activity, has been found to differ in the normal and failing adult and fetal human heart at the protein level. Different isoform expression is associated with changes in the Ca^{2+} responsiveness of the myofilaments during force development. cTnT3 is the dominant isoform in the adult heart whereas cTnT4 is expressed in the fetal heart and reexpressed in the failing adult heart [130]. The Ca^{2+} activation and Ca^{2+} binding properties of myofibrillar TnC are altered in developing cardiac myofibrils. The changes in these properties may be influenced by changes in the TnT isoforms present in the myofibril.

TnI is the inhibitory component of Tn, the thin filament regulatory complex in striated muscle. Hunkeler et al. characterized the expression of the different cardiac TnI isoforms in the human heart [138]. The expression of mRNA and protein of TnI isoforms have been found in normal infant hearts, as well as infant and adult hearts with congenital heart disease. However, there is no detectable TnI mRNA expression in the normal adult heart.

Surprisingly, recent data from our lab have indicated that there is no significant change of myofibrilar contractile function in CHF. In Triton skinned trabeculae, the

force-SL relationship and the F_{max} development are similar in both the CHF rats and the control rats. EC_{50}s of F_{max} development are at the same level in the two groups [56]. The result indicates that the depressed myocyte function is caused by the dysfunction of the elements other than the contractile machinery-myofilaments or protease effects.

3.4 Alteration of cytoskeleton in CHF

The cytoskeleton is a supporting structure within a cell. Similar to other type of cells, the cytoskeleton of cardiac myocytes serves to control the cell shape and size, and stabilize the arrangement of other intracellular organelles. There are three kinds of cytoskeleton fibers: microtubules, microfilaments, and intermediate filaments. The microtubules are composed of tubulin, and the microfilaments are composed of actin. Intermediate filaments consist of a set of different subclasses of intermediate proteins [139]. These proteins attach the myofibrils to the sarcolemma.

The changes of cytoskeleton in CHF have been reported in many aspects. Recently, Schaper et al. have demonstrated in human CHF a disproportionate increase in the relative abundance of cytoskeletal proteins [140]. Tsutsui et al. have reported that the microtubule component of cardiac myocytes increases in the case of pressure overload hearts with a depression of contractile function [141]. Some researchers have proposed that there is a reduction in the myofilament protein titin. This change of the amount of titin could result in the increase of the stiffness and the decrease of the compliance of myocardium [142].

Controversial data regarding the role of cytoskeleton change in CHF have been published as well. Several laboratories have failed to show a correlation between the change of cytoskeleton and the contraction dynamics [143]. Therefore, whether changes in

the cytoskeleton composition impact on ventricular function in CHF remains unclear at present.

3.5 Summary

First, it has been shown rather conclusively that Ca^{2+} handling is altered in end-stage CHF and VH. This change of Ca^{2+} handling is particularly manifested by the depressed function of the SR Ca^{2+} pump and the enhanced activity of the Na^{+}/Ca^{2+} exchanger. The Ca^{2+} handling may be affected without any change in the individual components involved in the cardiac ECC. It appears that the coupling between the sarcolemmal Ca^{2+} channels and the SR Ca^{2+} release channels is abnormal, which plays a role in CHF animal models. This hypothesis needs to be further tested in human CHF.

Second, it is less clear whether the contractile protein function is altered in heart failure. TnT could be notably altered in CHF. Whether the change will affect the contractile protein function in CHF is still not known yet. On the other hand, the cytoskeleton is significantly changed in CHF, but the functional consequence of this alteration is unclear.

Last, the mechanism of CHF is a complicated process, therefore, whether any of these mechanisms plays a causal role in the development of heart failure is not known at present. Most of the experimental models of CHF suggest that altered Ca^{2+} handling may be the underlying cause of the decreased myocyte function that is seen at end-stage CHF. Clearly, it is necessary to study further Ca^{2+} handling and myofilament function in detail in CHF in order to resolve this important issue.

Chapter 4

Objectives and Experimental Methods

4.1 Objectives of the study

Based on the previous introduction, Ca^{2+} ions are important in the carciac ECC, especially the free Ca^{2+} ions directly determine the activation level of myofilaments and the force development.

During cardiac cycle, the movement of Ca^{2+} ions between different Ca^{2+} compartments: the extra- and intra-cellular space, the SR, and Tn causes the heart rhythmic contraction and relaxation. The supply of Ca^{2+} can be either the Ca^{2+} influx through the sarcolemma L-type Ca^{2+} channels from the extracellular space or the Ca^{2+} release from the SR cavity. The total amount of Ca^{2+} in myocytes must be kept balanced, otherwise the SR can overload or deplete its Ca^{2+} content, which can cause lusitropic or inotropic failure in the heart.

The myocyte Ca^{2+} buffering system affects the cardiac function through its effects on the free Ca^{2+} level in the cytosol. The cytosolic free Ca^{2+} ions are directly associated with the cardiac power output by binding to TnC. The binding of Ca^{2+} on TnC removes the inhibition of TnI on actin, then actin can interact with myosin to form cross-bridges to generate force. The amount of Ca^{2+} available for the activation of TnC is affected by the myocyte Ca^{2+} buffering system and the SR Ca^{2+} pump. The free Ca^{2+} is only a small fraction of the total Ca^{2+}, ranging from 0.02% to 1% in resting myocytes as reported by different investigators. Because of the high Ca^{2+} buffering capacity of myocytes and the inconsistency of the buffering capacity reported, the total Ca^{2+} in myocyte can not be

determined. It is necessary to quantitatively further study the myocyte Ca^{2+} buffering system and clarify the myocyte Ca^{2+} buffering capacity.

At the same level of the free Ca^{2+}, the work which the heart can be done is affected by other facts, such as the length. Like Frank-Starling's law tells us that an increase of muscle length results in an augment of force output. This phenomenon can be explained that an increase of SL increases the myofilament Ca^{2+} sensitivity in the cellular level. This responsiveness of myofilament to the change of SL is determined by the derivatives of SL, i.e. the lattice spacing and the number of cross-bridges, not the length itself, as I describe in detail in Chapter 2.

Skinning is a valuable technique in the study of the force-length relationship, which allows investigators to study the pure function of myofilaments without the effects of the sarcolemma and the SR. However, skinning permeabalizes the cellular membrane, which may cause loss of Ca^{2+} sensitizers in the cytosol and increase of the lattice spacing. Both of the two factors can result in a decreased myofilament Ca^{2+} sensitivity in skinned preparation. Besides, the previous skinned studies have been done with high $[Mg^{2+}]$, ranging from ~1-5 mM, which is far off the physiological level, 0.7 mM as reported by Gao et al. The high $[Mg^{2+}]$ can affect the electrical signal propagation, which results in the reduction Ca^{2+} supply, and also affect myofilament contractile function, which causes inhibition of myofilament activation in the cardiac ECC, as a consequence, lower the force development.

The purpose of this study is to quantitatively determine the availability of the Ca^{2+} for the activation of myofilaments. By using Fura-2, the free $[Ca^{2+}]$ was detected by ratioing measurement of fluorescence intensities 340 nm over 380 nm, and the total

$[Ca^{2+}]$ was controlled in the skinned myocytes. Both the Ca^{2+} buffering capacity of the bulk myocyte suspension and pure myocytes were determined under my experimental protocol.

The length-tension relationship is the high point of the study of the Frank-Starling's law. In this study, I restored the physiological lattice spacing in the triton X-100 skinned cardiac trabeculae and kept $[Mg^{2+}]$ at ~0.7 mM. I studied force-SL relationships under the corrected $[Mg^{2+}]$ and osmolality in skinned trabeculae. From the study, I inferred the extent of the effect of the increased lattice spacing in hypertrophied or failing hearts on the cardiac function.

4.2 Free $[Ca^{2+}]$ measurement with fluorescence dye fura-2

4.2.1 Introduction for measuring Ca^{2+} buffering capacity in Saponin skinned myocytes

The skinning technique allows investigators to control the experimental conditions while mimicking in vivo physiological conditions. In this study, I used isolated rat myocytes skinned by saponin from both ventricles. The total $[Ca^{2+}]$ in the experimental bath was controlled. Fura-2 was used as a Ca^{2+} indicator to measure the free $[Ca^{2+}]$ in the bath. Free $[Ca^{2+}]$ was measured by calculating the ratio of fluorescence intensity 340 nm over 380 nm. In order to increase the amplitude of the fluorescence signal, a small bath, with a volume of 500 μl, was introduced in the study. There was a propeller in the bath, which mixed the fluid in the bath continuously. Myocytes were added into the bath and fluorescence intensity at excitation wave lengths 340 nm and 380 nm was measured at controlled total $[Ca^{2+}]$.

4.2.2 The device for fluorescence measurement

Figure 4-1 is the schematic drawing of the set up for fluorescence measurement. An arc lamp (Model 6292, Oriel Instruments) seated in front of an elliptical mirror was ignited by a power supply (Model LPS-220, Proton Technology International). The lamp was adjusted so that it generated high light intensity in the second focal plane of the elliptical reflector. A mirror reflected UV light from the arc lamp into an optic fiber. A rotary solenoid control shutter (29A45GCw35-36-87, Magnuson Engineers Inc) controlled the UV light path. Then, the UV light was separated into two identical quartz optic fiber guides facing a 340 nm filter (340FS10-25, Oriel) and a 380 nm filter (03FIU014, Oriel), respectively. There was a chopper located behind the filters and it turned at a controlled rate. This chopper allowed light to pass through one filter only, either 340 nm or 380 nm. The light passing through the filters was collected by an Y shaped fiber optics and reflected by a dichroic mirror (400DPLC, Nikon) on a 20X-fluo objective lens (Nikon, Canada). The light was then focused in the bath to excite fluorescence. The emission of the fluorescence was conveyed to the objective lens and transferred back through the dichroic mirror. Finally, the fluorescence light passed through a 510 nm filter and projected on to a photodetector. The photodetector consisted of a photomultiplier tube with a DA type socket assembly (PMT-R2693, C1053-01, Hamamastu, Japan). The PMT signal was recorded on a chart recorder (Gould, Cleveland, Ohio) and computer.

4.2.3 Fura-2 signal calibration

Fura-2 is one of the sensitive Ca^{2+} dyes, which has been widely used in a wide range of research settings. This major Ca^{2+} dye has contributed tremendously to the

Figure 4-1: Schematic drawing for the free [Ca^{2+}] measurement. 1: stirring bar, 2: myocyte bath chamber, 3: microscope, 4: UV light source (ARC lamp), 5: UV light beam, 6: Chopper, 7: excitation light filters (340nm and 380 nm), 8: wheel, 9: excitation light beam (340 nm or 380 nm), 10: excitation light beam projection on the myocyte chamber, 11: emission light beam, 12: dichroic mirror, 13: 510 nm filter, 14: photomultiplier tube (PMT), 15: universal amplifier, 16: computer, 17: Gould chart recorder.

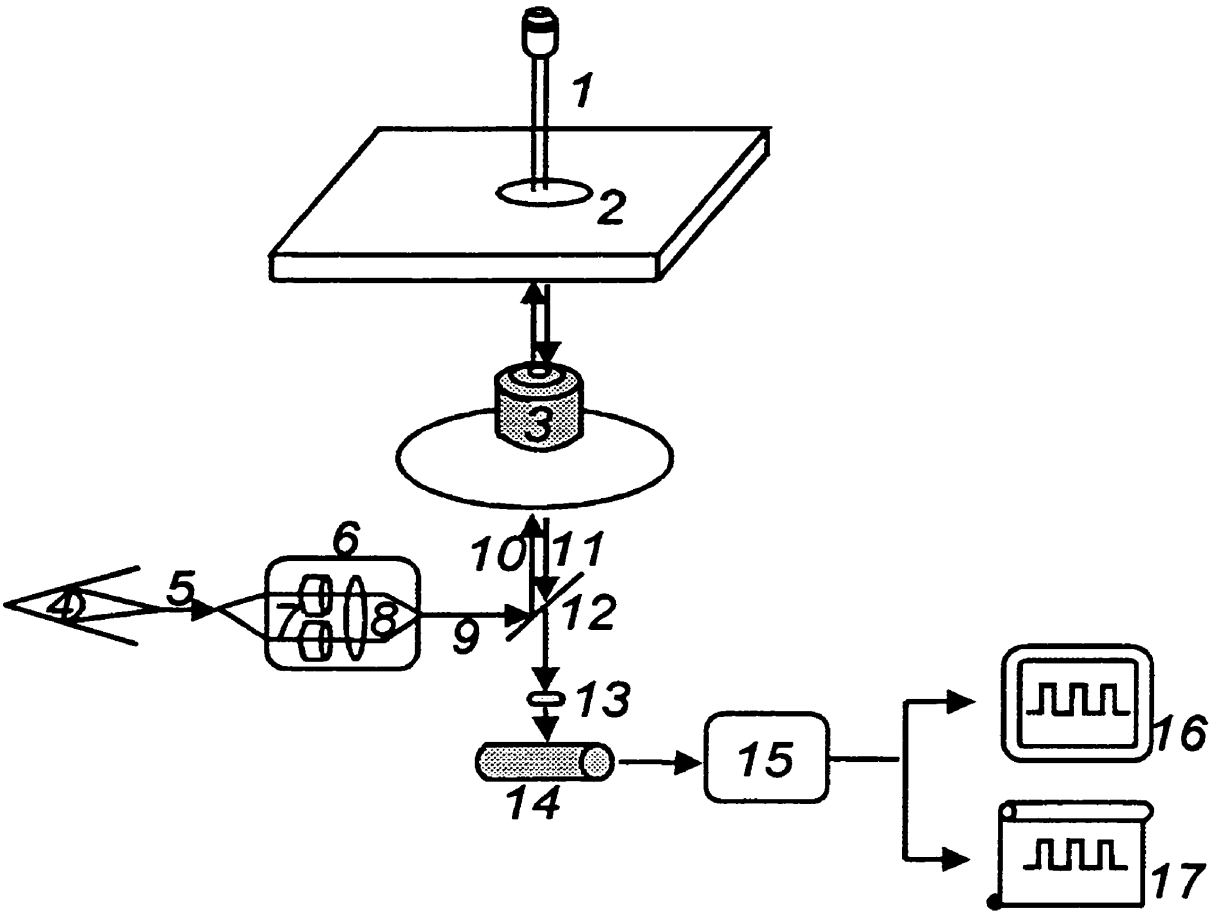
1
2
3
4
5
6
7
8
9
10
11
12
13
14
15
16
17

understanding of the role of Ca^{2+} in cellular regulation. The ability to make ratio measurement is one of fura-2's properties. The largest dynamic range for Ca^{2+}-dependent fluorescence signals is obtained by exciting the fura-2 at 340 nm and 380 nm. The ratio of the fluorescence intensities was detected at emission light ~510 nm. At low concentrations of the indicator, use of the 340/380 nm excitation ratio for fura-2 allows accurate measurements of the $[Ca^{2+}]_i$. Measurement of the fluorescence ratio can reduce the effects of uneven dye loading, leakage of dye and photo-bleaching, as well as the problems associated with measuring Ca^{2+} in preparations of unequal thickness or time varying.

In order to accurately measure free $[Ca^{2+}]$ in cytosol, it is necessary to first calibrate fura-2. The UV lamp light, metal components in the solution can affect the fura-2 calibration curve and the accuracy of free $[Ca^{2+}]$ measurement. In this fura-2 calibration experiment, I used Ca^{2+} calibration buffer kit #1 (Purchased from Molecular Probes). The calibration curve is shown in Figure 4-2.

4.2.4 Skinning techniques

There are mechanical and chemical skinning methods, which allow investigators to make the membrane structure permeable. The chemical skinning method is most commonly used in laboratory experiments. Saponin is one of the detergents, which is generally used in skinned preparations and makes uniform pits or holes on the surface membrane structure. Saponin acts on cholesterol molecules and specifically on the surface membrane without affecting the SR membrane since the content of cholesterol in the SR membrane is much less than that of the surface membrane. Sapnoin [144]. Triton X-100 is another detergent, which removes barriers on both the surface membrane and SR

Figure 4-2: Fura-2 calibration curve by using a commercial fura-2 calibration buffer kit 1#. This is a typical fura-2 sigmoidal calibration curve. R_{min} =0.163, R_{max} =7.48, β=15.00, Kd=78.08 nM. R_{min} and R_{max} are the ratio of fluorescence intensities of 340 nm over 380 nm at minimal and maximal $[Ca^{2+}]$, respectively. β is the ratio of fluorescence intensity of 380 nm at zero $[Ca^{2+}]$ over saturated $[Ca^{2+}]$. Kd is fura-2 absolute binding constant to Ca^{2+}. Based on the formula:

$$[Ca^{2+}]_{free} = Kd \times (R-R_{min})/(R_{max}-R) \times \beta$$

the free $[Ca^{2+}]$ can be measured from the ratio measurement of the intensity of 340 nm and 380 nm.

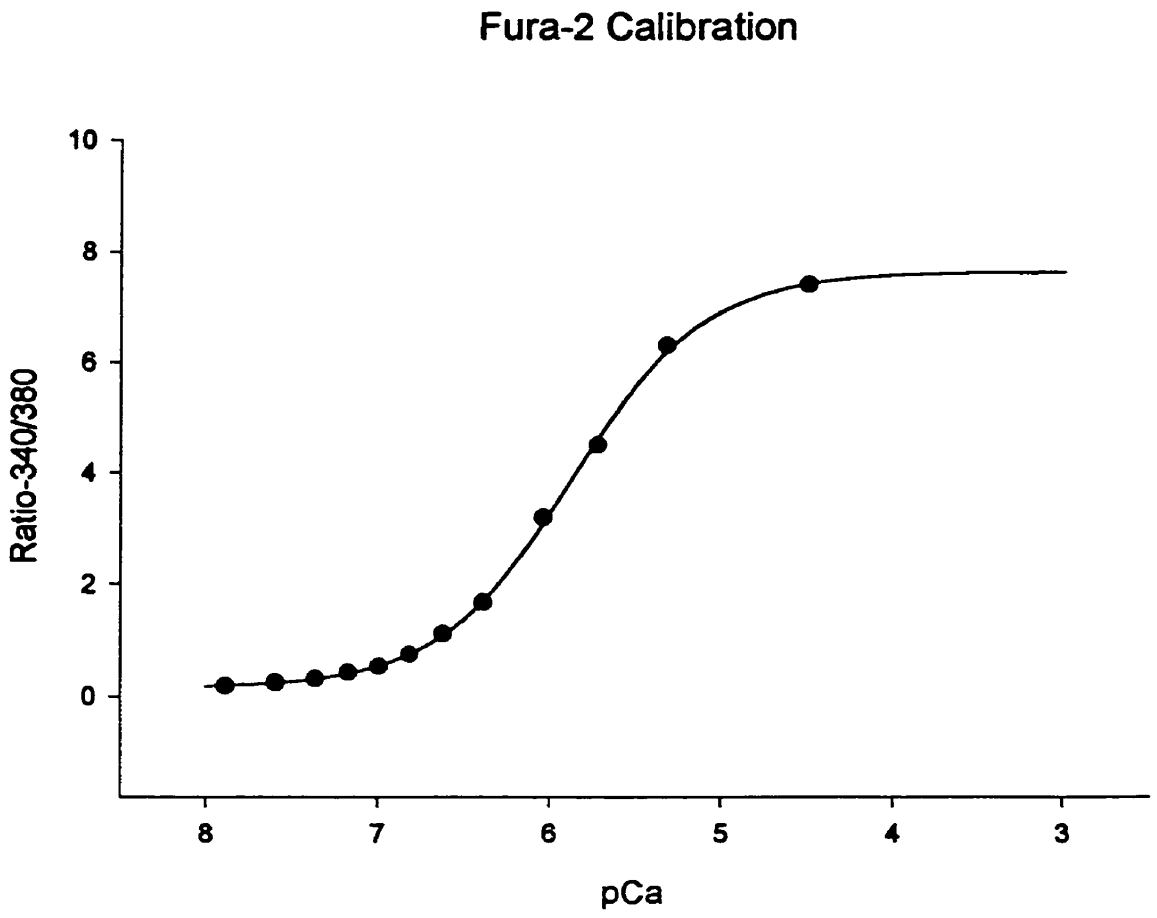
Fura-2 Calibration
Ratio-340/380
10
8
6
4
2
0
8
7
6
5
4
3
pCa

membrane. This detergent dissolves ~80% of the protein, and nearly all the phospholipid from SR membrane [145].

Kargacin et al. reported that saponin skinning produced uniform pits or holes with a diameter 70-80 Å and density ~$2x10^6/cm^2$ on the cellular membrane and caused a loss of ~30% of intracellular protein in smooth muscle cells [146]. Triton skinning procedure causes a 50% protein loss [147]. The proteins lost through the permeable membrane are soluble and low-molecular-weight cytosolic proteins not attached to the cytoskeleton. The levels of myosin and actin remain unaffected. Skinned isolated cells retain their major structural and contractile proteins. Acrylamide gels show that both myosin and actin are retained by the skinning procedure. The studies of Kargacin et al. indicate that a minimum saponin concentration of 25 μg/ml could be used to routinely to skin isolated cells [146].

Triton X-100 is another useful detergent in skinning studies, which solubilizes both the sarcolemma membrane and the SR membrane but does not destroy the Ca^{2+}-dependent acto-myosin ATPase activity [145]. In isolated muscle or cell studies, the force-length relationship in skinned preparations is very similar to that of intact preparations [55], which demonstrates that the skinned cardiac muscles retain their ability to shorten and also indicates that the Ca^{2+} regulatory mechanism present in intact muscle is retained after skinning. The maximum shortening velocity in skinned preparations is also similar to the maximal velocity of shortening of intact preparations [148], which suggests that the kinetics of the contractile process have not been altered significantly by the skinning procedure.

4.3 Force-pCa-SL relationship studies

4.3.1 Experimental method for Force-SL-pCa studies

The experiments were conducted under strictly controlled conditions. In skinned preparations, I maximally mimicked the in vivo condition. [Mg^{2+}] was controlled to the level close to that in vivo in the skinning solutions and the lattice spacing was corrected by adding 5% Dextran. In this way, I tried to match physiological environment in my study.

1.) Experimental procedure:

1) Dissected trabeculae from anesthetized LBN rats.
2) Skinned the trabeculae with 1% Triton X-100 for 30 minutes to mimic in vivo conditions.
3) Controlled free [Mg^{2+}] at 0.7 mM which was close to the concentration in vivo.
4) Corrected osmotic pressure by adding 5% Dextran T500 to decrease the lattice spacing.
5) Controlled experimental temperature at ~25°C.
6) Measured force at controlled SL ana [Ca^{2+}].

2.) Device for SL and force measurements

The SL was measured by laser diffraction patterns. The detailed method was described by ter Keurs et al. [54]. Briefly, a laser beam was generated by a 15 mW He-Ne laser light (Spectra-Physics model 106-2, Eugene, OR) (632.8 nm). The cross section of the laser beam was reduced to 350 μm by a converging lens system mounted in the laser beam path and the intensity of the laser light was adjusted by a polarizer. Then, the laser beam was projected on the trabeculae and it was symmetrically diffracted into multiple

orders by the striations of the sarcomeres. The angle between the zero order and first order diffraction bands was proportional to the laser wave length (λ) and reciprocal to SL (d) and obeys the following equation:

$$Sin\theta = n\lambda/d$$

where n is the diffraction order of the diffracted beam. The diffracted light was detected by a photodiode array (model RC 105, Reticon, Sunnyvale, CA). The spatial resolution of the diffractometer is 4 nm and temporal resolution is 500 μs. The photodiode array could scan the diffracted light intensity and generate a profile of light intensity along the array. With automatic subtraction of the zeroth-order skirt, the median position of the first order intensity distribution was determined from the integral of the pattern distribution. An electronic calculation system converted the scanning signals to SL. The SL measuring system was calibrated by a 10 μm standard grating before each experiment.

Force was measured by a modified silicon strain gauge (model AE-801, Sensonor, Horten, Norway) attached to a micromanipulator. In order to increase the sensitivity of the force transducer, a ~1.5 cm carbon fiber extension was glued on the tip of the silicon gauge. A platinum wire basket was glued on the end of the carbon fiber. The outside of the elements of the force transducer was covered by silicone glue mixed with carbon black and toluene. This procedure ensured that the transducer become water and light resistant. The platinum basket provided a stable-mounting cradle for the muscle block of the trabeculae. The transducer was calibrated by six different weight metal hooks. The noise of the transducer was <15 μN. The schematic drawing for the experimental setup is shown in Figure 4-3.

4.3.2 Data acquisition

Force and SL were recorded on a pen-recorder (model 2800, Gould Electronics, Cleveland, OH) equipped with amplifiers (model 56-1340-00, Gould Electronics, Cleveland, OH). Force and SL signals were also displayed on an oscilloscope (model 610, Data Precision, Danver, MA) during the experiments for monitoring the force and SL signal changes.

4.3.3 Data analysis

Data were stored in a computer and processed with Excel and SigmaPlot software programs. Statistical analysis was done using the "primer of bio-statistics" software program [149]. The comparisons between the experimental groups were tested by one way ANOVA and unpaired t-test.

Figure 4-3: Schematic drawing of the setup for the force and SL measurement. 1: motor arm, 2: He-Ne laser beam, 3: force transducer, 4: muscle bath chamber, 5: trabecula, 6: mirror, 7: telescopic lens, 8: planoconvex lens, 9: reticon, 10: microscope objective, 11: video camera, 12: TV monitor, 13: computer, 14: Gould chart recorder.

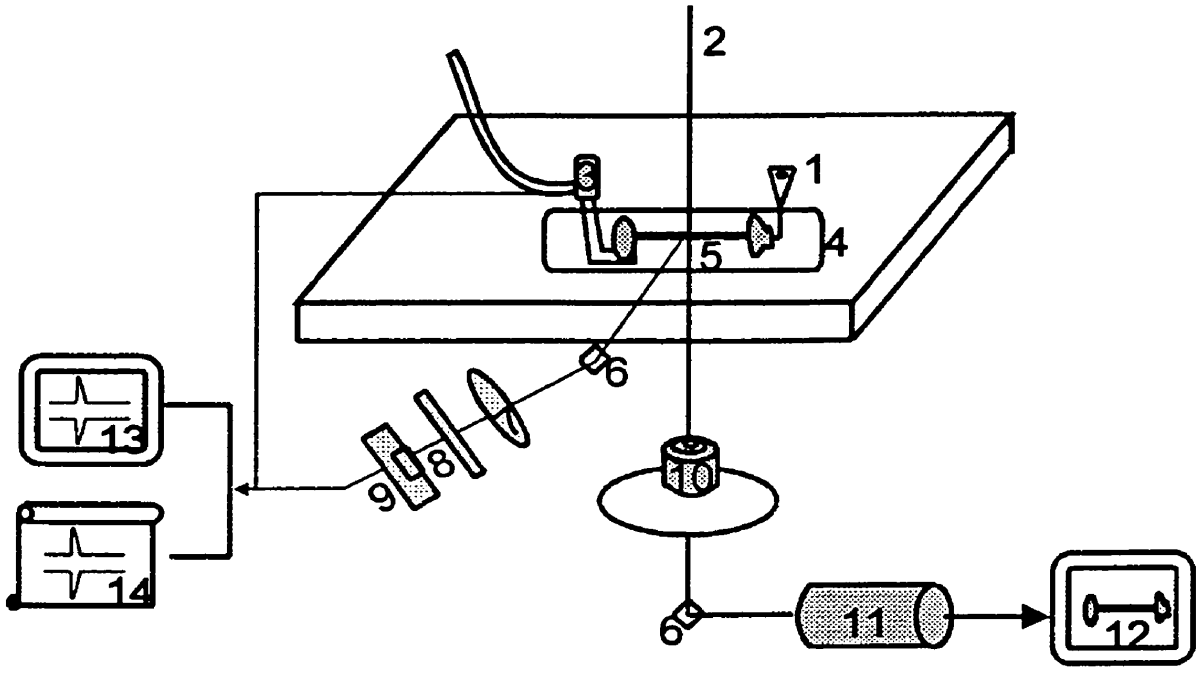
2
1
4
5
6
13
14
9
8
10
11
12

Chapter 5

Physiological Ca^{2+} buffering in rat cardiac myocytes

5.1 Introduction

It is an increase in the intracellular free [Ca^{2+}] that couples electrical excitation to mechanical contraction [150]. During excitation, Ca^{2+} enters through L-type Ca^{2+} channels from the extracellular space into intracellular space and causes CICR. The total [Ca^{2+}] increased is buffered by a cellular Ca^{2+} buffering system, including intracellular ligands and proteins. The active force generated is associated with free [Ca^{2+}].

Different investigators have reported quite different value for intracellular Ca^{2+} buffering capacity. Isenberg et al. proposed that the intracellular Ca^{2+} buffering system has high-affinity binding sites and low-affinity binding sites [30]. The former refers to the ligands in the myoplasm that compete with TnC for Ca^{2+}, the latter are the activation sites, TnC. Isenberg et al. suggested that high affinity sites have a buffering capacity 5500:1 and low affinity sites have a buffering capacity 700:1 for Ca^{2+} ions in intact guinea-pig ventricular cells [30], which means 99.98% Ca^{2+} is bound to cellular buffering system at rest. Fabiato et al. demonstrated that the ratio between total [Ca^{2+}] and free [Ca^{2+}] was from 140:1 to 35:1 corresponding to different level of force generated [150]. Sipido and Wier et al. showed that there was 100-fold difference between the total [Ca^{2+}] and free [Ca^{2+}] in guinea-pig cardiac cells [151].

The above studies of the Ca^{2+} buffering system show a high buffering capacity of the cardiac cells. Because the Ca^{2+} buffering capacity of myocytes is so high, the various results between different studies result in tremendous differences in estimates of the total [Ca^{2+}] inside the cells. The quantitation of the interaction of free cytosolic [Ca^{2+}] and

function are extremely important in cardiac ECC study, especially in the studies of SR Ca^{2+} uptake and the properties of the contractile apparatus in skinned preparations.

Dysfunction of SR Ca^{2+} uptake has been observed in isolated failing cardiac myocytes. However, it is more meaningful to study SR Ca^{2+} pump function in skinned isolated cardiac trabeculae than in isolated myocytes. Isolated trabeculae are closer to "physiological conditions" than single myocytes since, during the cell isolation procedure, the myocytes may be damaged in important ways. It is crucial to measure the Ca^{2+} buffering capacity of the solutions in order to accurately measure the SR Ca^{2+} uptake rate in skinned cardiac trabeculae.

Also, the high Ca^{2+} buffering capacity of cardiac cells makes the control of free $[Ca^{2+}]$ important in force-length relationship studies in skinned trabeculae. Skinning allows investigators maximal control of free $[Ca^{2+}]$, pH and ionic strength (IS) in experiments. An accurate control of free $[Ca^{2+}]$ in the skinning solutions is critical for the interpretation of force measurements. In order to best control the free $[Ca^{2+}]$ in my study of the force-length relationship, it was necessary to clarify the cardiac Ca^{2+} buffering capacity.

In this study, I measured Ca^{2+} buffering capacity after correction for ATP-bound Ca^{2+} in saponin skinned myocytes from LBN rats and compared my results with the results from previous published studies.

5.2 Materials and Methods

The hearts of male Lewis Brown-Norway rats (LBN, Harlan Sprague Dawley, Inc), with weight ~250 g, were perfused on Langendorff apparatus. The ventricular myocytes were isolated by an enzymatic method.

5.2.1 Isolation of myocytes

1.) Solutions:

1) Modified Krebs-Henseleit (KH) solution (in mM): 120 NaCl, 5 KCl, 1.2 $MgSO_4$, 1.37 Na_2HPO_4, 0.43 NaH_2PO_4, 19 $NaHCO_3$, 10 glucose, 10 taurine, pH 7.35 and Ca^{2+} free.
2) Digestion solution: 1.5 mg/ml collagenase (Worthington, type I, ~210 unit/mg) and 5% bovine serum albumin (BSA, Sigma, fraction V) in 50 ml of Ca^{2+} free KH solution. BSA increased the colloid osmotic pressure in the solution.
3) HEPES solution (in mM): 140 NaCl, 5 KCl, 2.8 Na-acetate, 1.2 $MgSO_4$, 10 HEPES, 10 glucose, 10 taurine and 0.5% BSA, adjust pH to 7.35 with NaOH at room temperature.

2.) Cell Isolation Procedure

Before myocyte isolation, the Ca^{2+} free KH solution (300~500 ml), collagenase solution (50 ml) and Hepes solution (25 ml) were pre-incubated at 37 °C. The LBN rat was anaesthetized using ether. The heart was quickly transferred to the Langendorff perfusion apparatus and perfused with Ca^{2+} free KH solution through the aorta at ~5 ml/min at 37 °C for 8-10 minutes. The perfusion of Ca^{2+} free KH solution loosened the connection between the myocytes. Meanwhile, the surrounding tissue of the heart was trimmed and the pulmonary artery was cut open. The heart was then perfused with collagenase solution for 12-15 minutes until the heart became soft and its color became beige. After that, the atria were removed and the heart was cut into 3-4 pieces and incubated in 20 ml Hepes at 37 °C with gentle stirring for 5 minutes. The myocytes were filtered and collected through 8 layers of gauze sponge. The collected solution was centrifuged at 500 rpm for 1 minute to let the cells settle down. The cells were stored in

fresh Hepes solution and purified a few times by gravity. The cell viability and density were measured by a standard hemocytometer chamber. Successful myocyte isolation was characterized by 70-85% of the cells in rod shape with a density of 165,000 cells per ml suspension solution.

5.2.2 Saponin skinning in isolated myocytes

After the myocytes were isolated, they were washed 3 times by an ATP solution containing (in mM): 120 KCl, 5 $MgCl_2$ (~0.36 mM $[Mg^{2+}]_{free}$), 10 ATP-Na_2, 20 HEPES, 1.25 dithiothreitol (DTT), 0.03 ruthenium red without addition of EGTA. Then the myocytes were skinned by 25 μg/ml saponin for 5 minutes. After skinning, the myocytes were washed with the ATP solution 5 times to ensure that saponin was completely washed away. The Milli Q water contained on average a free $[Ca^{2+}]$ ~700 nM (5 measurements from the water). This amount of contaminated Ca^{2+} increased free $[Ca^{2+}]$ 110 nM in the experimental bath.

5.2.3 Fura-2 calibration curve:

It is important to determinate the fura-2 binding constant to Ca^{2+} in vitro condition to measure the free $[Ca^{2+}]$. The fura-2 fluorescence was calibrated with 5 uM fura-2 penta-potassium (Molecular Probe, Eugene, Oregon). The components of calibration solution were as following (in mM): 120 KCl, 5 $MgCl_2$ (~0.36 mM $[Mg^{2+}]_{free}$), 2.0 EGTA, 10 ATP-Na2, 20 HEPES, 1.25 dithiothreitol (DTT), 0.03 ruthenium red and different concentrations of Ca^{2+}, pH 7.15 at room temperature. The free $[Ca^{2+}]$ in the solution was calculated using a computer program provided by Dr. Kentish (1986). The ionic strength of the solution and binding constant of compounds were adjusted according

to the study of Harrison and Bers[152]. The fura-2 fluorescence-[Ca^{2+}] relationship was fitted by the following equation:

$$R=R_{min}+ (R_{max}-R_{min})*[Ca^{2+}]/(K+[Ca^{2+}])$$

R_{min} was the ratio of F340/F380 at zero Ca^{2+} and R_{max} was the ratio of F340/F380 at saturated Ca^{2+}. The fura-2 calibration curve is shown in Figure 5-1.

5.2.4 Total [Ca^{2+}] control in the Ca^{2+} capacity measurement:

After the myocytes were skinned by saponin, they were stored in the ATP solution, described above. Then 500 μl of myocyte suspension was pipetted into the bath and loaded with fura-2 at 3 μM/L. 5 nmol/ml of thapsigargin was also added in the bath. A propellor stirred the suspension constantly and evenly. During the free [Ca^{2+}] measurement, I added concentrated $CaCl_2$ from a stock solution to produce a total [Ca^{2+}] at 0, 10, 20, 30, 50, 100 and 150 μM. The added Ca^{2+} became bound to the myocytes and to the ATP which I had added. The theoretical free [Ca^{2+}] was calculated after consideration of the amount of Ca^{2+} ion bound to ATP. The detailed calculation is shown in Table 5-1 and theoretical Ca^{2+} binding to ATP is shown in Figure 5-2.

5.2.5 Determination of the amount of Ca^{2+} bound with myocyte Ca^{2+} buffering system

The Ca^{2+} added in the experimental bath included three parts: Ca^{2+} bound with myocyte Ca^{2+} buffering system, Ca^{2+} bound with ATP and free Ca^{2+} in the cell suspension. The relationship between the different Ca^{2+} distributions was fitted into the following equation:

$$\text{Total } Ca^{2+} = Ca^{2+}\text{-myocyte} + Ca^{2+}\text{-ATP} + \text{Free } Ca^{2+}$$

The amount of free Ca^{2+} in the bath was detected by Fura-2 and the amount of Ca^{2+} bound with ATP could be theoretically calculated by a compute program provided by Dr.

Kentish. Since the total amount of Ca^{2+} added was controlled, the amount of Ca^{2+} bound with myocyte was then determined by the above equation. Based on the average cell density in the experimental bath (165,000 cells/ml) and average cell volume 30 pl, the myocyte Ca^{2+} buffering capacity was calculated.

5.3 Results

The added Ca^{2+} bound to both ATP and myocytes. In Table 5-1, I calculated the $[Ca^{2+}]$ bound to ATP and free $[Ca^{2+}]$ in the test solution without myocytes. The relationship between the amount of ATP-bound Ca^{2+} and free $[Ca^{2+}]$ in the ATP solution is shown in Figure 5-2. In the 500 µl bath chamber, there were total 5000 nmol ATP molecules. The theoretical relationship between free $[Ca^{2+}]$ (pCa) and the amount of ATP bound Ca^{2+} (nmol) was sigmoidal over the full range. In my study, I worked in the low range of the sigmoidal curve (<200 µM). From the calculation with Kentish's program, the change of IS and other conditions of the test solution caused by the addition of Ca^{2+} to the experimental bath chamber was negligible in this working range.

The total Ca^{2+} in the cellular suspension included three fractions: ATP-bound Ca^{2+}, Ca^{2+} bound with cellular buffer and free Ca^{2+}. From the ratio measurement of fluorescence intensity, the free $[Ca^{2+}]$ in the cellular suspension could be measured and determined. The result of free $[Ca^{2+}]$ is shown in Table 5-1. The relationship between the total Ca^{2+} added, Ca^{2+}-ATP, Ca^{2+}-myocytes and free Ca^{2+} in the cellular suspension is shown in Figure 5-3. From this figure, it can be seen that myocyte bound 40.1 nmol for 75.7 nmol Ca^{2+} added. The average density of myocyte in the bath chamber was 165,000 cells/ml. The average volume of myocyte is 30 pl, so the Ca^{2+} buffering capacity of myocytes could be calculated from free $[Ca^{2+}]$ 10.9 µM with total $[Ca^{2+}]$ 8.04 mM per

Table 5-1: The calculation of $[Ca^{2+}]$ and measured free $[Ca^{2+}]$ in the cell suspension. "Total $[Ca^{2+}]$" was the Ca^{2+} ions, which were added into the cell suspension; "Calculated $[Ca^{2+}]$" was the $[Ca^{2+}]$ calculated by the computer program in the absence of myocytes; "Free $[Ca^{2+}]$" was the actual $[Ca^{2+}]$ measured by fura-2. IS = ~0.2 M, Ie = 0.17 M. The total $[Ca^{2+}]$ is the sum of controlled $[Ca^{2+}]$ and contaminated $[Ca^{2+}]$ from the chemicals used. The second and third columns are the free $[Ca^{2+}]$ and ATP bound $[Ca^{2+}]$ in the pure testing solutions without myocytes theoretically calculated by the computer program provided by Dr. Kentish. The free $[Ca^{2+}]$ was measured by Fura-2. In the whole study, the $[Mg^{2+}]$ was kept constant at ~0.36 mM.

Controlled $[Ca^{2+}]$ μM	Contaminated $[Ca^{2+}]$ μM	Calculated free $[Ca^{2+}]$ μM	Calculated ATP-$[Ca^{2+}]$ μM	Measured free $[Ca^{2+}]$ μM	Free $[Mg^{2+}]$ mM
0	0.74	0.11	0.63	0.21	0.36
10	0.74	1.62	9.12	0.37	0.36
20	0.74	3.13	17.61	0.54	0.36
30	0.74	4.65	26.09	0.73	0.36
40	0.74	6.17	34.57	0.97	0.36
50	0.74	7.69	43.05	1.27	0.36
100	0.74	15.4	85.34	3.69	0.36
150	0.74	23.1	127.6	10.9	0.37

Figure 5-1: the fura-2 calibration curve. Calibration solution containing (in mM): 120 KCl, 5 $MgCl_2$ (~0.36 mM $[Mg^{2+}]_{free}$), 2.0 EGTA, 10 ATP-Na_2, 20 HEPES, 1.25 dithiothreitol, 0.03 ruthenium red and different concentration of Ca^{2+}, pH 7.15 at room temperature. In this calibration experiment, R_{min}=0.162, R_{max}=3.380, the apparent dissociation constant (Kd') of fura-2 to Ca^{2+} was 935.414 nM. The effective dissociation constant (Kd) was 113.00 nM and ß=8.278. Free $[Ca^{2+}]$ could be calculated from the following equation:

$$[Ca^{2+}]_{free} = Kd \times (R-R_{min})/(R_{max}-R) \times ß$$

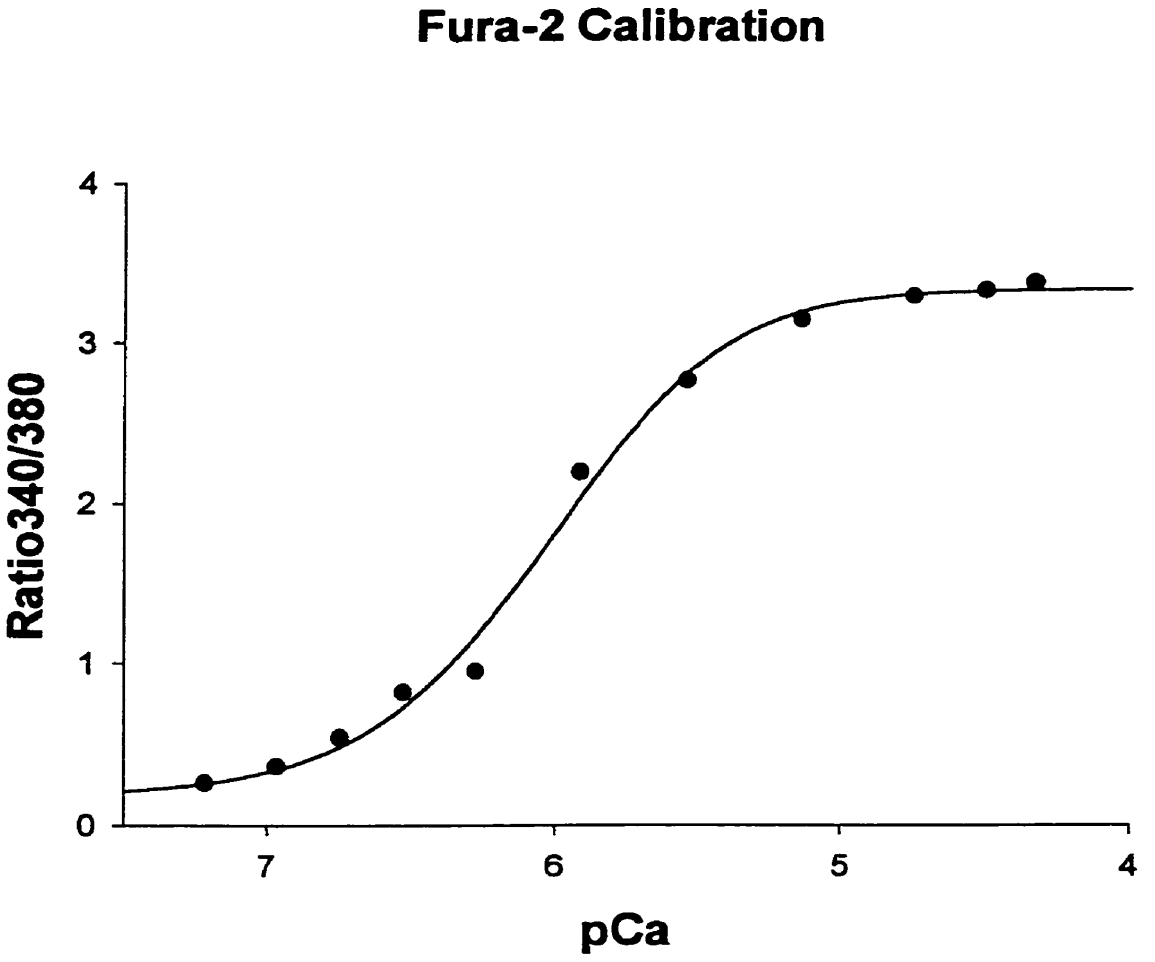
Fura-2 Calibration
Ratio340/380
4
3
2
1
0
7
6
5
4
pCa

Figure 5-2: Ca^{2+} bound to ATP is a sigmoidal fraction of free [Ca^{2+}] with a maximum in the range of total 5000 nmol ATP molecules added. This figure shows predicted Ca^{2+} bound to ATP in both at high free [Ca^{2+}] and low range of free [Ca^{2+}]. ATP bound a substantial amount of Ca^{2+} added. The Ca^{2+}-ATP binding in the low [Ca^{2+}] range was used to calculate the myocyte Ca^{2+} buffering capacity.

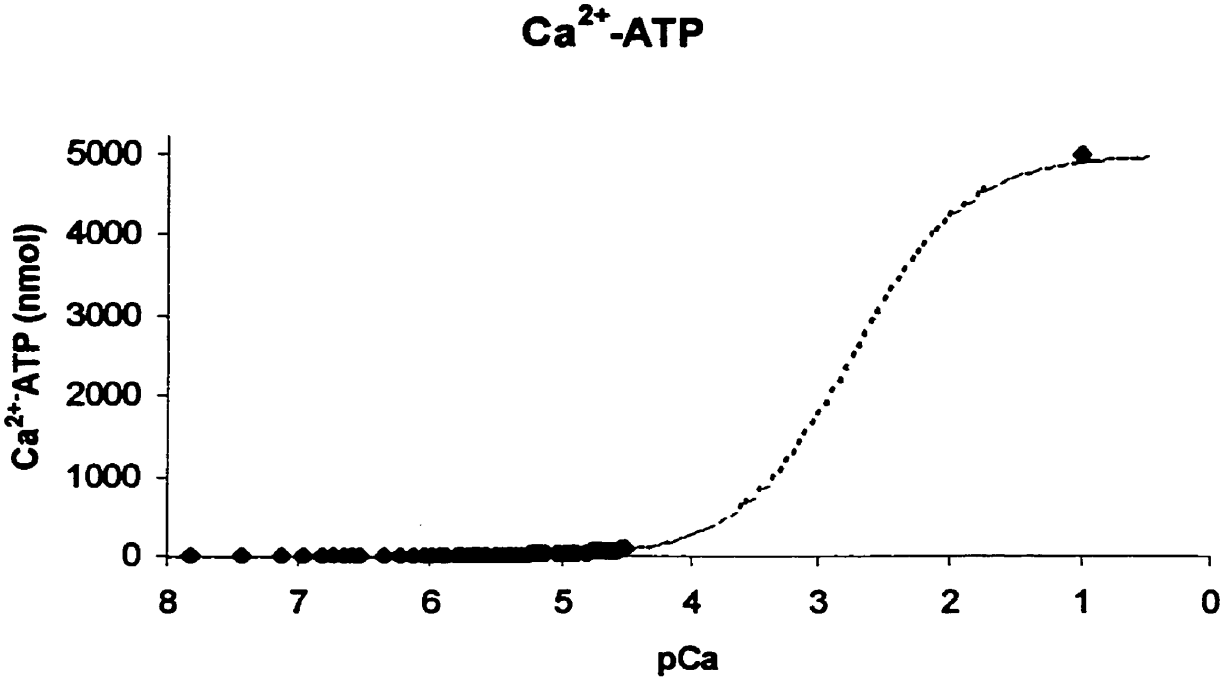
Ca2+-ATP
5000
4000
3000
2000
1000
0
Ca2+ATP (nmol)
8
7
6
5
4
3
2
1
0
pCa

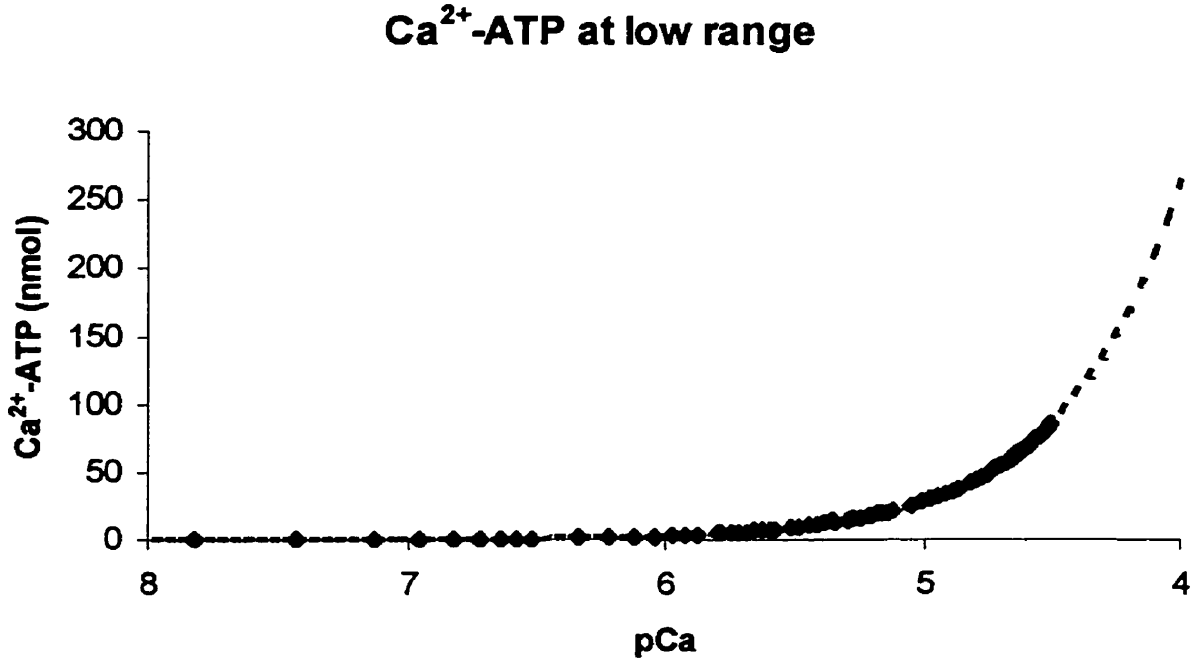
Ca2+-ATP at low range
300
250
200
150
100
50
0
Ca2+-ATP (nmol)
8
7
6
5
4
pCa

Figure 5-3: This figure shows the Ca^{2+} distribution in the cellular suspension. In the suspension, the total Ca2+ added in the experimental bath included three fractions of Ca^{2+}: Ca^{2+} bound to ATP, Ca^{2+} bound to myocyte buffer and free Ca^{2+}. The free Ca^{2+} ions were detected by Fura-2, and the amount of Ca2+ ions was theoretically calculated by the computer program provided by Dr. Kentish. Based on the equation:

$$\text{Total } Ca^{2+} = Ca^{2+}\text{-Myocyte} + Ca^{2+}\text{-ATP} + \text{Free } Ca^{2+},$$

The amount of Ca^{2+} bound with myocytes in the bath could be determined. At the minimal amount of Ca^{2+} added, in total 5 nmol Ca^{2+} ions, 4 nmol Ca^{2+} ions were bound with myocyte Ca^{2+} buffering system, which gave a myocyte Ca^{2+} buffering capacity 99.98%. At the highest amount of Ca^{2+} added, in total 76 nmol Ca^{2+} ions, 40 nmol Ca^{2+} ions were bound, which corresponded to a Ca^{2+} buffering capacity 99.93%.

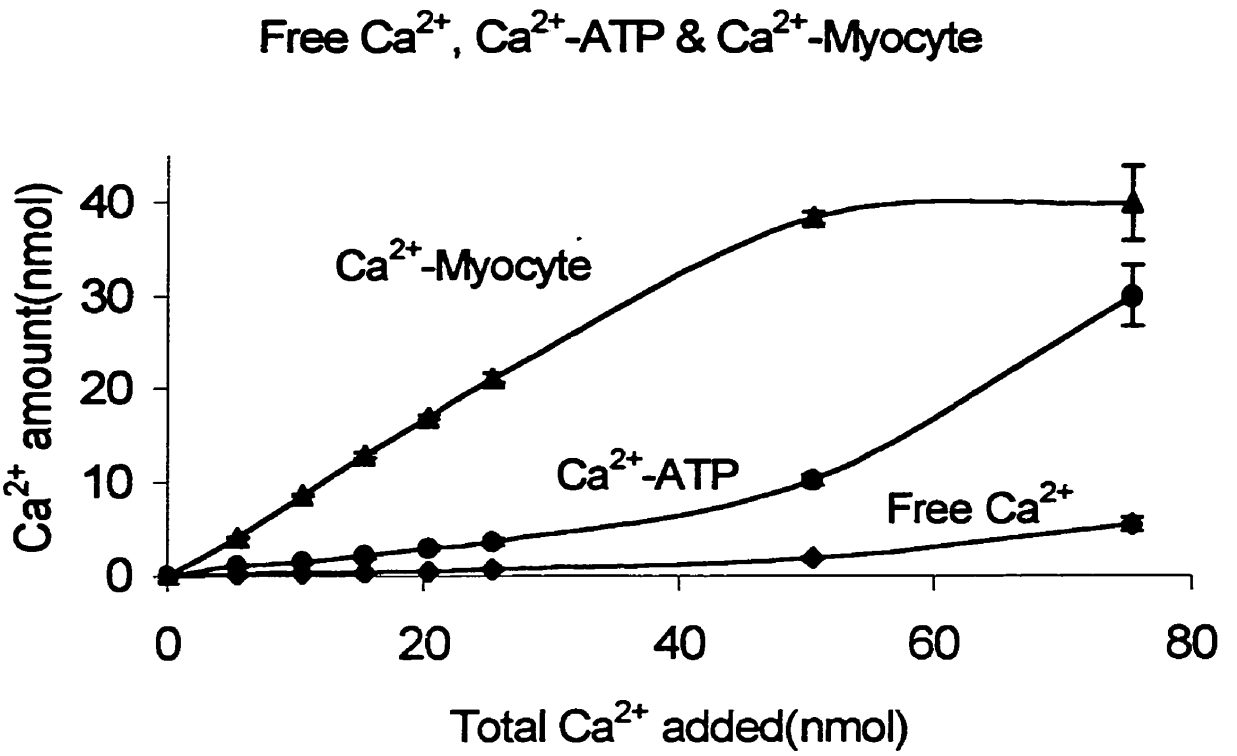
Free Ca2+, Ca2+-ATP & Ca2+-Myocyte
Ca2+ amount(nmol)
40
30
20
10
0
Ca2+-Myocyte
Ca2+-ATP
Free Ca2+
0
20
40
60
80
Total Ca2+ added(nmol)

Figure5-4 shows the relationship between the total [Ca^{2+}] and the free [Ca^{2+}] in the myocyte suspension: in the full range of total [Ca^{2+}] in the experiments. Free [Ca^{2+}] gradually increased with the increase of total [Ca^{2+}] in the cell suspension. At lower total [Ca^{2+}], the increase of free [Ca^{2+}] was less steep. When total [Ca^{2+}] was over 100 μM, as the total [Ca^{2+}] increased, the increase of free [Ca^{2+}] became steeper. There was a non-linear relationship between the total and free [Ca^{2+}].

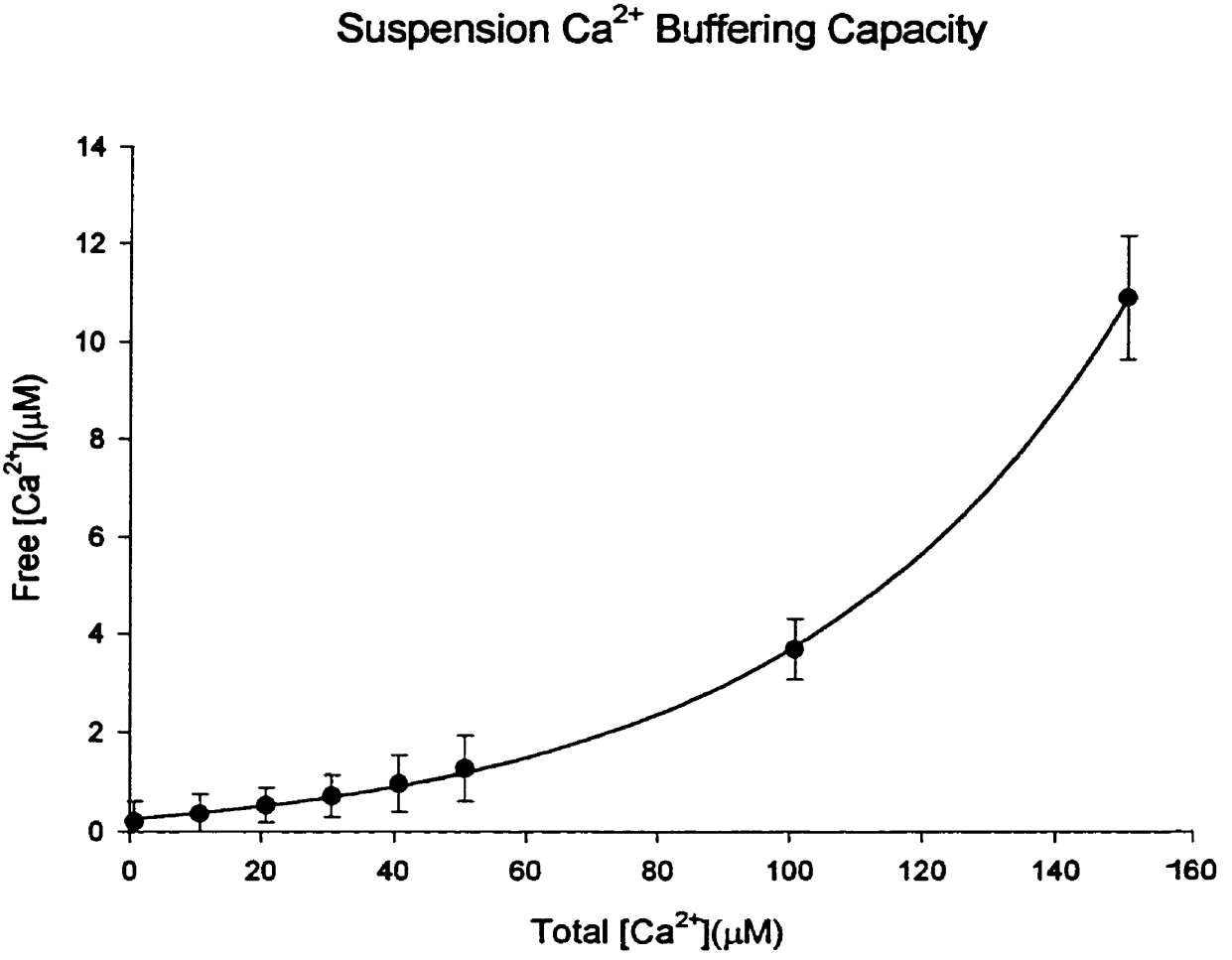
Suspension Ca2+ Buffering Capacity
Free [Ca2+](μM)
Total [Ca2+](μM)
0
2
4
6
8
10
12
14
0
20
40
60
80
100
120
140
160

Figure 5-5: In the low range of the total [Ca^{2+}] tested in the experiments, the relationship between the total [Ca^{2+}] and free [Ca^{2+}] was linear. Increase of total [Ca^{2+}] increased free [Ca^{2+}] and the ratio between total [Ca^{2+}] and the free [Ca^{2+}] is 50:1. The y-intercept was 0.14 μM. This number was possibly caused by the source of Ca^{2+} contamination. Ca^{2+} contamination from the milli Q water was considered to be unlikely, but the Ca^{2+} could be from the chemicals used in the experiments. The solutions used lacked a strong Ca^{2+} buffer-EGTA, which was another possible reason to cause the Ca^{2+} contamination.

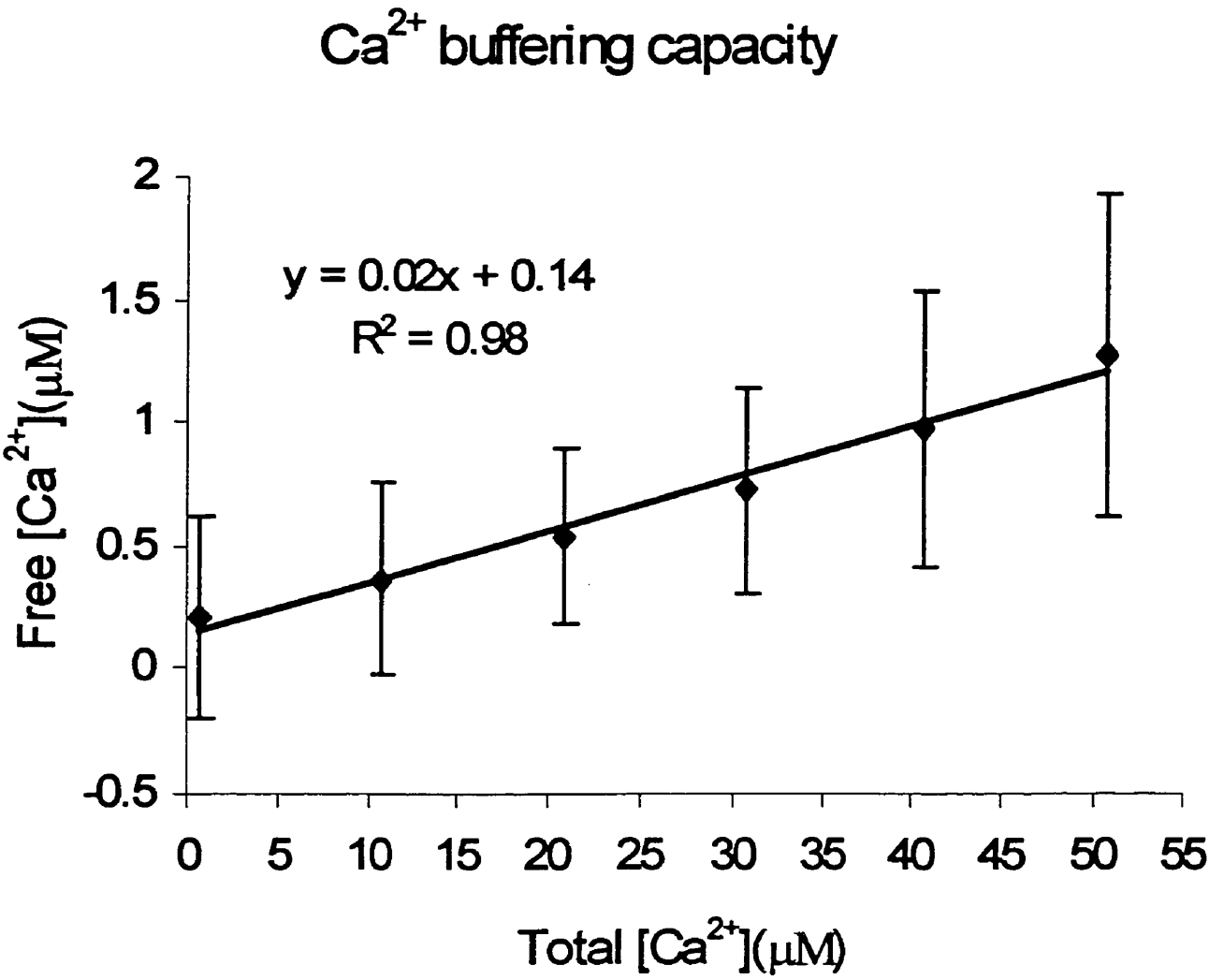
Ca2+ buffering capacity
y = 0.02x + 0.14
R2 = 0.98
Free [Ca2+](μM)
Total [Ca2+](μM)
2
1.5
1
0.5
0
-0.5
0
5
10
15
20
25
30
35
40
45
50
55

liter cells at highest level of Ca^{2+} added (added Ca^{2+}: 75.7 nmol). In this experiment, 99.93% Ca^{2+} added was bound to cellular buffer. At the low end of total Ca^{2+} added, 4.13 nmol out of total 5.37 nmol Ca^{2+} ions added were bound to myocytes, which corresponded to Ca^{2+} buffering capacity 99.98%.

The free [Ca^{2+}] was dependent on the total [Ca^{2+}] in the bath solution. Increase of total [Ca^{2+}] gradually increased the free [Ca^{2+}]. In the full range of total [Ca^{2+}], the relationship between total and free [Ca^{2+}] was nonlinear, whereas in the low range of total [Ca^{2+}], the relationship was linear. The slope between the free [Ca^{2+}] and the total [Ca^{2+}] was ~1:50 in the low range of total [Ca^{2+}] (total [Ca^{2+}]<50 μM).

5.4 Discussion and conclusion

The data from my study show that in the low range of the amount of Ca^{2+} added, the myocyte Ca^{2+} buffering capacity is higher than that in the high range. In my study, the myocyte Ca^{2+} buffering capacity is 99.98% and 99.93% at the low and high range of Ca^{2+} added, respectively.

The myocyte Ca^{2+} buffering capacity of the present study is higher than those of Fabiato et al. and Sipido et al.. Fabiato et al. used mechanically skinned cardiac myocytes and reported that the resting myocytes had a free [Ca^{2+}] 0.05 μM with a total [Ca^{2+}] 7 μM[150]. Based on these numbers, the myocyte Ca^{2+} buffering capacity is (7-0.05)/7=99.29%. This low value of buffering capacity likely results from their experiment approach. In their study, the intracellular total [Ca^{2+}] was measured by atomic absorption spectrophotometry in the homogenated myocytes. Disrupted sarcolemma and cellular suspensions could have Ca^{2+} binding sites, which were removed during their experiments. Further, the total [Ca^{2+}] measurement by the atomic absorption

spectrophotometry needs a long rest period, which can result in Ca^{2+} loss in cytosol through rest decay by the Na^{+}/Ca^{2+} exchanger [153]. Sipido and Wier et al. studied Ca^{2+} buffering capacity in single myocyte with whole patch clamp to control the amount of Ca^{2+} entered into the myocytes. These researchers reported that free $[Ca^{2+}]$ is 0.01 of the total $[Ca^{2+}]$ in the cell [151], and this corresponds to the myocyte Ca^{2+} buffering capacity of 99%. This low Ca^{2+} buffering capacity is also due to the underestimated total $[Ca^{2+}]$ in their study. In their calculation of intracellular total $[Ca^{2+}]$, they assumed that total amount of Ca^{2+} is the Ca^{2+} entered into the cells through L-type Ca^{2+} channels during depolarization when 10 mM caffeine was applied to deplete SR Ca^{2+} store. This may not be true. Isenberg et al. pointed out that 10 μM ryanodine did not deplete the SR Ca^{2+} store, neither did 10 mM caffeine completely release all SR Ca^{2+} content [30]. In the studies of Sipido and Wier et al., there were probably substantial Ca^{2+} ions bound with buffering proteins in the SR lumen, resulting in the underestimation of total $[Ca^{2+}]$. Besides the factor mentioned above, 10 mM caffeine can increase myofilament Ca^{2+} affinity and increase the Ca^{2+} binding to TnC [153], which also result in the estimation of total $[Ca^{2+}]$.

The results of current study agree with the data of Isenberg et al. Isenberg et al. have reported that 5499 out of 5500 Ca^{2+} ions are bound to the myocyte buffering system, which indicates that 99.98% of Ca^{2+} is bound to myocytes at rest. Once myocytes are depolarized, 699 out of total 700 Ca^{2+} ions are bound to intracellular ligands, corresponding to a buffering capacity 99.86% [30]. Two different experimental approaches were used in Isenberg's study and mine. Isenberg et al. used isolated intact guinea-pig myocytes with electron microprobe microanalysis (EPMA) to measure myocyte Ca^{2+}

buffering capacity. The EPMA is the most direct method for measuring the intracellualr total [Ca^{2+}]. In the present study, I used saponin-skinned rat myocytes and total [Ca^{2+}] was controlled. Despite the two distinct experimental methods applied, the results are consistent. Based on the above myocyte Ca^{2+} buffering capacity, the total [Ca^{2+}] of myocytes at rest is ~0.4-0.5 mM.

The real myocyte Ca^{2+} buffering capacity could be higher than I found. In the present study, I added 5 nmol/mg protein thapsigargin during measurement of free [Ca^{2+}] in the cell suspension. Thapsigargin inhibits the SR from taking up Ca^{2+} from the cytosol. Cardiac cells have a [SR] of 47 μM/l cell water [154]. In the SR lumen, the Ca^{2+} buffering protein calsequestrin binds ~35-40 Ca^{2+} ions/molecule [155]. Based on this number, Bers et al. proposed that there are 5-14 mM Ca^{2+} binding sites per liter of SR [153]. Therefore, in the presence of thapsigargin inhibition on SR function, the myocyte cytosolic Ca^{2+} buffering capacity is underestimated although the exact number for the SR lumenal [Ca^{2+}] is unkown. Another possible factor may be the decreased buffering capapcity of peameablized sarcolemma by saponin. Lullmann proposed the existence of the E_m-sensitvive Ca^{2+} binding sites on the inner sarcolemma surface, which were mainly negatively charged phospholipids. These binding sites could be as much as 500-1000 μmol/kg ww [156]. Therefore, the peameablization of sarcolemma by saponin also results in the underestimation of the bound Ca^{2+} in myocytes. But the quantitative role of these sarcolemma Ca^{2+} binding sites is still questionable. Rich et al. reported that after the extracellular space Ca^{2+} ions were removed, there was no Ca^{2+} released from these binding sites when the cellular surface was depolarized [157]. These sarcolemma Ca^{2+}

binding sites are probably additional Ca^{2+} binding sites in the myocyte Ca^{2+} buffering system, which does not affect physiological myocyte Ca^{2+} buffering capacity.

The cardiac myocytes have a strong Ca^{2+} buffering capacity, even the highest capacity reported by Isenberg et al. could be underestimated the real total [Ca^{2+}] in myocyte. The EPMA used to measure total [Ca^{2+}] has some limitations, e.g. dispersion of X-ray beam into other regions and geometry of junctional SR within the depth of section, which may result in the underestimation of Ca^{2+} buffering capacity.

Because of the properties of skinned preparations, it is inevitable that some Ca^{2+} binding proteins are lost once the membrane is permeablized. In my experiments, after the myocytes were skinned by saponin, I washed the myocytes five times. In the washing procedure, Ca^{2+} binding ligands and cytosolic proteins were lost and this may lower the Ca^{2+} buffering capacity. In experiments with smooth muscle, previous investigators have found that saponin skinning causes loss of CaM from cytosol [158; 159]. Kargacin et al. reported that the total amount of protein lost in saponin-skinned preparations could reach 30% [146]. The data from our laboratory showed that Langendorff-perfused hearts lost 15% cytosolic proteins once skinned with saponin for 10 minutes. The lost CaM by skinning in smooth muscle is substantial, however, the [CaM] is much lower in cardiac muscle than that of smooth muscle (personal communication from Dr. Walsh: 50-fold higher in smooth muscle), so it will not be the case in cardiac saponin skinned cells. The detail of the lost proteins by skinning needs to be further studied.

Except the above mentioned shortcoming in the studies of myocyte Ca^{2+} buffering system, under the current technology, the results from Isenberg's study and mine give the

closest value to the real myocyte Ca^{2+} buffering capacity, which indicate that 99.98% Ca^{2+} ions are bound with buffering system in resting myocytes.

In the whole range of total [Ca^{2+}] in the bulk myocyte suspension, there is a non-linear relationship between the free and total [Ca^{2+}]. An increase of total [Ca^{2+}] gradually increases the free [Ca^{2+}] (Figure 5-4). In the low range, total [Ca^{2+}] below 60 μM, the relationship between the free and total [Ca^{2+}] is linear. There is a 50-fold difference between the free and total [Ca^{2+}] (Figure 5-5). This number is valuable for my future study of the SR Ca^{2+} uptake rate. The curves depicting the relationship between free [Ca^{2+}] and total [Ca^{2+}] have a y-intercept with free [Ca^{2+}] 140 nM instead of 0, which is probably caused by Ca^{2+} contamination. Since I did not use the Ca^{2+} buffer, EGTA, in order to measure the pure myocyte Ca^{2+} buffering capacity, it is possible that trace amount of Ca^{2+} from some of the chemicals used, namely ATP or KCl (listed by the company as 99.5% and 99% pure, respectively) may have contaminated my solutions. Such contamination may have affected my results although I did consider all the sources of Ca^{2+} contamination, even the amount of Ca^{2+} in the Milli Q water was counted.

The following conclusion can be made from the present study:

The results indicate there is a strong Ca^{2+} buffering system in the cytosol of myocytes, which makes the free [Ca^{2+}] control more important in the study of length-dependent myofilament Ca^{2+} sensitivity in skinned cardiac muscles. A small variation of free [Ca^{2+}] corresponds to a large difference to the total [Ca^{2+}] in the cell.

The results shows that there is a ~50 fold difference between the total [Ca^{2+}] and the free [Ca^{2+}]. This number indicates the myocyte suspension Ca^{2+} buffering capacity

under my own protocol. The result is applicable for future studies for measuring the SR Ca^{2+} uptake in skinned isolated trabeculae using the same protocols.

Chapter 6

Length-dependent Ca^{2+} sensitivity in skinned rat cardiac trabeculae at physiological $[Mg^{2+}]$ and osmotic compression

6.1 Introduction

6.1.1 Similarities and dissimilarities of F-SL-pCa relationship in intact and skinned trabeculae

In previous studies of length-dependent myofilament Ca^{2+} sensitivity, investigators have shown that intact cardiac muscle and skinned cardiac trabeculae have similarly shaped force-SL relationships. Kentish et al. studied length dependence of Ca^{2+} sensitivity of cardiac muscle and indicated that the force-SL relationship in intact and skinned cardiac muscle was not different [55]. The force-SL relations for the intact muscles at an extracellular $[Ca^{2+}]$ of 1.5 mM were similar to the curves at $[Ca^{2+}]$ of 8.9 μM in the skinned preparations, which were curved away from the SL axis, whereas the curves at an extracellular $[Ca^{2+}]$ of 0.3 mM in intact muscles fell between the relations at $[Ca^{2+}]$ of 2.7 μM and 4.3 μM in the skinned preparations, which were curved toward the SL axis. Recently, further data from skinned-trabeculae studies in our laboratory have shown a similar relationship between force and SL [56]. The force-SL relationships of intact and skinned muscle both have shown that at low $[Ca^{2+}]$, the relationships are convex toward the SL-axis; at high $[Ca^{2+}]$, the curves are convex toward the F-axis. The difference of concavity and convexity reflects different activation levels of myofilaments at various $[Ca^{2+}]$. Thus, the cardiac muscle shows an increase of Ca^{2+} sensitivity with an increase of $[Ca^{2+}]$. On the other hand, at constant $[Ca^{2+}]$, the increase of SL results in increased force

development, which indicates that in the working range of cardiac SL, an increase in SL can augment myofilament Ca^{2+} sensitivity and increase active force production.

One distinct difference between intact muscle and skinned trabeculae is that the former has higher myofilament Ca^{2+} sensitivity than that of skinned cardiac fibers [55; 160]. One possible cause is that the investigators used relatively higher [Mg^{2+}] compared with that in vivo. Mg^{2+} competes with Ca^{2+} in many aspects in activating cardiac muscle. So, different [Mg^{2+}] in the test solutions for skinned studies results in different level of activation of cardiac muscle. In the skinned cardiac muscle studies from Kentish et al., the investigators reported that skinned cardiac muscle had an EC_{50} ~3.77 μM [55]. Gao et al. reported that skinned muscle had an EC_{50} ~2.2 μM and 0.93 μM with [Mg^{2+}] 1.2 mM and 0.5 mM in the skinning solutions, respectively. From work in our laboratory, the EC_{50} was found to be ~2.80 μM in skinned studies with [Mg^{2+}] 1.0 mM [56]. This result is consistent with that of Gao's. Whereas in intact muscle, the EC_{50} was 0.62 μM with free [Mg^{2+}] ~0.7 mM in Gao's study [160].

The second possible reason is that essential proteins may be lost from the cytosol during skinning. Gao et al. suggested that despite the significant effect of Mg^{2+} on the force-Ca^{2+} relation in skinned muscle, the Ca^{2+} responsiveness of the myofilaments was still altered by skinning [160]. Skinning causes loss of ~30% proteins from cytosol, especially when muscle are skinned by Triton X-100, cytosolic proteins are lost to a greater extent than that in saponin skinned preparations (~20% more loss of proteins)[146;147]. The lost proteins may contain Ca^{2+} sensitizers so that skinning can result in decrease of myofilament Ca^{2+} sensitivity.

Another effect of the loss of proteins is decreased osmolality in the cytosol, which results in swelling of the muscle and increased lattice spacing in skinned experimental preparations [93]. The lattice spacing can greatly affect the force generation by influencing either the number of cross-bridges formed in force development or the force developed by individual cross-bridges.

6.1.2 Mg^{2+} competes with Ca^{2+} in vivo

The effect of [Mg^{2+}] is not well understood but, to date, the data have shown that abnormal Mg^{2+} can greatly affect cardiac muscle contraction in many ways. At physiological concentration, Mg^{2+} acts like a modulator [161]. The influence of Mg^{2+} on myocardium includes two aspects: an effect on electrical activity and an effect on contractility. These two aspects are closely linked.

Effects of Mg^{2+} on electrical activity in ECC

Mg^{2+} affects myocardial electrical activity by influencing the resting membrane potential and Ca^{2+} influx through sarcolemma. Mg^{2+} increases the inward rectifying K^+ current and increases the threshold current requirements for activation of the triggered response [162]. Mg^{2+} also has an inhibitory effect on Ca^{2+} channels. It inhibits Ca^{2+} influx through L-type Ca^{2+} channels in the sarcolemma [163]. Investigators also suggested that Mg^{2+} could stimulate protein phosphatase and dephosphorylate Ca^{2+} channels [164]. Aomine et al. reported that Mg^{2+} may shift the threshold of various ion channels to less negative potentials, so it decreases Ca^{2+} influx through Ca^{2+} channels [165].

Mg^{2+} affects SR Ca^{2+} handling. Low [Mg^{2+}] increases the SR Ca^{2+} ATPase affinity for Ca^{2+} and the uptake rate can be increased by ~800% by low [Mg^{2+}] (<1mM)[166]. Karaki et al. reported that the contraction induced by caffeine is greatly

augmented in the absence of Mg^{2+} [167]. Kawano et al. suggested that Mg^{2+} could block the ryanodine receptor Ca^{2+} release channel in cardiac SR [168]. These investigators suggested that Mg^{2+} reduced the opening probability of SR Ca^{2+} release channels by competing with Ca^{2+} for the activation site on the SR membrane or binding to low affinity inhibition sites, which do not discriminate between Ca^{2+} and Mg^{2+}. Evidence has supported the concept that Mg^{2+} is a naturally occurring weak Ca^{2+} antagonist.

Effects of Mg^{2+} on contractile machinery

The most important effect of Mg^{2+} in skinned preparations is that Mg^{2+} has a direct effect on the contractile system. Some investigators have suggested that Mg^{2+} competes with Ca^{2+} to bind to high-affinity site on actin, which affects the conformation of actin and its ability to form nuclei and hydrolyze ATP [169]. Morimoto et al. pointed out that Mg^{2+} affected Ca^{2+} binding to TnC. They claimed that Ca^{2+} binding to the low- and high-affinity sites of TnC in myofibrils was affected by Mg^{2+} competitively and that myofibrillar ATPase activity was modulated through a competitive action of Mg^{2+} on Ca^{2+} binding to the low-affinity sites [170]. Other investigators have also proposed the mechanism that the major effect of Mg^{2+} is to reduce the rate of Ca^{2+} binding to the sites that bind Ca^{2+} and Mg^{2+} competitively due to the slow dissociation of bound Mg^{2+} from the binding sites in Tn [171].

By a variety of mechanisms, Mg^{2+} greatly affects Ca^{2+} functions in cardiac muscle. So, it is expected that the lowering $[Mg^{2+}]_{free}$ will increase the myofilament Ca^{2+} sensitivity.

6.1.3 Swollen skinned fibers

Skinning produces a "high-permeability state" of the cellular membrane. By increasing the membrane permeability, both in isolated cells and in isolated muscle strips, the ionic concentrations can be controlled and particular molecules can be introduced to the experimental milieu.

However, the removal of the sarcolemma results in swelling of the fibers, which can be recovered by the addition of polymers. This muscle swelling is caused by swelling of the myofilament lattice [99].

Effects of addition of polymer on lattice spacing

Skinned cardiac myocytes were only expanded radially with no visible alteration to longitudinal organization in any location within the cells. In skinned-fibers, physiological force development can be restored by adding polymers in skinning solutions without affecting contractile properties. Endo was the first who found that development of force was affected by osmotic compression in skinned skeletal muscles[172]. Later, Godt et al. showed that Triton skinning increases the width of muscle fiber by 20% with a 15% decrease of F_{max} and adding 4% or 5% Dextran T500 could reduce the width of skinned muscle to the intact myocyte without affecting F_{max}, whereas, adding 10% Dextran reduced the width to 86% of its intact level and decreased F_{max} to 85% [93]. Maughan et al. reported that the myofilament lattice spacing of cardiac papillary muscle increased by 8% after skinned [173]. The author suggested that swelling of the myofilament lattice in a skinned cell could be prevented by addition of 2.5% concentration of either PVP or Dextran T-500 in isolated myocyte preparations [173].

Addition of polymers, i.e. PVP and Dextrin T500, do not affect muscle striation and SL[174].

Loss of regulatory proteins in skinned fibers

It has been proven that skinning procedure causes loss of some Ca^{2+} sensitizers in cytosol. Gardner et al. reported that CaM was significantly lost in a time-dependent manner after smooth muscle was skinned by saponin or Triton X-100 [147]. In their studies, Gardner et al. demonstrated that at the end of a 1-h skinning period, tissues exposed to saponin lost 30% of total CaM and Triton X-100 skinned tissue lost 50% of the total CaM; whereas during 5-h continuous skinning procedure, total tissue CaM continued to decline. CaM loss affects the Ca^{2+} sensitivity of the myofilament in smooth muscles [158]. Triton X-100 skinned preparations tend to lose more CaM and have a lower Ca^{2+} sensitivity than that of saponin-skinned muscles [147].

Some substances have been proposed as the lost Ca^{2+} sensitizers in the skinned preparation studies of cardiac muscel. Gao et al. suggested that many factors were responsible for the disparity in the force-pCa relation between intact and skinned muscles[160]. In their studies, Gao et al. claimed that skinning caused a loss of carnosine-like compounds and taurine. Both of the two substances are natural Ca^{2+} sensitizers. The carnosine-like compounds can mildly increase Ca^{2+} sensitivity and F_{max}. Taurine can increase Ca^{2+} sensitivity without affecting F_{max} [175; 176]. Gao et al. also suggested that skinning caused the loss of CaM and MLC kinase, which impaired the phosphorylation of MLC and decrease Ca^{2+} sensitivity [177].

6.2 Hypotheses

This study aimed to detect myofilament Ca^{2+} sensitivity at physiological [Mg^{2+}] and lattice spacing in skinned cardiac muscle preparations. I studied whether physiological [Mg^{2+}] and osmotic compression could restore myofilament Ca^{2+} sensitivity in skinned rat cardiac muscle to the level of intact trabeculae. From the results of this study, I infer whether the increased lattice spacing caused by swelling of the muscle in cardiac hypertrophy and heart failure affects myofilament Ca^{2+} sensitivity. I intended to test the following hypothesis:

Myofilament Ca^{2+} sensitivity in skinned muscle was identical to intact muscle at similar [Mg^{2+}] and similar filament lattice spacing.

6.3 Materials and Methods

6.3.1 Preparation of the skinning solutions

In the skinning solutions, I mimicked intracellular conditions and strictly controlled the fractions of components in test solutions.

First, the purity of each chemical used in the experiments was considered, especially the purity of EGTA, which greatly affects the free [Ca^{2+}] in the skinning solution. Second, the pH of the skinning solutions was kept constant at 7.10 in order to mimic the in vivo condition. The experimental temperature was controlled at 25°C. Third, a computer program provided by Dr. Kentish was used to calculate free concentrations for metals and ligands in the experimental solutions.

Determining the purity of EGTA

1% error of EGTA purity can theoretically cause up to 20% error of free [Ca^{2+}] in the final test solutions[178], so the accuracy of EGTA purity is crucial.

In my experiments, the EGTA purity was determined by back-titration method [179]. In this method, I used Ca^{2+} to replace H^+ in H_4EGTA to test the actual purity. In the first step, I made 100ml of 100 mM $CaCl_2$ solution. In making this stock solution, every step was taken with extra caution, including carefully weighing and volume measuring. I assumed that this solution was 100% accurate. Then, another solution was made, which contains: 98 mM chelexed KPr, 2 mM chelexed BES, and 2mM K_2H_2EGTA. The pH of this solution was adjusted to ~9.4 by chelexed 1 M KOH. The volume of the solution was adjusted to 100 ml while the pH was kept constant ~9.4. Finally, 25 ml of 2 mM K_2H_2EGTA solution was titrated by $CaCl_2$ in very small steps (initially 50 μl and later 10 μl) at room temperature. The reaction is described by the following equation:

$$K_2H_2EGTA + Ca^{2+} \rightarrow CaK_2EGTA + 2H^+$$

A titration curve of pH vs. $CaCl_2$ volume was plotted and it had a "V" shaped curve. The concentration of H_2K_2EGTA was deduced from the $CaCl_2$ volume added. If H_2K_2EGTA was 100% pure, the [$CaCl_2$] would be 2 mM. In my experiment, I found the value of $CaCl_2$ used in my experiment was 1.92 mM, so the actual purity of EGTA I used was 96% (company report showed 97%). The actual purity of EGTA was derived from the following equation:

Actual purity = actual concentration / theoretical concentration

pH measurement

pH measurement is important in making skinning solution since pH greatly affects the force-pCa relationship. First, in order to keep pH value constant, I chose a strong pH buffer BES, which has a pKa of 7.1 at 23°C and decreases 0.016 unit per degree increase of temperature. Second, I calibrated the pH electrode (Ross-combination

electrode, Orion, Boston, MA) with two standard solutions: pH 4.01 buffer and pH 7.00 buffer (Orion Research Inc., Beverly, MA) each time I made skinning solutions. Last, a substantial junction potential could contribute a big error in the pH measurement [180]. We (including previous investigators in our laboratory) checked the liquid junction potential of the pH electrode and found the effect was minimal so, subsequently it was ignored.

Determining solution compositions on a computer program

The free concentrations for all compositions were determined by a computer program. The detailed procedure was described by Kentish et al. [55]. All binding constants were originally taken from Martell and Smith at 0.1 mM IS and 20 °C [181]. Then the constants were adjusted to 0.2 mM IS and 25 °C according to the procedure of Harrison and Bers [152]. Two important equations were used to adjust binding constants:

1) Correction of the binding constant for different temperature: Van't Hoff equation:

$\text{Ln } K_2 = \text{Ln } K_1 + (\Delta H/R)(1/T_1 - 1/T_2)$

K_2 and K_1 are binding constant at temperature T_1 and T_2 respectively. R is the gas constant. ΔH is the molar enthalpy.

2) Correction of the binding constant for different IS: Debye-Huckel limiting equation:

$\text{Log } K_2 = \log K_1 + 2xy\ (\log f_1 - \log f_2)$

K_2 and K_1 are binding constants at ionic equivalence I_{e2} and I_{e1} respectively, f_1 and f_2 are coefficient constants of K_1 and K_2 respectively, x and y are the valence of the metal and ligand.

$\log f_1 = A[I_{e1}^{0.5}/(1+ I_{e1}^{0.5})-0.25\ I_{e1}]$

$\log f_2 = A[I_{e2}^{0.5}/(1+ I_{e2}^{0.5})-0.25\ I_{e2}]$

$A=1.8246*106(\epsilon T1)-1.5$, ϵ is the dielectric constant of solvent.

Table 6-1: Corrected binding constants for Ca^{2+} at ionic strength 0.2 M and 25 °C (mol/L).

LIGAND-ION COMPLEX	BINDING CONSTANT for Ca^{2+}
HBES	7.61
H_2EGTA^{2-}	18.2
H_4EGTA	22.9
$NaEGTA^{3-}$	1.38
$CaHEGTA^{1-}$	14.4
$MgHEGTA^{1-}$	12.6
H_2ATP^{2-}	10.5
$NaATP^{3-}$	1.20
$CaHATP^{1-}$	8.23
$MgHATP^{1-}$	8.38
MgHCP	1.30
$HEGTA^{3-}$	9.36
H_3EGTA^{1-}	20.9
$KEGTA^{3-}$	0.96
$CaEGTA^{2-}$	10.6
$MgEGTA^{2-}$	4.96
$HATP^{3-}$	6.49
$KATP^{3-}$	0.90
$CaATP^{2-}$	3.45
$MgATP^{2-}$	3.80
CaHCP	1.15
Hprop	4.72

HBES: pKa=7.10 at 22.8 °C. dpKa/dt=-0.016/°C[182] was used to correct pKa at 25 °C.

Ie=0.5 Sum(Zi^2*Ci), Zi and Ci are charge and concentration of ion i, respecitvely. The corrected binding constants are shown in Table 6-1.

Removal of possible contaminated Ca^{2+}

The resin CHLEX 100 was chosen to remove all contaminated Ca^{2+} from compounds used and containers. CHLEX 100 has a very high affinity for Ca^{2+}, Mg^{2+}, Fe^{2+} and Cu^{2+}. The solutions chelexed included: KOH solution, BES buffer solution, and KPr solution.

1) KOH chelexing

1M KOH was made from mixing KOH tablets 56.11 g with 1L Milli Q water.

In order to remove Ca^{2+}, CHELEX 100 was first converted to the K^+-CHELEX form from the Na^+- CHELEX form. A 130-150 ml volume of CHELEX 100 was mixed with 100 ml of 1 M HCl. In a plastic beaker, this mixture was stirred with a teflon stirrer for 10-15 minutes; then the beads were allow to settle. The HCl was decanted and another 100 ml 1M HCl was added and the above step was repeated once. CHELEX 100 was converted from the Na^+ form to the H^+ form and the volume of the resin shrank about 50%. The resin was washed once with ~100 ml deionized water for 5 minutes. After that, the resin was poured into a column and a pump (Econo-column pump, Bio-Rad) continuously sucked the water out at a rate of 1 drop/s. Before the water level was below the resin, a small volume of KOH was carefully added into the column. After that, the volume of the resin gradually expanded while it changed from the H^+-CHELEX form to the K^+- CHELEX form. During this procedure, pH was carefully monitored. The initial exiting solution with pH ~0.5 was discarded. KOH collection was started when the existing solution's pH was ~14 at room temperature. This volume of resin was capable of

chelexing ~1500 ml KOH and the chelexed KOH was stored in 4 °C refrigerator or room temperature.

This procedure involved two chemical changes:

$$\text{Na-Chelex} + \text{HCl} \leftrightarrow \text{H-Chelex} + \text{NaCl}$$

$$\text{H-Chelex} + \text{KOH} \leftrightarrow \text{K-Chelex} + H_2O$$

2) BES buffer and KPr chelexing

Another 120 ml of H- CHELEX 100 was prepared as described the above. Then the resin was washed with 100 ml deionized water. The resin was allowed to settle down and half of the water was decanted. After that, the resin was titrated with chelexed KOH in very small steps while being stirred. The pH was monitored to ensure that the pH never exceeded 7.10. When the pH was close to 7.10, a few extra minutes were allowed to pass between each addition of chelexed KOH because pH rose rapidly and dropped gradually with addition of KOH. It was crucial to keep pH below 7.10 otherwise additional propionic acid was required, but this was not ideal because this chemical had not been chelexed. At this moment, the volume of the resin returned to its initial size but it was in K^+-CHELEX form. Then, the resin was poured into a column and the water was constantly sucked out by a pump.

A 500 ml volume of 500 mM stock BES buffer was prepared by dissolving 53.30 g of BES in deionized water. The pH was corrected to 7.10 with chelexed KOH. KPr was made by titrating 200 ml 1M chelexed KOH with pure concentrated (~13.5M) propionic acid to pH 7.1 at 25 °C.

Before the water level was below the resin, BES buffer was carefully added into the column without disturbing the resin bed. The initial exiting 50~100 ml solution was

discarded. When the existing solution had a pH value close to ~7.10, the solution was collected in a plastic container. Before the BES buffer level had fallen below the resin, KPr was added into the column and the solution started to be collected until the exiting solution had a pH value ~7.10. Then, the collected BES and KPr were stored in –20°C.

Stock solution making procedure

The stock solution was made at 1.25 times of the concentrations of the final testing solutions. The detailed concentration of each component was shown in Table 6-2.

K_2H_2EGTA and CaK_2EGTA solutions

The final test solutions were made by mixing K_2H_2EGTA and CaK_2EGTA solutions in different proportions to keep the [EGTA] and [Mg^{2+}] constant while free [Ca^{2+}] varied. Briefly, H_2K_2EGTA was made from EGTA titrated with chelexed KOH. Since Ca^{2+} was bound much more strongly to EGTA than was Mg^{2+}, $MgCl_2$ was added to the solution and the amount was 5 times the difference between the total [Mg^{2+}] in relaxation solution (RS) and total [Mg^{2+}] in the activation solution (AS): 5 x (5.30-4.95) = 1.75 mM. pH was corrected to 7.0 at 25 °C by chelexed KOH. CaK_2EGTA was prepared by mixing equal molar concentrations of $CaCO_3$ and free acid H_4EGTA. 1 M chelexed KOH was used to dissolve EGTA and adjust the pH to 7.10 at 25 °C. Both H_2K_2EGTA and CaK_2EGTA solutions were made 5 times more concentrated than their final concentrations so that they could be diluted when they were mixed with the stock solution in a 1:4 ratio.

AS, RS, testing solutions and skinning solution

Skinning solutions (SK), RS and concentrated AS have the same basic components except that the skinning solution has 1% Triton X100, and activating

solutions have different amount of Ca^{2+}. The basic components in the experimental solutions are (in mM): BES 100, Na_2ATP 6.8, Na_2CrP 10, KPr 55, $MgCl_2$ 5, DTT 1, and EGTA 10. In all solutions, ionic strength was 0.2 M, net charge was ~0.000 and pH was 7.1. [Mg^{2+}] was kept ~0.7 mM in all solution. Both RS and AS contained 5% Dextran in order to increase osmolality.

The AS or RS was made by mixing of 4 units of stock solution and 1 unit either of CaK_2EGTA or H_2K_2EGTA solution, respectively. The concentrations of components were shown in Table 6-3 and Table 6-4.

The test solutions were prepared by mixing AS and RS in different proportions. Details are shown in Table 6-5. When various volumes of AS and RS were mixed, the concentration of EGTA and [Mg^{2+}] were always kept constant with [Ca^{2+}] varied from 0 to 23.7 μM.

The quality of the solutions made was tested by fura-2 measurement. In a series of measurements, fura-2 never detected any Ca^{2+} in RS and skinning solutions. The actual free [Ca^{2+}] measured by fura-2 in testing solutions was identical to calculated values.

Triton X-100 skinning solution was made by addition of 1 % Triton X-100 in RS.

6.3.2 Materials and general methods

Trabeculae were taken from right ventricles of 250 to 300g male LBN (Lewis Brown Norway) rats. The rats were anesthetized by diethyl ether and the thoraxes were opened acutely. The hearts were excised and perfused by HEPES solution with [Ca^{2+}] 0.3 mM and high [KCl] 20 mM within a few seconds. Only thin, long, straight and rectangularly shaped trabeculae were selected. The average length, width, and thickness of the trabeculae were 3.37±0.13 mm, 0.24±0.04 mm, and 0.10±0.01 mm

Table 6-2. The concentrations of the components in the stock solution and the final test solutions, at 25°C, pH 7.10, 0.20 M IS and a net charge of 0.000.

Species	Stock Solution (1.25X) mM	Final Solution (mM)
BES buffer	125	100
Na2ATP	8.5	6.8
Na2CrP	12.5	10
KPr	68.8	55.0
MgCl2	6.19	4.95
DTT	1.25	1.0

Mixing the stock solution with either H_2K_2EGTA or CaK_2EGTA in 4:1 ratio made the final AS and RS solutions.

DTT can prevent the generation of oxygen free radicals, so it can increase the stability of the muscle.

Table 6-3. Total concentration (in mM) of final components in AS and RS solutions at 25°C, pH 7.10, 0.20 M IS and a net charge of 0.000. AS is concentrated high [Ca^{2+}] solution, which was diluted to make final test solutions.

Species	AS	RS
BES	100	100
KPr	55.0	55.0
$MgCl_2$	4.95	5.30
Na_2ATP	6.80	6.80
Na_2CP	10.0	10.0
DTT	1.00	1.00
EGTA	10.0	10.0

Table 6-4. Free concentrations (in mM) of final components in AS and RS solutions at 25°C, pH 7.10, 0.20 M IS and a net charge of 0.000.

Species	AS	RS
$HBES/BES^-$	48.3/51.7	48.3/51.7
K^+	139	139
Na^+	33.1	33.1
Mg^{2+}	0.71	0.70
Ca^{2+}	0.02	0.0
$MgATP^{2-}$	4.09	4.11
Cl^-	9.90	10.6
Pr^-	54.8	54.8
$HCrP^-$	9.86	9.86
$EGTA^{4-}$	0.00	0.00

Table 6-5: $[Ca^{2+}]$ and $[Mg^{2+}]$ in the testing solutions at 25°C, pH 7.10. Ionic strength is ~0.20 mM, ionic equivalent is 0.17 mM, and net charge is 0.000.

AS (μl)	RS (μl)	Total $[Mg^{2+}]$ (mM)	Free $[Mg^{2+}]$ (mM)	Total $[Ca^{2+}]$ (mM)	Free $[Ca^{2+}]$ (μM)	pCa
1000		4.95	1.04	12.5	915	3.04
1000	0	4.95	0.71	10.0	23.7	4.63
990	10	4.95	0.70	9.90	13.7	4.86
980	20	4.96	0.70	9.80	8.84	5.05
975	25	4.96	0.70	9.75	7.39	5.13
950	50	4.97	0.70	9.50	3.89	5.41
900	100	4.99	0.70	9.00	1.89	5.72
875	125	4.99	0.70	8.75	1.47	5.83
850	150	5.00	0.70	8.50	1.19	5.92
800	200	5.02	0.70	8.00	0.84	6.07
775	225	5.03	0.70	7.75	0.73	6.14
750	250	5.04	0.70	7.50	0.63	6.20
700	300	5.06	0.70	7.00	0.49	6.31
600	400	5.09	0.70	6.00	0.32	6.50
500	500	5.13	0.70	5.00	0.21	6.68
400	600	5.16	0.70	4.00	0.14	6.85
300	700	5.20	0.70	3.00	0.09	7.04
200	800	5.23	0.70	2.00	0.05	7.28
100	900	5.27	0.70	1.00	0.02	7.63
0	1000	5.30	0.70	0.00	0.00	

(mean±SE, n=15), respectively. The trabeculae were equilibrated in HEPES buffer (mM): NaCl 140, KCl 4, Na-Acetate 2.8, $MgSO_4$ 1.2, HEPES 10, glucose 10, taurine 10, $CaCl_2$ 0.7 and pH 7.4. During the equilibrating period at ~25°C, the trabeculae were stimulated 1.5 times threshold at 0.5 Hz for 30 to 60 minutes.

Then the trabeculae were skinned by a standard skinning solution containing 1% Triton X-100 for 30 minutes. Following this step, the muscles were washed in relaxing solution (Ca^{2+} free) 5 times to ensure that all Triton X-100 was totally washed out. Force was measure by a silicon strain gauge (Sensonor AE801, Horten, Norway). A carbon fiber extension was glued on the element of the force transducer in order to increase the sensitivity of the force transducer. The noise of the transducer is < 15 μN. The trabeculae were mounted in a steel basket glued on the carbon fiber. The valve side of the muscle was hooked on a motor arm. The muscle length or SL was changed by controlling the position of the motor arm.

The SL was measured by laser diffraction techniques, as described by ter Keurs et al. [54]. A laser beam was projected on the trabecula and diffracted into multiple orders. The angle between zero order and the diffracted beam was reciprocal to the SL. The diffracted beam was sensed by a reticon. In this way, change of SL can be detected.

During the experiments, the relative zero force point was set at SL ~1.86 μm in relaxation solutions. Then, the trabeculae were set at resting SL 2.10 μm before each activation. The trabeculae were activated by 6 activating solutions containing free [Ca^{2+}] ranging from 0.49 μM to 3.89 μM. In some experiments, increase of the [Ca^{2+}] to 7.39 μM revealed no further increase of developed force in the presence and absence of Dextran. At this high [Ca^{2+}], the SL diffraction pattern deteriorated. After each activating,

the trabeculae were put back into relaxation solutions to relax for 2 minutes, and the force baseline was checked and adjusted again if it had changed. In most experiments, the trabeculae were activated from highest ($[Ca^{2+}]$:3.89 μM) to the lowest activating solution ($[Ca^{2+}]$: 0.49 μM) since the active force gradually decreased in the skinned fibers [55]. In this way, the error of force measurement was minimized. In a few experiments, the trabeculae were activated from the lowest to the highest activating solution. The results from the two methods were similar. In each individual experiment, the reference force was measured at $[Ca^{2+}]$ 3.89 μM and SL ~2.15 μm at the end of experiments. If the reference force decreased over 20%, the result was discarded. All experiments were completed in ~1 hour so that the force decrease was minimized.

In all the steps during experiments, the temperature was controlled ~25 °C as that temperature was used by investigators previously for in intact trabeculae studies.

6.3.3 Data analysis

F-SL relationship was fitted into the equation[55]:

$$F=a(SL-SL_0)^b,$$

where SL_0 was the intercept with the abscissa. Passive force at different SL was fit the same equation.

Interpolated data from force-SL relationships were used to generate force-pCa relationships. The curves were fitted into Hill's relationship[55]:

$$F=F_{max}X^n/(EC_{50}{}^n+X^n),$$

where Fmax was the maximal force developed at the SL studied, EC_{50} was the free $[Ca^{2+}]$ of the half maximal force generated.

In the study of cooperativity, I plotted linearized force-pCa relationship: log[U/(1-U)] vs. pCa, whereas U was the ratio of the force developed over the F_{max} at the SL studied. This kinds of plot gave two values of Hill coefficient corresponding to the different level of $[Ca^{2+}]$, which reflect different level of coorperativity with different force development.

The data were subjected to one-way ANOVA or unpaired t-test for statistical analysis.

6.4 Results

6.4.1 Force-SL relationship in skinned cardiac rat trabeculae

Force-SL relationships with Dextran and without Dextran were studied in 6 different activating solutions, which contained free $[Ca^{2+}]$: 3.89, 1.89, 1.19, 0.84, 0.63 and 0.49 μM in SL ranging from 1.55 μm to 2.15 μm. Force was normalized by force generated at $[Ca^{2+}]$ 1.19 μM and SL 2.10 μm.

Eight trabeculae were studied in solutions containing Dextran T500. Figure 6-1 shows the raw data with the fitting curves for force-SL relationships. Figure 6-2 shows the force-SL relationships after the data were binned. At high $[Ca^{2+}]$ 3.89 μM, the sarcomeres could shorten to SL ~1.55 μm while developing ~60% of F_{max}. At short length (~SL 1.60 μm to 1.7 μm) and high $[Ca^{2+}]$, the curve of force-SL relationship was very steep, indicating that a small increase of SL developed substantial force. Further increase of SL increased active force less and at SL >2.10 μm, the active force development tended to reach a plateau. The trabeculae generated F_{max} at $[Ca^{2+}]$ 3.89 μM and SL 2.15 μm 108±6 mN/mm^2.

Seven trabeculae were studied in non-Dextran group as my controls. Figure 6-3 shows the force-SL relationships in non-Dextran group. The curves were similar to those in the Dextran group. Increasing SL increased force development. In this group of preparations, the muscle also developed F_{max} in $[Ca^{2+}]$ 3.89 μM at SL 2.15 μm. The F_{max} was 79±8 mN/mm^2 .

The data from the two groups confirm that $[Ca^{2+}]$ greatly affects the force-SL relationship. At low $[Ca^{2+}]$, the curves of force-SL relationship are convex toward SL-axis and at high $[Ca^{2+}]$, the curves are curved toward froce-axis. The presence or absence of Dextran had little effect on the shape of force-SL relationships. But the addition of 5% Dextran did indeed change the F_{max} developed between the two experimental groups.

6.4.2 Force-pCa relationship in skinned cardiac rat trabeculae

Figure 6-4 and Figure 6-5 shows the force-pCa relationships from interpolated force-SL data in the Dextran group and non-Dextran group. Force-pCa relationship is sigmoidal. With stretch, the F_{max} gradually increased and EC_{50} gradually decreased. The change of F_{max} and EC_{50} along with stretch is shown in the following Table 6-6 and Table 6-7.

6.5 Discussion

At physiological $[Mg^{2+}]$ and osmotic compression, the values of EC_{50} are lower than those in controls (Figure 6-6). These EC_{50} values (~1μM at SL 2.15 μm) in both Dextran treated and non-Dextran groups are substantially lower than those of previous skinned preparation studies done with high $[Mg^{2+}]$, in which EC_{50} ranged from 2 μM to 3 μM [55; 56; 160]. However, these EC_{50} values are still substantially higher than those of intact cardiac muscle. Gao et al. suggested that intact rat cardiac muscle had an EC_{50} of 0.62

Table 6-6: Change of F_{max} with the change of SL in with and without Dextran groups. All data are mean±SE. The statistical analysis shows the difference between the two groups is significant (ANOVA, $p<0.001$).

SL(μm)	F_{max}(mN/mm^2)(with Dextran)	F_{max}(mN/mm^2)(without Dextran)
1.90	94±3	71±4
1.95	97±3	73±5
2.00	100±4	75.±6
2.05	102±4	77±7
2.10	105±5	78±7
2.15	108±6	79±8

Table 6-7: Change of EC_{50} with the change of SL in with Dextran and without Dextran group. EC_{50} gradually decreases with increase of SL in both groups. All data are mean±SE. EC_{50} in with Dextran group is lower than that in without Dextran group (ANOVA, $p<0.05$). At longer SL (2.15 μm), the difference is negligible (unpaired t-test, $p>0.2$).

SL(μm)	EC_{50}(μM)(with Dextran)	EC_{50}(μM)(without Dextran)
1.90	1.41±0.05	1.55±0.09
1.95	1.33±0.05	1.48±0.11
2.00	1.25±0.05	1.40±0.12
2.05	1.17±0.05	1.32±0.13
2.10	1.10±0.06	1.21±0.13
2.15	1.03±0.06	1.06±0.14

Figure 6-1: Force-SL relationships from 8 trabeculae in Dextran group. The basic shape of force-SL is similar to that of intact rat cardiac muscle and skinned cardiac muscle with high [Mg^{2+}]. At high [Ca^{2+}] (3.89 μM and 1.89 μM), the curves are convex to the force-axis, whereas at low [Ca^{2+}] (0.49 μM, 0.63 μM, and 0.84 μM), the curves are convex to SL-axis, at intermediate [Ca^{2+}] (1.19 μM), the force-SL relationship is close to linear. Increase of SL increases force development. Force is normalized by the active force generated at [Ca^{2+}] 1.19 μM and SL 2.15 μm.

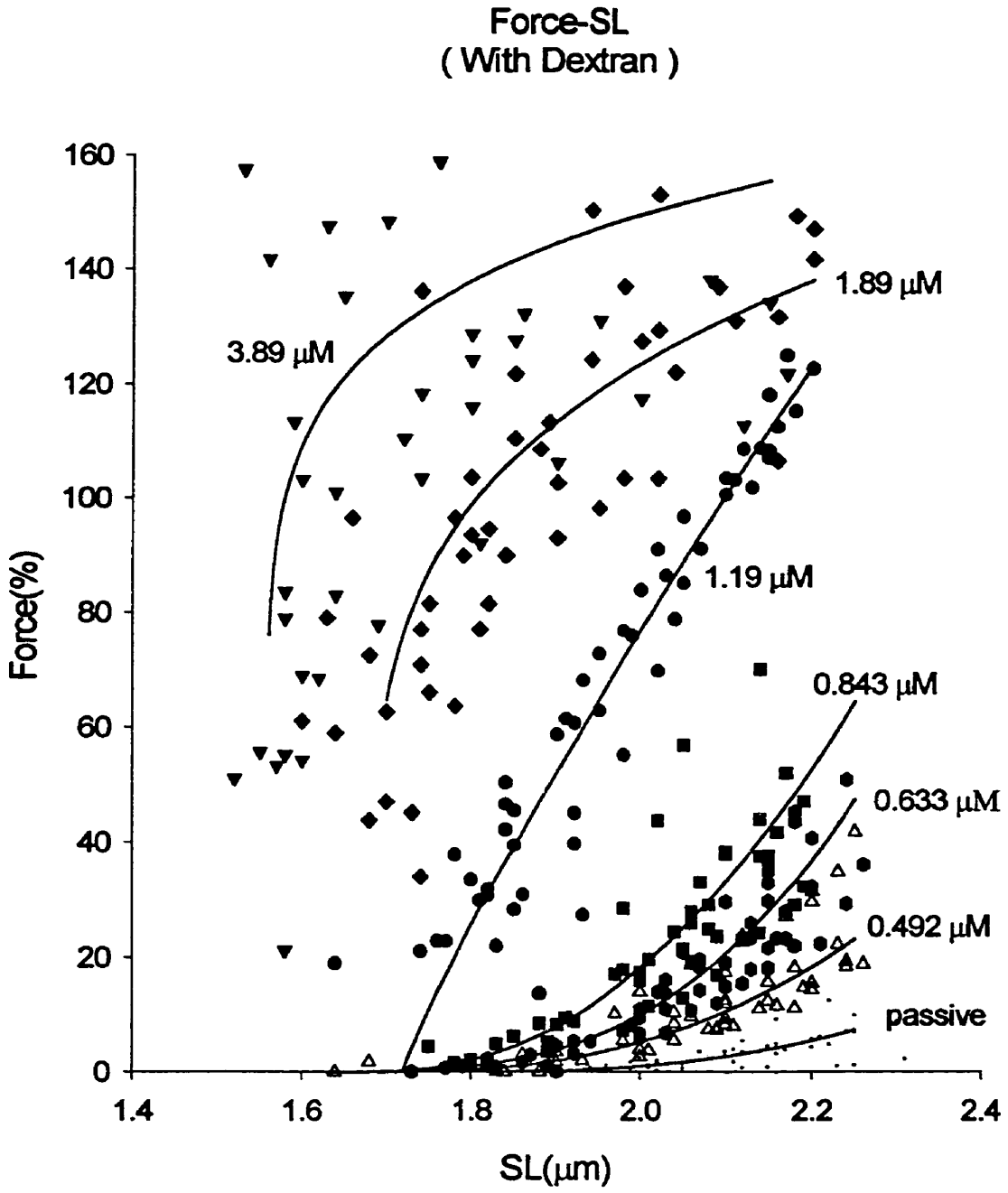
Force-SL
(With Dextran)
160
140
120
100
80
60
40
20
0
Force(%)
1.4
1.6
1.8
2.0
2.2
2.4
SL(μm)
3.89 μM
1.89 μM
1.19 μM
0.843 μM
0.633 μM
0.492 μM
passive

Figure 6-2: Force-SL relationships of binned data from 8 trabeculae. The curves are fitted into the equation: $F=a(SL-SL_0)^c$. The basic shape of F-SL after binning is similar to that in original fitting curves. At high $[Ca^{2+}]$, the curves are convex to force-axis; at intermediate $[Ca^{2+}]$, force-SL is close to linear and at low $[Ca^{2+}]$, the curves are convex to SL-axis. Increase of SL increases force development. All the constants: SL_0 (SL intercept) and c (curvature of the curves) are comparable to those published by Kentish et al.

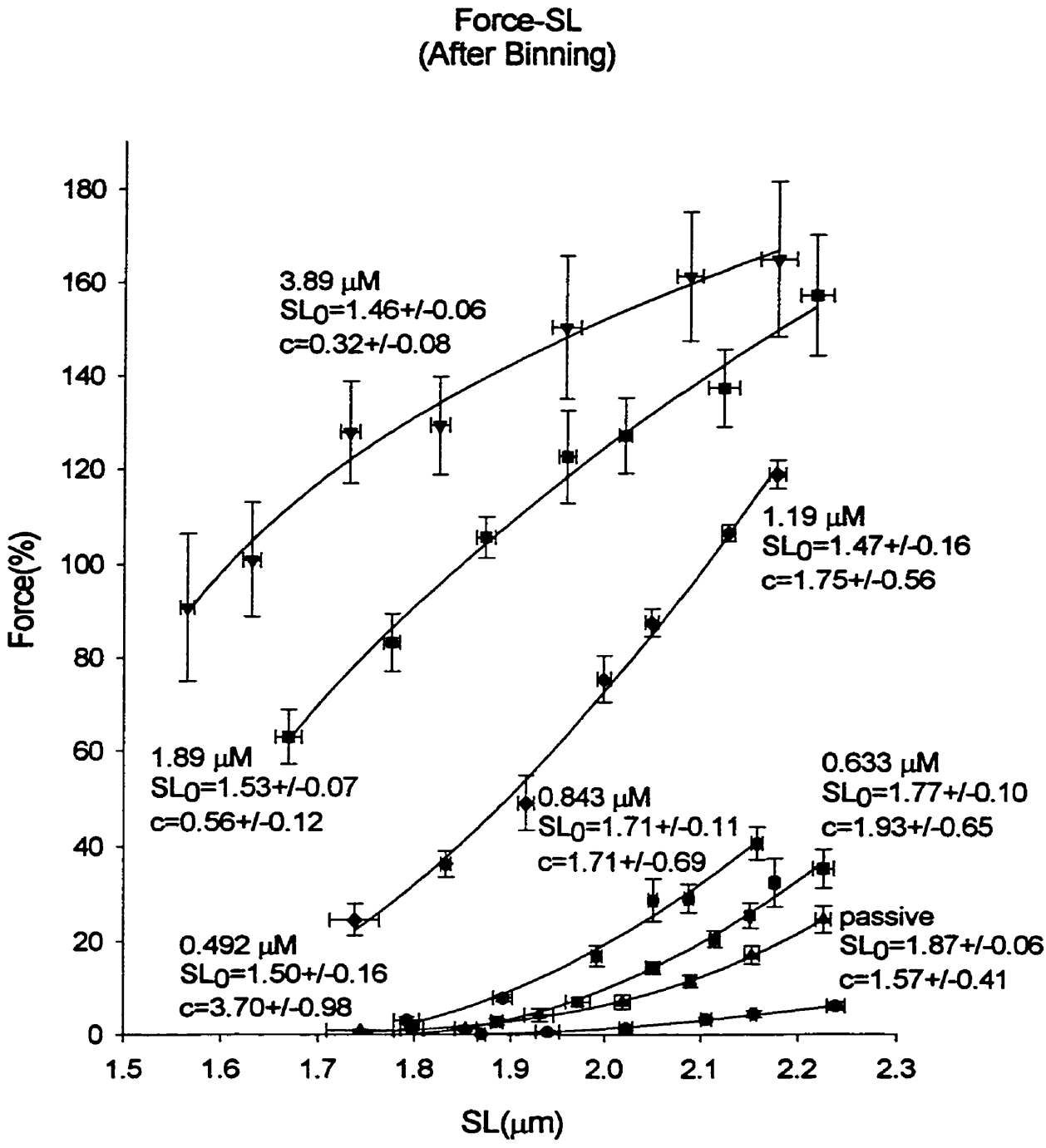
Force-SL
(After Binning)
Force(%)
SL(μm)
180
160
140
120
100
80
60
40
20
0
1.5
1.6
1.7
1.8
1.9
2.0
2.1
2.2
2.3
3.89 μM
SL0=1.46+/-0.06
c=0.32+/-0.08
1.89 μM
SL0=1.53+/-0.07
c=0.56+/-0.12
1.19 μM
SL0=1.47+/-0.16
c=1.75+/-0.56
0.843 μM
SL0=1.71+/-0.11
c=1.71+/-0.69
0.633 μM
SL0=1.77+/-0.10
c=1.93+/-0.65
0.492 μM
SL0=1.50+/-0.16
c=3.70+/-0.98
passive
SL0=1.87+/-0.06
c=1.57+/-0.41

Figure 6-3: Force-SL relationships from 7 trabeculae of binned data in the control group (without Dextran). The shape of the curves is similar to those in the Dextran group. The curvature of the curves shifts with the change of $[Ca^{2+}]$, which indicates that change of myofilament Ca^{2+} sensitivity along with the change of $[Ca^{2+}]$. At high $[Ca^{2+}]$, the curves of force-SL relationships are convex toward to force-axis, whereas at low $[Ca^{2+}]$, the curves are convex toward to SL-axis. At the intermediate $[Ca^{2+}]$, the force-SL relationship is linear. In all $[Ca^{2+}]$ tested, increase of SL results in increase of force development.

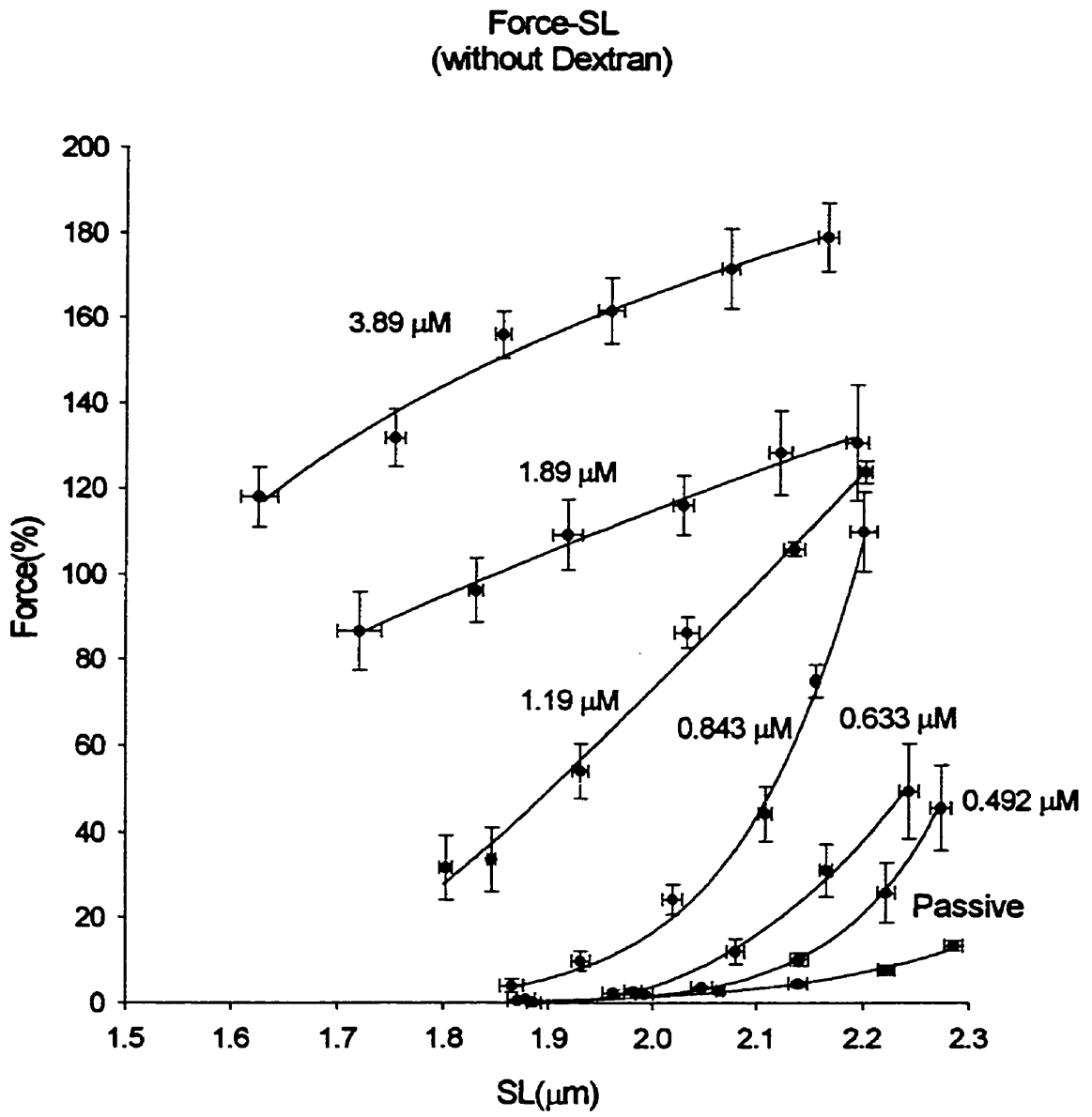
Force-SL
(without Dextran)
Force(%)
SL(μm)
200
180
160
140
120
100
80
60
40
20
0
1.5
1.6
1.7
1.8
1.9
2.0
2.1
2.2
2.3
3.89 μM
1.89 μM
1.19 μM
0.843 μM
0.633 μM
0.492 μM
Passive

Figure 6-4: Force-pCa relationships from interpolated force-SL data in the with Dextran group. For clarity, the different levels of force development corresponding to SLs are separated into two different groups. The top figure represents force generated at SL 1.85, 1.95, 2.05, 2.15 μm, respectively. The bottom figure represents force generated at SL 1.80, 1.90, 2.00, 2.10 μm, respectively. The force-pCa relationship is sigmoidal. With increase of SL, the curves shift leftward while the F_{max} gradually increases and EC_{50} gradually decreases, which indicates that increase of SL increases myofilament Ca^{2+} sensitivity. F_{max} in Dextran group is 108±6 mN/mm^2. The SLs are activated SLs during muscle contraction.

Force-pCa
(With Dextran)

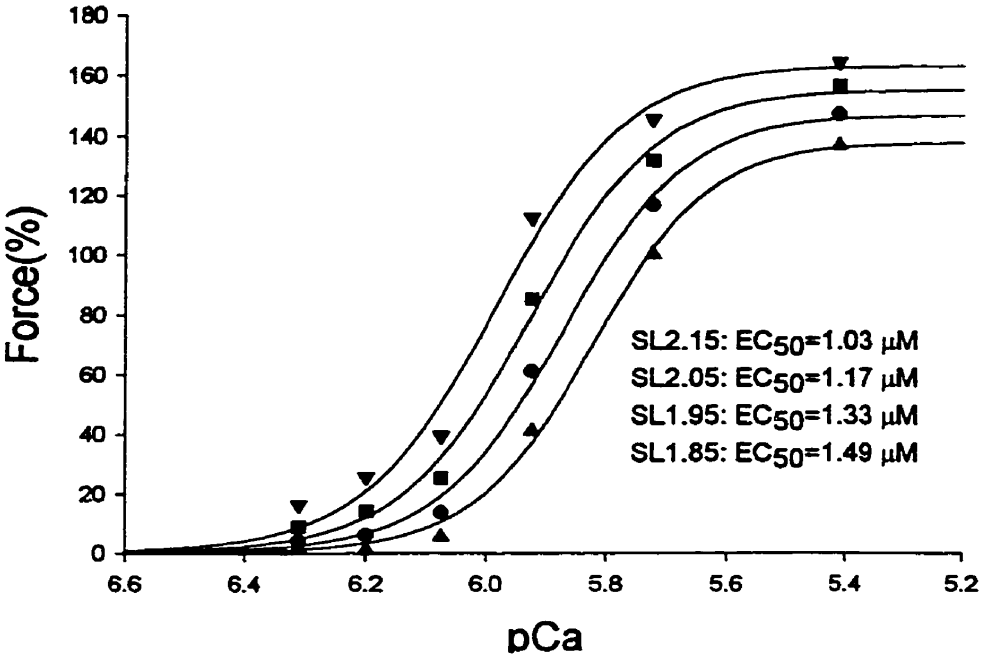

Force-pCa
(with Dextran)

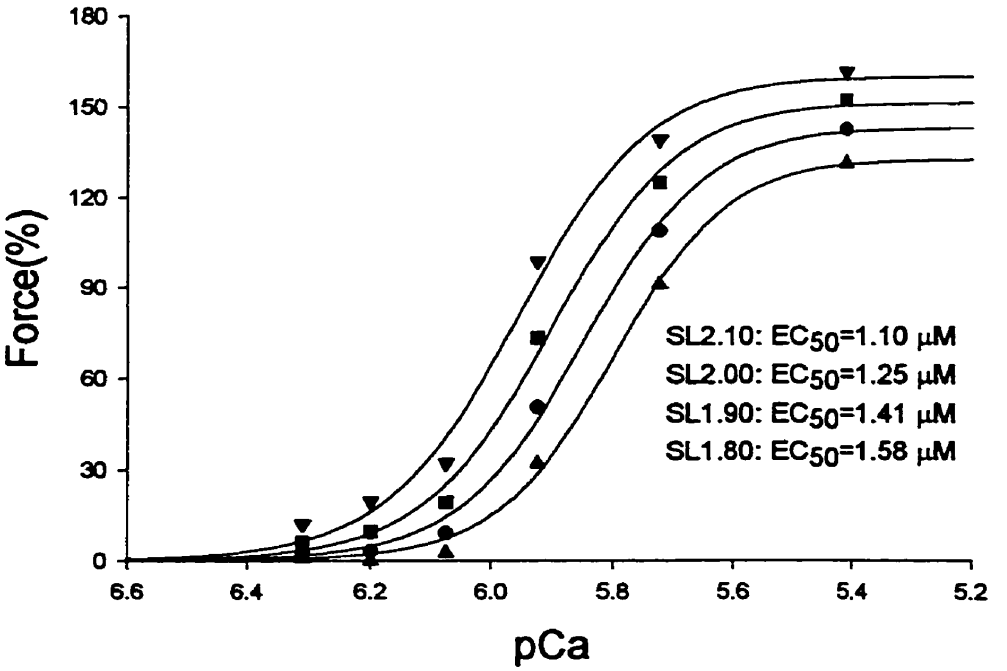

Figure 6-5: Force-pCa relationships from interpolated force-SL data in the non-Dextran group. For clarity, the different levels of force development at corresponding SLs are separated into two different groups. The top figure represents force generated at SL 1.95, 2.05, 2.15 μm, respectively. The bottom figure represents force generated at SL 1.90, 2.00, 2.10 μm, respectively. The F-pCa relationship is sigmoidal. With increase of SL, the F_{max} gradually increases and EC_{50} gradually decreases, which indicates that increase of SL increases myofilament Ca^{2+} sensitivity. F_{max} in non-Dextran group is 79±8 mN/mm^2. The SLs indicated are activated SLs during muscle contraction.

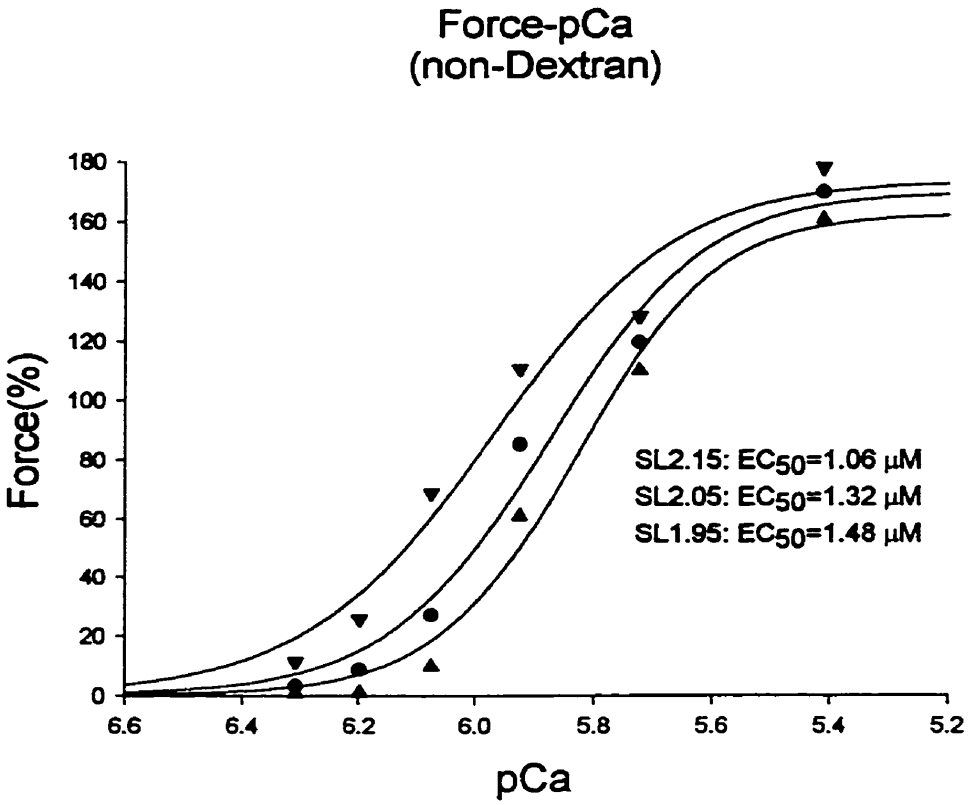
Force-pCa
(non-Dextran)
Force(%)
pCa
SL2.15: EC50=1.06 μM
SL2.05: EC50=1.32 μM
SL1.95: EC50=1.48 μM

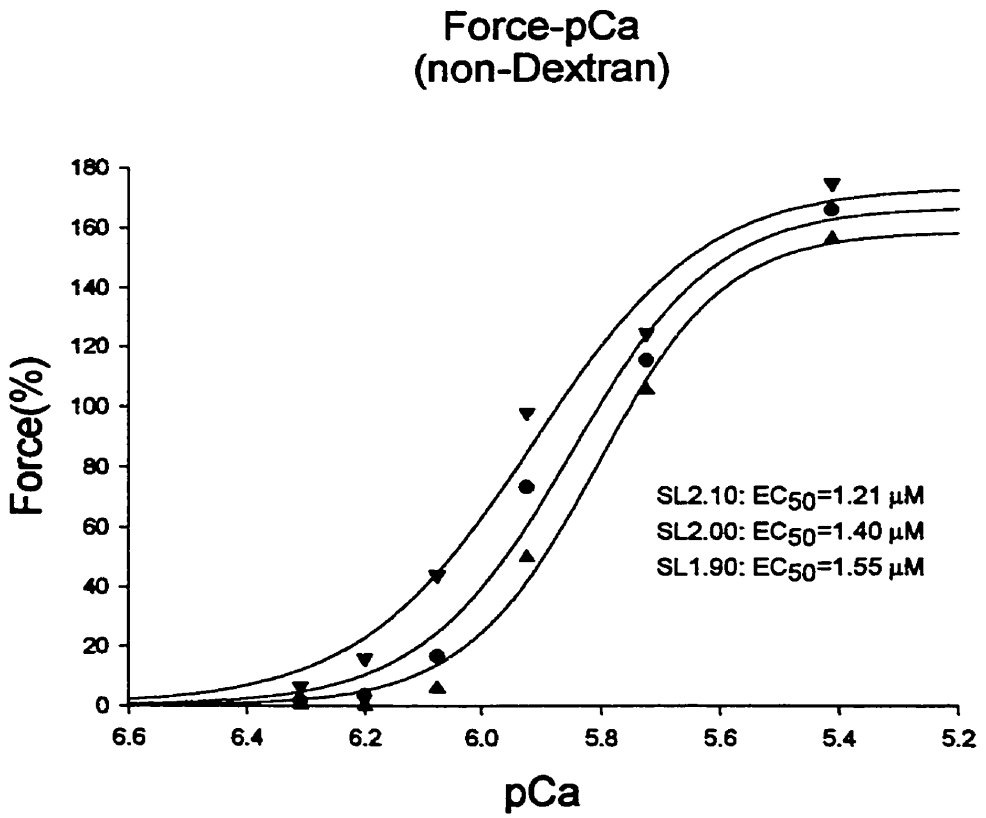
Force-pCa
(non-Dextran)
Force(%)
pCa
SL2.10: EC50=1.21 μM
SL2.00: EC50=1.40 μM
SL1.90: EC50=1.55 μM

μM [160]; Hollander et al. in our laboratory reported that the intact rat trabeculae had an EC_{50} of 0.38 μM from the same strain of rats [183]. It seems that skinned preparations decrease the Ca^{2+} sensitivity of the myofilament contractile apparatus. However, the correction of $[Mg^{2+}]$ and osmotic compression in my skinned preparation study did reduce the EC_{50} to 1.03 μM and 1.06 μM at SL 2.15 μm with and without Dextran T500, respectively, which indicates that the myofilament Ca^{2+} sensitivity increased to some extent compared with the data from previous studies on skinned trabeculae.

Many factors contribute to the low Ca^{2+} sensitivity for cardiac myofilaments in the skinned preparations. Temperature, $[Mg^{2+}]$, myofilament lattice spacing and cytosolic Ca^{2+} sensitizers are important elements that could affect cardiac myofilament Ca^{2+} sensitivity.

6.5.1 Effects of temperature on cardiac myofilament Ca^{2+} sensitivity

Temperature can greatly affect myofilament Ca^{2+} sensitivity. Temperature affects EC_{50} of myofilament Ca^{2+} sensitivity in a species-dependent manner. In rabbit cardiac muscle, Harrison and Bers et al. reported that increase of temperature increased active force development and increased myofilament Ca^{2+} sensitivity [184]. In intact cardiac trabeculae, from the same strain of rats I used in this study, de Tombe et al. in our laboratory found that increase of temperature decreased myofilament Ca^{2+} sensitivity from EC_{50} 0.66 μM at 20 °C to 1.73 μM at 30 °C [185], respectively. This could explain why EC_{50} is higher in my experiment compared with that in intact muscle from Gao's studies (1.03 μM vs. 0.62 μM). My experiments were conducted under 25 °C, where Gao et al. did their experiments at 22 °C. Higher temperature increased EC_{50} value and lowered myofilament Ca^{2+} sensitivity in rat skinned trabeculae.

6.5.2 Effects of [Mg^{2+}] on cardiac myofilament Ca^{2+} sensitivity

Gao et al. found that the free Mg^{2+} is approximately 0.7 mM in vivo [160], which is much lower than that used in previous skinned studies ranging from 1mM to 5 mM.

Mg^{2+} competes with Ca^{2+} in vivo in many ways, but the exact mechanism is still unknown. Mg^{2+} affects the Ca^{2+} sensitivity of myofilament in skinned preparations probably through its effects on Tn. Potter et al. reported that the major effect of Mg^{2+} was to reduce the rate of Ca^{2+} binding to the sites that bound Ca^{2+} and Mg^{2+} competitively due to the slow dissociation of bound $Mg^{2+}$from Tn [171]. In skinned muscle, Mg^{2+} affects Ca^{2+} binding to the low and high affinity sites of TnC [170]. Morimoto et al. claimed that Ca^{2+} binding to the low- and high- affinity sites of TnC in myofibrils was affected by Mg^{2+} competitively and that myofibrillar ATPase was modulated through a competitive action of Mg^{2+} on Ca^{2+} binding to the low- affinity sites. By a variety of mechanisms, Mg^{2+} affects Ca^{2+} functions in cardiac muscle. It is expected that the lower $[Mg^{2+}]_{free}$ will increase the myofilament Ca^{2+} sensitivity and higher $[Mg^{2+}]_{free}$ tends to lower myofilament Ca^{2+} sensitivity.

Since $[Mg^{2+}]$ greatly affects myofilament Ca^{2+} sensitivity, it is crucial to mimic the exact in vivo $[Mg^{2+}]$ in the skinning solution preparations. In different skinning preparations, investigators have reported different EC_{50} values for cardiac myofilament Ca^{2+} sensitivity. From rat cardiac trabeculae, Gao et al. reported skinned muscle had an EC_{50} of 2.2 μM and 1.13 μM using skinning solutions with $[Mg^{2+}]$ 1.2 mM and 0.5 mM[160], respectively; Kentish et al. suggested that skinned rat cardiac trabeculae had an EC_{50} of 3.77 μM using skinning solutions with $[Mg^{2+}]$ 1.5 mM [55]; Zhang et al. in our laboratory found skinned cardiac muscle had an EC_{50} of 2.88 μM using skinning

solutions with [Mg^{2+}] 1.0 mM [186]. The data from my current skinned fibers studies shows that at SL 2.15 μm, the skinned rat trabeculae had an EC_{50} of 1.03 μM and 1.06 μM with Dextran and without Dextran, respectively. EC_{50} from my skinned preparation studies are lower than most of the previous results from skinned preparations with high [Mg^{2+}] and is comparable with Gao's data from skinning experiments with low [Mg^{2+}] of 0.5 mM (EC_{50} 1.03 μM vs.1.13 μM, respectively). Thus, high [Mg^{2+}] decreased the myofilament Ca^{2+} sensitivity.

6.5.3 Effects of osmotic compression on cardiac myofilament Ca^{2+} sensitivity

Changed force development and Ca^{2+} sensitivity by alteration of lattice spacing

Several investigators have found that removal of the sarcolemma results in swelling of fibers, which results in increased lattice spacing of the myofilaments as revealed by X-ray diffraction [99; 187]. It is possible that cross-bridge properties, especially cross-bridge kinetics, would change, resulting in a decrease of force development and Ca^{2+} sensitivity for myofilaments.

Godt et al. demonstrated that the influence of osmotic compression on the force-pCa relationship of skinned rabbit skeletal fibers was bi-phasic [93]. Skinned myofilaments had highest Ca^{2+} sensitivity when skinned fibers were progressively compressed by 5% Dextran T500 from the swollen size to the intact size. This phenomenon is confirmed by our experiment results. In the Dextran group, the F_{max} development is significantly higher than that of the non-Dextran group in the SL range from 1.80 μm to 2.15 μm (Table 6-6 and Figure 6-7: F_{max} 107.60±6.24 mN/mm^2 vs. 78.65±8.08 mN/mm^2 with and without Dextran at SL 2.15 μm, respectively). The F_{max} in the Dextran group is close to the F_{max} of intact cardiac muscle reported previously in our laboratory, 107 mN/mm^2 [183]. The F_{max}

in non-Dextran group is consistent with the F_{max} of skinned studies with high [Mg^{2+}], 87 mN/mm^2 [55]. Myofilament Ca^{2+} sensitivity is higher in Dextran treated group than that of control in the SL range from 1.90 μm to 2.15 μm (Table 6-7 and Figure 6-6: EC_{50}s are lower in Dextran treated trabeculae than those of trabeculae in the control group). Increase of SL decreases the EC_{50} difference between the two experimental groups and at SL 2.15 μm, the difference is negligible (t-test, $p>0.2$).

Possible mechanism for increased myofilament Ca^{2+} sensitivity by alteration of lattice spacing

Change of lattice spacing could result in a change of cross-bridge angle or the attachment-detachment rate constants, which would be expected to influence force generated from the cross-bridges [93]. The enhancement of Ca^{2+} sensitivity might be greatest when interfilament spacing is near that of intact muscle (i.e. in 5% Dextran solutions) where the angle of cross-bridge attachment might be "optimal"and the number of cross-bridge formed is at maximal state. At higher concentration of polymer (i.e. 10% Dextran T500 solutions), the fiber is compressed below its in situ size and the F_{max} developed is inhibited [187]. In high osmolality, Krasner et al. reported that the maximal Ca^{2+}-activated ATPase of skinned fibers was inhibited [188], which resulted in a decrease in force development.

Millman et al. proposed that the influence of moderate [Dextran T500] increasingly compressed the cross-bridges against the backbone of the thick filaments primarily by electrostatic repulsive forces between the contractile filaments, and the interaction between the contractile filaments was minimal. At high [Dextran T500], there was a considerable shrinkage of lattice space, and the contractile filament interaction

(viscoelastic, rather than attachment) increased dramatically [189], which caused decreased force in highly compressed lattice spacing. This proposal was confirmed by the studies of Roos et al. These investigators demonstrated that the slope of the stiffness-width relationship increased sharply at about the 4% concentration of Dextran [174].

6.5.4 Force feedback mechanism in skinned fibers

A Hill co-efficient larger than unity reflects cooperativity between the cross-bridges of thick filaments, actin, and Tn binding to Ca^{2+}. In my experimental results, the force-pCa relationships interpreted from the data of force-SL relationships show that, although the force-pCa relationships are well fitted by sigmoidal curves, the individual data points are not perfectly fitted into the curves. This sigmoidal curve fitting procedure can result in the error of Hill co-efficient (Figure 6-4 and Figure 6-5). Moss et al proposed that there were two different classes of Ca^{2+} binding sites involved in the force development, thus there were probably more than one values for Hill coefficient [190]. The linearized force-pCa relationships are best fitted by not one but two straight lines as described previously, with Hill coefficient n_{high} and n_{low} corresponding to the different levels of myofilament activation [191]. The value of n_{low} determines the steepness of the force-pCa curve. In order to minimize the error of analysis of cooperativity, I plotted linearized force-pCa relationship, Log(U/1-U) vs pCa, at each SL studied in both groups(Figure 6-8).

The data from these experiments show that moderate osmotic compression by 5% Dextran T500 treatment, which restores the physiological lattice spacing, increases the cardiac myofilament Ca^{2+} sensitivity since there are more cross-bridges formed with close to the optimal lattice spacing. From the current study, the values of n_{low} are higher

in the control group than those in the Dextran treated group; whereas the difference of n_{high} becomes negligible between the Dextran and non-Dextran groups (Figure 6-8). At sub-maximal activation conditions, stretch of the trabeculae decreases the lattice spacing and increases attached cross-bridges more in the control group than that in the Dextran-treated group. Under osmotic compression by 5% Dextran, stretch induces less reduction of lattice spacing and increases force less. At the high [Ca^{2+}], the activation of the thin filament is close to maximum, thus stretch increases force little in both the control and Dextran-treated groups, which, therefore, increases force feedback little and the difference of Hill co-efficient between the two groups becomes negligible. Further, the results of this study show that n_{high} is saturated at ~4-5 in both groups. This implies that the force feedback to Ca^{2+} binding on TnC has reached a maximal level. Further increases of [Ca^{2+}] or stretch cannot increase the cooperativity of filaments.

6.5.5 Effects of loss of cytosolic Ca^{2+} sensitizers on cardiac myofilament Ca^{2+} sensitivity

EC_{50} from skinned cardiac fibers at physiological [Mg^{2+}] and after osmotic compression is still higher than intact trabeculae and it does not restore myofilament Ca^{2+} sensitivity to that of intact cardiac muscle. A possible reason is that skinning causes loss of Ca^{2+} sensitizers in cytosol [146; 147]. These data show that at physiological [Mg^{2+}] and osmolality, skinned rat cardiac trabeculae have an EC_{50} of 1.03 μM at SL 2.15 μm, which is substantially higher than that of intact cardiac muscle of the same strain rats 0.34 μM[183]. EC_{50} in intact muscle from our laboratory is lower than that from other investigators, which probably is due to the different experimental preparations. EC_{50} from Gao et al. is 0.62 μM [160]. In their experiments, these investigators did not measure activated SL. When the cardiac muscle is activated, internal shortening takes place. This

change of SL during muscle activation can substantially affect the force-pCa relationship, thus EC_{50}.

Triton X-100 is a strong chemical detergent and it dissolves all membrane structures, including the sarcolemma membrane and SR membrane. Not only does it cause muscle swelling, it also causes loss of proteins. The composition of the lost proteins is not clear, but might include Ca^{2+} sensitizers. SDS gels of Triton and saponin skinning suspension from the heart reveal many proteins which are lost within 10 minutes (data from our lab's previous study). The molecular weight of the lost proteins can reach 200 kD. Small proteins are easily lost during skinning, i.e. CaM.

Steel et al. proposed that the lost Ca^{2+} sensitizers include carnosine-like compounds and taurine (MW 125), which are known as natural Ca^{2+} sensitizers [176]. In the millimolar range, the carnosine-like compounds (or histidyl derivatives) can increase myofilament Ca^{2+} sensitivity although its effect is small. Taurine can increase myofilament Ca^{2+} sensitivity without affecting F_{max} developed. In Triton-skinned trabeculae, 30 mM taurine decreased EC_{50} from 3.02 to 2.56 μM.

In smooth muscle studies, investigators have showed that skinning causes loss of CaM from cytosol [147]. CaM is a Ca^{2+} sensitizer, with a molecule weight ~18 kD. After addition of CaM into skinning solutions, it results in increase of myofilament Ca^{2+} sensitivity. Studies have shown that 5 μM CaM increases 10-fold the speed of development of isometric tension and pCa_{50} shifts from 5 to 6.2 in smooth muscles [158]. [CaM] is lower in cardiac muscle (~1 μM/L cell, information from Dr. Walsh) than that of smooth muscle (~30-50 μM/L cell, information from Dr. Walsh), so CaM probably

plays different roles in cardiac ECC. Further studies are needed to accurately measure [CaM] in myocytes and elicit the role of CaM in cardiac ECC.

6.6 Conclusion

Increase of SL reduces double overlap of thin filaments and decreases the lattice spacing. This may increase the number of attached cross-bridges, thus generating more force. At longer SL, the attachment of cross-bridges tends to be maximal and the osmotic compression has less effect on the number of attached cross-bridges. The latter effect may explain why the EC_{50} at SL 2.15 μm is insensitive to Dextran. This length-dependent force generation is a clear manifestation in skinned cardiac fibers.

Increase of osmolality by addition of 5% Dextran, which reduces lattice spacing to that of intact level, increases F_{max} developed. After correction of $[Mg^{2+}]$ and osmotic compression, skinned cardiac fibers are capable to generate F_{max} to that of intact cardiac muscle.

Mg^{2+} competes with Ca^{2+} binding to Tn. Low $[Mg^{2+}]$ increases the myofilament Ca^{2+} sensitivity.

However, the correction of $[Mg^{2+}]$ and osmotic compression together do not restore the myofilament Ca^{2+} sensitivity to that observed in vivo cardiac muscle, which suggests the presence of (a) Ca^{2+} sensitizer(s) in the cytosol of cardiac myocytes.

Figure 6-6: Comparison of EC_{50} between the control and Dextran groups. EC_{50} is higher in the control than that in the Dextran group. With increase of SL, EC_{50} gradually decreases in both groups (ANOVA, $p<0.001$). At longer SL (SL=2.15 μm), the change of EC_{50} becomes insensitive to the presence of Dextran since EC_{50} is at similar level in both groups at SL 2.15 mm. Overall, EC_{50} is higher in the control group than that of with Dextran group (ANOVA, $p<0.05$).

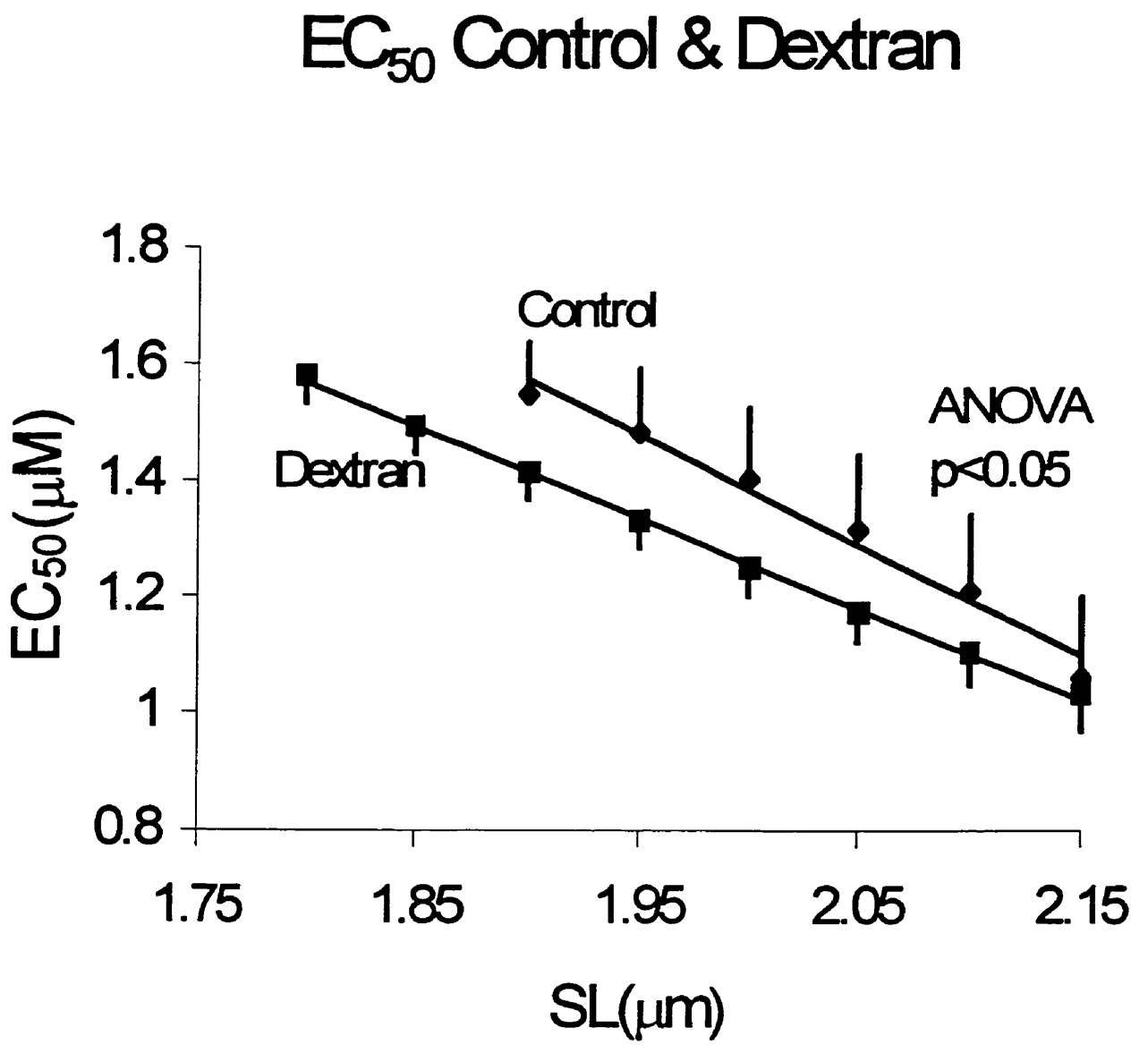
EC50 Control & Dextran
1.8
1.6
1.4
1.2
1
0.8
EC50(μM)
Control
Dextran
ANOVA
p<0.05
1.75
1.85
1.95
2.05
2.15
SL(μm)

Figure 6-7: Comparison of F_{max} developed between the control group and Dextran group. At corresponding SLs from 1.90 μm to 2.15 μm, F_{max} is higher in Dextran group than that of control group (ANOVA, $p<0.001$). Also, with increase of SL, F_{max} gradually increases in both groups (ANOVA, $p<0.001$). At SL 2.15 μm, F_{max} is 107±6 mN/mm^2 and 79±8 (mean±SE) mN/mm^2 in Dextran and non-Dextran groups, respectively.

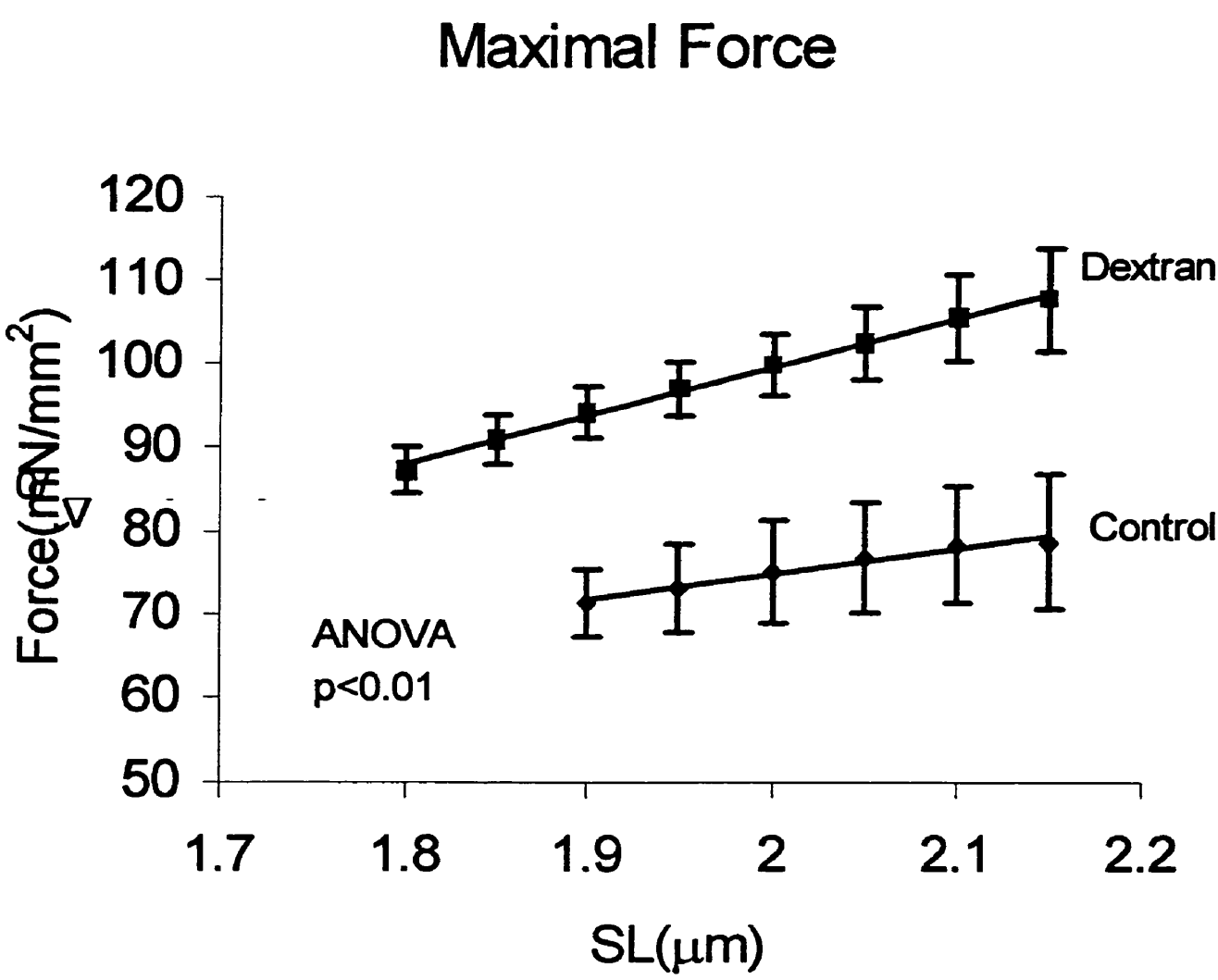
Maximal Force
120
110
100
90
80
70
60
50
Force(mN/mm²)
Dextran
Control
ANOVA
p<0.01
1.7
1.8
1.9
2
2.1
2.2
SL(μm)

Figure 6-8: Comparison of Hill co-efficient between the control group and the Dextran group. The Hill coefficient reflects cooperativity between the thin and thick filaments and Ca^{2+}. The plots of log(U/1-U)-pCa show that there are two phases of cooperativity: at low $[Ca^{2+}]$ and at high $[Ca^{2+}]$. At high $[Ca^{2+}]$, the cooperativity reaches maximal at Hill co-efficient ~4. The values of n_{low} are higher in the control group and the difference is statistically significant (ANOVA, $p<0.01$). The 95% confidence interval of n_{low} in the control group is far away from the fitting curve of n_{low} in the Dextran group. This is possibly caused by more increased force generated with stretch in the control group. At high $[Ca^{2+}]$, the difference of n_{high} becomes smaller and is not statistically significant (ANOVA, $p=0.11$), as it is shown in this figure, the 95% confidence interval of n_{high} is overlap with the fitting curve n_{high} in the Dextran group.

Hill co-efficient in Dextran group

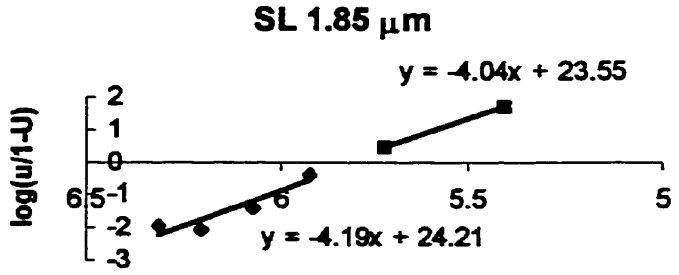

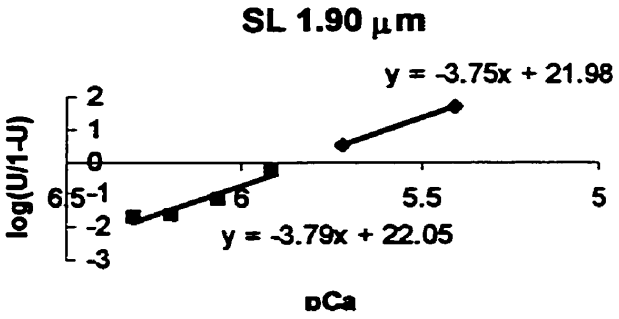

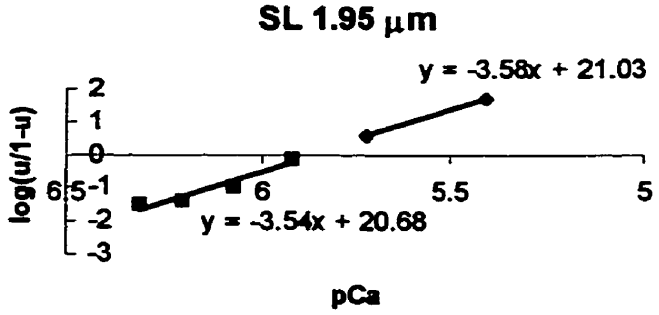

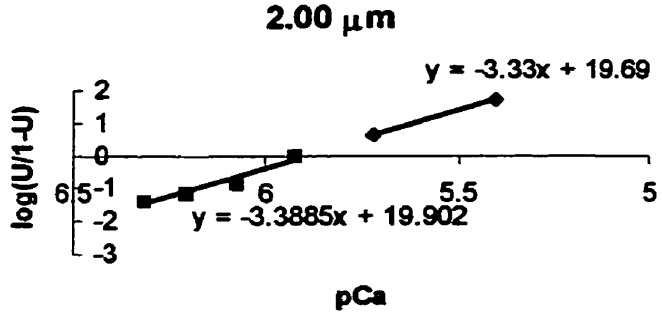

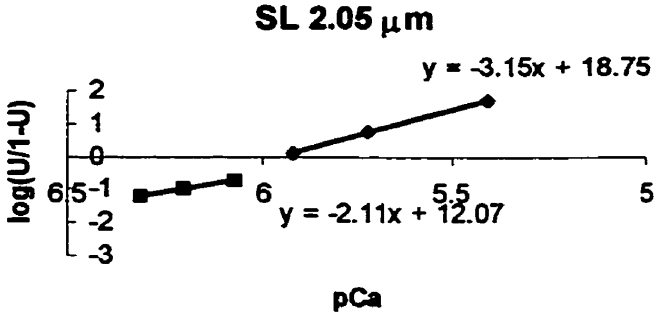

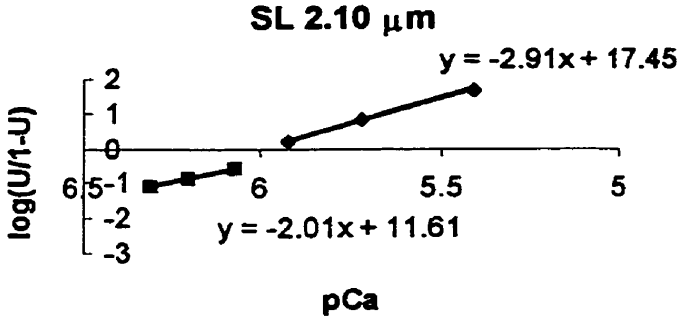

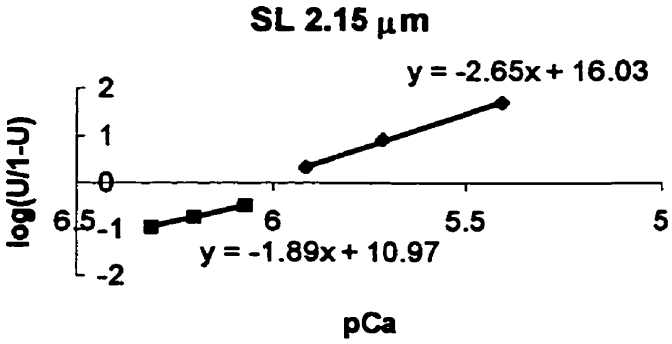

Hill co-efficient in non-Dextran group

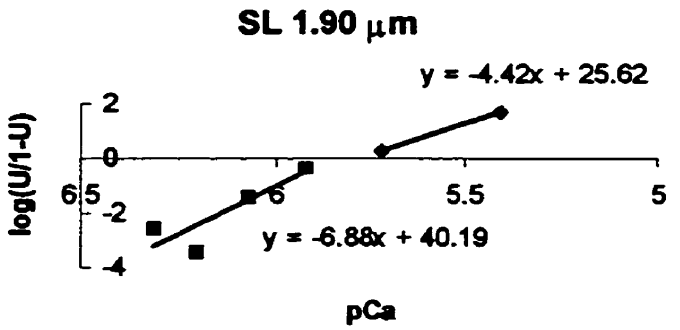

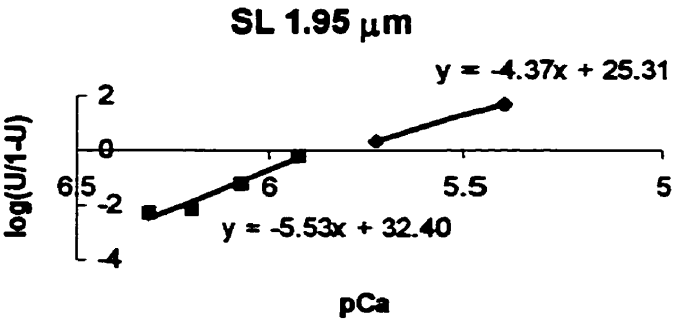

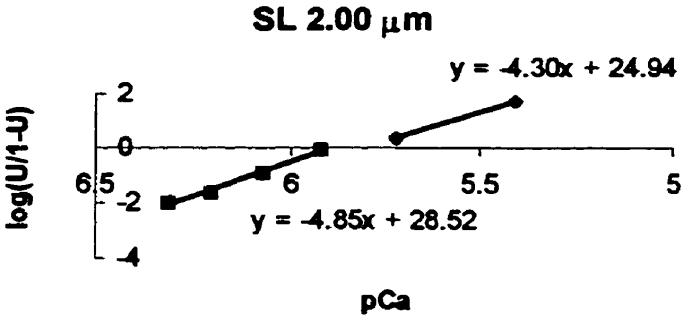

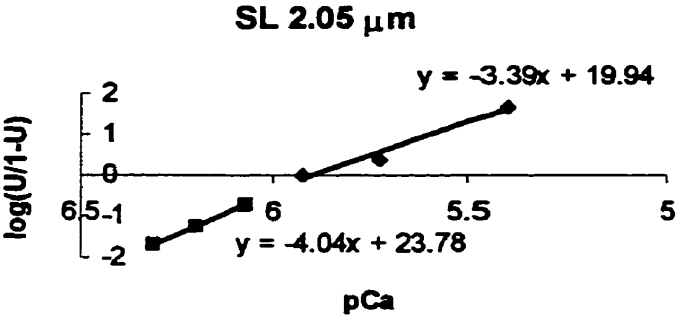

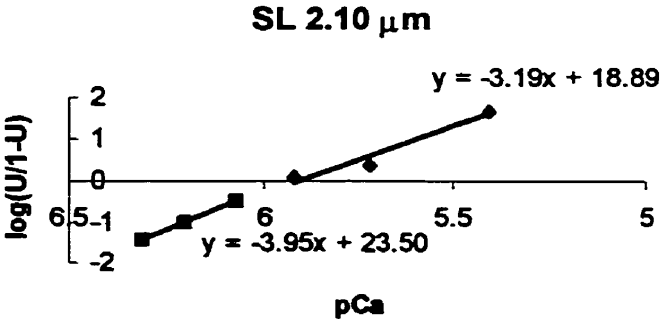

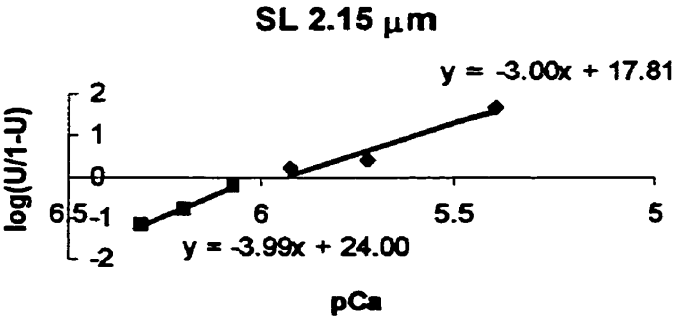

Comparison of n_{low} and $_{nhigh}$

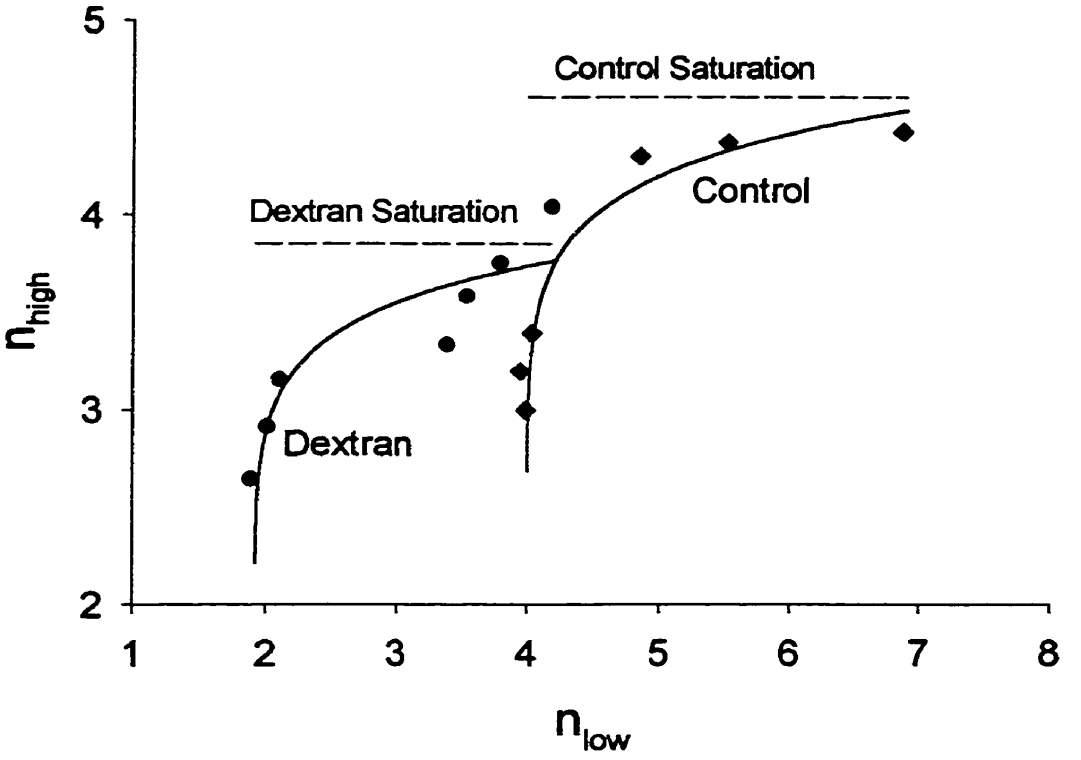

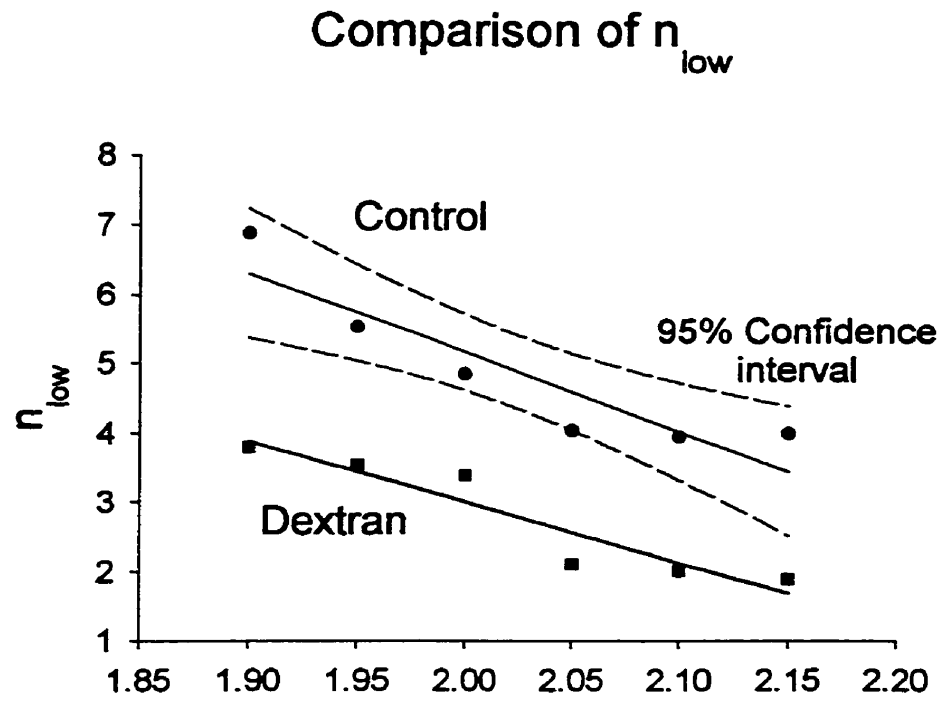
Comparison of n low
8
7
6
5
4
3
2
1
n low
Control
95% Confidence interval
Dextran
1.85
1.90
1.95
2.00
2.05
2.10
2.15
2.20

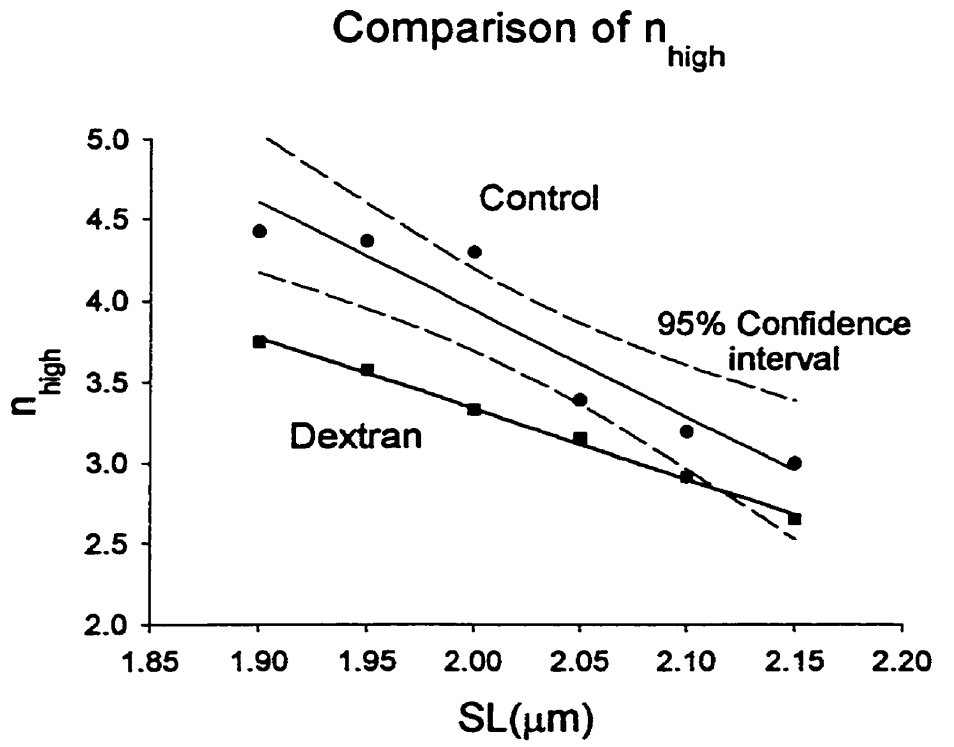
Comparison of n high
5.0
4.5
4.0
3.5
3.0
2.5
2.0
n high
Control
95% Confidence interval
Dextran
1.85
1.90
1.95
2.00
2.05
2.10
2.15
2.20
SL(μm)

Chapter 7

Future Studies in ECC

CICR is a characteristic of cardiac ECC. Although previous studies have shown the ultrastructural organization of the DHPRs and RyRs in chick-heart cells, it is still not clear in mammalian cardiac cells. The number of RyRs per cell may be much greater in mammalian heart cells, which may imply differences in ultrastructure. Furthermore, the reaction between DHPRs and RyRs needs further study. How many of DHPRs and RyRs are involved in a Ca^{2+} spark release is still unknown. Moreover, where does the triggering Ca^{2+} come from? Does it enter through the L-type Ca^{2+} channel or by the Na^{+}/Ca^{2+} exchanger, or by both? Some research evidence has shown that extracellular Ca^{2+} can enter into cytosol by the Na^{+}/Ca^{2+} exchanger in the absence of Ca^{2+} entry through the voltage-dependent Ca^{2+} channel. Cannell et al. suggested that both L-type Ca^{2+} current and the reversed Na^{+}/Ca^{2+} exchange current contribute to CICR [25]. The authors claimed that it is clear that the Na^{+}/Ca^{2+} exchanger can trigger the SR Ca^{2+} release, but these investigators failed to identify the physiological role of this kind of SR Ca^{2+} release. At present, there is no direct evidence to exclude the above theory.

There are also some puzzles regarding uptake of Ca^{2+} by the SR Ca^{2+} pump. First, the Ca^{2+}-ATPase binds two Ca^{2+} ions with high affinity at cytosolic Ca^{2+} binding sites. Researchers are still puzzling whether the translocation of the two Ca^{2+} ions into the SR is sequential or non-sequential. Some people think the Ca^{2+} ions pass through the Ca^{2+} channel sequentially. The first Ca^{2+} entering the channel is the first to exit on the lumenal side of the membrane of the SR [192]. Others suggest that the two Ca^{2+} ions become indistinguishable as they dissociate from the Ca^{2+}-ATPase into the SR lumen. Second, it

is still uncertain whether there are two or four Ca^{2+} binding sites in the SR Ca^{2+} pump. Some investigators proposed the four Ca^{2+} binding sites model. These investigators suggested the two Ca^{2+} ions are bound initially to the high affinity cytoplasmic Ca^{2+} binding sites, and are then translocated after phosphorylation of the enzyme by ATP to distinct low-affinity lumenal sites, followed by non-sequential Ca^{2+} release into the SR lumen. But this proposal is hard to fit into a single Ca^{2+} channel mode since, if four Ca^{2+} ions occupy the SR Ca^{2+} uptake channel, it might cause electrostatic constraints [193]. Recently, some researchers presented a two-channel model [194]. The transmembrane domains M_4, M_5, M_6 and M_8 have been proven to interfere with the high-affinity Ca^{2+} binding site and contribute to the Ca^{2+} channel(s) of the Ca^{2+}-ATPase. Recent data also show the effects of M_3 helix on high-affinity Ca^{2+} binding and thapsigargin sensitivity [195]. The data also suggest that the effects of mutation on the two high-affinity Ca^{2+} sites can be separated. In the two-channel model, the investigators proposed that these two interacting Ca^{2+} channels were gated by phosphorylation of the Ca^{2+}-ATPase at a single site. The helices M_2, M_3, M_4 and M_5 form a channel and the other channel was formed by the helices M_4, M_5, M_6, and M_8. This hypothesis needs to be tested further, as does the variable stoichiometry of the Ca^{2+} binding sites in the SR Ca^{2+} ATPase [195]. The choice among the various possible Ca^{2+} translocation mechanisms requires more information about the structure of the Ca^{2+} uptake channel than those currently available.

Most of the previous studies on SR Ca^{2+} uptake have been done on isolated myocytes. Isolated cells are equally exposed to experimental solutions, so the problem of uneven skinning in isolated tissue preparation can be avoided. However, isolated cells are in "pathophysiological" conditions since structural changes usually occur in the cell

isolation procedure. In order to measure SR Ca^{2+} uptake function in conditions much closer to physiological states, isolated cardiac trabeculae should be considered.

In order to measure SR Ca^{2+} uptake accurately, the measurement of intracellular Ca^{2+} buffering capacity is very important. Previous studies have reported different values for [CaM] in the myocytes with a 20 fold difference. Fabiato et al. reported a [CaM] 2.38 μmol/kg tissue wet wt [150], whereas Wier et al. showed a [CaM] 50 μmol/L cell [196]. This inaccuracy of [CaM] affects the measurement of myocyte Ca^{2+} buffering capacity, and thus affects the study of SR Ca^{2+} uptake. Although there are some technical difficulties in measuring [CaM] in cardiac cells, this needs to be done in order to further study SR Ca^{2+} pump function.

The cross-bridge sliding theory has been established for a long time, but the detailed mechanism is not completely known. Not many studies have enlightened the theory in a quantitative way. During studies of force-length relationship in this project, we tried to use BDM (2,3-butane-dione-monoxime) to stop ATP hydrolysis and cross-bridge cycling, so that the cross-bridges were kept attached in order to measure the absolute number of cross-bridges at different level of Ca^{2+} activation. But in the experiments, we found that 20 mM BDM did not stop force development in skinned cardiac fibers, as it has been reported to do in intact muscle. Even with 200 mM of BDM, we still observed substantial force development (F_{max} ~10% of that in intact muscle) in Triton X-100 skinned trabeculae. This preliminary experiment result indicates that BDM stops force development in intact muscle probably through a second-messenger system in the sarcolemma. Not many studies regarding the effects of BDM on force development in

skinned fibers have been done so far. It is absolutely necessary to clarify the effects of BDM in the force- generating system in skinned preparations.

It is a very attractive and ambitious goal to measure the absolute number of cross-bridges at different levels of myofilament activation. In this way, we could clarify the force feedback mechanism in the force development, especially in a quantitative way. Some new tools and new chemicals need to be discovered to stop cross-bridge cycling while cross-bridges are kept attached without affecting the experimental conditions in milieu.

From the present study, skinned cardiac fibers show lower myofilament Ca^{2+} sensitivity even after correction of $[Mg^{2+}]$ and lattice spacing to their physiological state. The cause I have proposed from the available data is the loss of Ca^{2+} sensitizers from cytosol during skinning. SDS gels of skinned myocyte suspensions in our laboratory revealed that hundreds of kinds of proteins were lost. In future studies, western blot and specific antibody labeling study should be considered. Several candidates, i.e. taurin and CaM, can be tested in future skinned preparations. The effects of addition of possible Ca^{2+} sensitizers in skinning solutions on EC_{50} will test the validity of my conclusion.

Biblioglophy

1. Katz AM: *Physiology of The Heart*. New York, Taven Press, 1992, 235-238

2. Bers DM: *Excitation-contraction coupling and cardiac contractile force*, ed1, Boston/London, Kluwer Academic, 1991, 1-16

3. Carl SL, Felix K, Caswell AH: Immunolocalization of sarcolemmal dihydropyridine receptor and sarcoplasmic reticular triadic and ryanodice receptor in rabbit ventricle and atrium. *J.cell Biology* 1995;129:673-682

4. Sun X, Protasi F, Takahashi M, Takeshima H, Furgeson DG, Franzini-Armstrong C: Molecular architecture of membranes involved in excitation-contraction coupling of cardiac muscle. *J.Cell Biology* 1995;129:659-671

5. Gordon MW: *Cardiac Action Potential*, in Sperelakis N (ed): *Cell Physiology*. San Diego, California, Academic Press, 1998, 783-785

6. Balshaw DM, Millette LA, Wallick ET: *The Sodium Pump*, in Sperelakis N (ed): *Cell Physiology*. San Diego, California, Academic Press, 1998, 216-224

7. Fabiato A, Fabiato F: Calcium release from the sarcoplasmic reticulum. *Circ.Res.* 1977;40:119-129

8. Streissnig J, Scheffauer F, Mitterdorfer, J., Schirmer M, Glossmann H: Identification of the benzothiazepine-binding polypeptide of skeletal muscle calcium channels with (+)-cis-azidodiltiazem and anti-ligand antibodies. *J.Biol.Chem.* 1990;265:363-370

9. O'Callahan CM, Ptasienski J, Hosey MM: Phosphorylation of the 165-kDa dihydropyridine/phenylalkylamine receptor from skeletal muscle by protein kinase C. *J.Biol.Chem.* 1988;263:17342-17349

10. Nastainczyk W, Rohrkasten A, Siever M, Rudolph C, Schachtele C, Marme D, Hofmann F: Phosphorylation of the purified receptor for calcium channel blockers by cAMP kinase and protein kinase C. *Eur.J.Biochem.* 1987;169:137-142

11. Flockerzi V, Oeken H-J, Hofmann F, Pelzer D, Cavalie A, Trauwein W: Purified dihydropyridine-binding site from skeletal muscle t-tubule is a functional calcium channel. *Nature* 1986;323:66-68

12. Lew WYW, Hryshko LV, Bers DM: Dihydrpyridine recptors are primarily functional L-type calcium channels in rabbit ventricular myocytes. *Circ.Res.* 1991;69:1139-1145

13. Song LS, Sham JS, Stern MD, Lakatta EG, Cheng H: Direct measurement of SR release flux by tracking 'Ca^{2+} spikes' in rat cardiac myocytes. *J.Physiol.* 1998;512:677-691

14. Block BA, Imagawa T, Campbell KP, Franzini-Armstrong C: Structural evidence for direct interaction between the molecular components of the transverse tubule/sarcoplasmic reticulum junction in skeletal muscle. *J.Cell Biology* 1988;107:2587-2600

15. Banijamali H, Gao WD, MacIntosh B, ter Keurs HEDJ: Force-interval relations of twitches and cold contractures in rat cardiac trabeculae; effect of Ryanodine. *Cir.Res.* 1998;69:937-948

16. Xu, L and Meissner, G. Regulation of cardiac muscle Ca^{2+} release channel by sarcoplasmic reticulum lumenal Ca^{2+}. *Biophys. J.* 1998;75(5):2302-2312

17. Ockleford C: The confocal laser scanning microscope (CLSM) [editorial]. [Review] [15 refs]. *J.Pathol.* 1995;176:1-2

18. Cheng H, Lederer WJ, Cannell MB: Calcium sparks: elementary events underlying excitation-contraction coupling in heart muscle. *Science* 1993;262:740-744

19. Rousseau E, Meissner G: Single cardiac sarcoplasmic reticulum Ca^{2+}-release channel: activation by caffeine. *Am.J.Physiol.* 1989;256:H328-H333

20. Cannell, M. B., Cheng, H., and Lederer, W. J. The control of calcium release in heart muscle. *Science* 1995;268:1045-1050

21. Cheng, H., Lederer, M. R., and Xiao, R. P. Excitation-contraction coupling in heart: new insight from Ca^{2+} sparks. *Cell Calcium* 1996;20(2):129-140

22. Kohmoto O, Levi AJ, Bridge JHB: Relation between reverse Na^{+}-Ca^{2+} exchange and SR Ca^{2+} release in guinea pig ventricular cells. *Circ.Res.* 1994;74:550-554

23. Lederer WJ, Sheu SS: Heart rate-dependent changes in intracellular sodium activity and twitch tension in sheep cardiac purkinje fibres. *J.Physiol.* 1983;44P:345-345

24. Levi AJ, Brooksby P and Hancox JC: A role for depolarization induced contraction in rat ventricular myocytes. *Cardio. Res.* 1993;27:1677-1690

25. Cannell MB, Grantham CJ, Main MJ and Evans AM: The roles of the sodium and calium current in triggering calcium release from the sarcoplasmic reticulum. *Ann. N.Y. Acad. Sci.* 1996;779:443-451

26. Sham JS, Cleemann L, Morad M: Gating of the cardiac Ca^{2+} release channel: the role of Na^{+} current and Na^{+}-Ca^{2+} exchange. *Science* 1992;255:850-853

27. Eisner DA, Trafford AW, Diaz ME, Overend CL., and O'Neil SC: The control of Ca^{2+} release from the cardiac sarcomplasmic reticulum: regulation versus autoregulation. *Cardio. Res.*1998;38:589-604

28. Santana LF, Cheng H, Gomez AM, and Cannell MB: Relation between the sarcolemmal Ca^{2+} current and Ca^{2+} sparks and local control theroies for cardiac excitation-contraction coupling. *Cir.Res.* 1996;78:166-171

29. Leblanc N, Hume JR: Sodium current-induced release of calcium from cardiac sarcoplasmic reticulum. *Science* 1990;248:372-376

30. Isenberg G, Wendt-Gallitelli MF: Binding of calcium to myoplasmic buffers contributes to the frequency-dependent inotropy in heart ventricular cells [editorial]. *Basic. Res. in Cardiol.* 1992;87:411-417

31. Kieval RS, Bloch RJ, Lindenmayer GE, Ambesi A, and Lederer WJ: Immunofluorescence localization of the Na^{+}-Ca^{2+} exchanger in heart cells. *Am.J.Physiol.* 1992;263:C545-C550

32. Nicoll DA, Longoni S, Philipson KD: Molecular cloning and functional expression of the cardiac sarcolemmal Na^{+}-Ca^{2+} exchanger. *Science* 1990;250:562-565

33. Burk SE, Lytton J, MacLennan DH, Shull GE: cDNA cloning, functional expression, and mRNA tissue distribution of a third organellar Ca^{2+} pump. *J.Biol.Chem.* 1989;264:18561-18568

34. MacLennan DH, Brandl CJ, Korczak B, Green NM: Calcium ATPase: Contribution of molecular genetics to our understnading of structure and function., in Hille B, Frambrough DM (eds): *Proteins of Excitable Membranes.* New York, John Wiley & Sons, Inc., 1987, 287-300

35. Clarke DM, Loo TW, Inesi G, MacLennan DH: Location of high affinity Ca^{2+}-binding sites within the predicted transmembrane domain of the sarcoplasmic reticulum Ca^{2+}-ATPase. *Nature* 1989;339:476-478

36. Mitchell RD, Simmerman HKB, Jones LR: Ca binding effects on protein conformation and protein interactions of canine cardiac calsequestrin. *J.Biol.Chem.* 1988;263:1376-1381

37. Koss KL and Kranias EG: Phospholamban: a prominent regulator of myocardial contractility. *Cir.Res.* 1996;79(6):1059-1063

38. Le Peuch CJ, Haiech J, De Maille JG: Concerted regulation of cardiac sarcoplasmic calcium transport by cyclic adenosine monophosphate dependent and calcium-calmodulin-dependent phosphorylations. *Biochemistry* 1979;18:5150-5157

39. Simmerman HKB, Collins JH, Theiber JL, Weger AD, Jones LR: Sequence analysis of phospholamban:Identification of phosphorylation sites and two major structural domains. *J.Biol.Chem.* 1986;261:13333-13341

40. Mattiazzi A, Hove-Madsen L, Bers DM: Protein kinase inhibitors reduce SR Ca^{2+} transport in permeabilized cardiac myocytes. *Am.J.Physiol.* 1994;267:H812-H820

41. Fabiato A: Use of aequorin for the appraisal of the hypothesis of the release of calcium from the sarcoplasmic reticulum induced by a change of pH in skinned cardiac cells. *Cell Calcium* 1985;6:95-108

42. Tada M, Yamada M, Kadoma M, Inui M, Ohmori F: Calcium transport by cardiac sarcoplasmic reticulum and phosphorylation of phospholamban. *Mol.Cell.Biochem.* 1982;46:74-95

43. Dupont Y: Kinetics and regulation of sarcoplasmic reticulum ATPase. *Eur.J.Biochem.* 1977;72:185-190

44. MacLennan, D. H., Clarke, D. M., Loo, T. W., and Skerjanc, I. S. Site-directed mutagenesis of the Ca^{2+}-ATPase of sarcoplasmic reticulum. *Acta.Physiol.Scand.* 1992;146:141-150

45. Frank O: Zur Dynamik des Herzmuskels. *Zeitschrift fuer Biologie* 1895;32:370-437

46. Patterson SW, Starling EH: On the mechanical factors which determine the output of the ventricles. *J.Physiol.* 1914;48:3.7-379

47. ter Keurs HEDJ: Heart failure and Starlings Law of the heart. *Can.J.Cardiol.* 1996;12:1047-1057

48. Allen DG, Kentish JC: The cellular basis of the length-tension relation in cardiac muscle. [Review] [87 refs]. *J.Mol.Cell.Cardiol.* 1984;17:821-840

49. Gordon AM, Huxley AF, Julian FJ: Tension development in highly stretched vertebrated muscle fibres. *J.Physiol.* 1966;184:143-169

50. Gordon AM, Huxley AF, Julian FJ: The variation in isometric tension with sarcomere length in vertebrate muscle fibres. *J.Physiol.* 1966;184:170-192

51. Edman KAP: The relation between sarcomere length and active tension in isolated semitendinosus fibres of the frog. *J.Physiol.* 1966;183:407-417

52. Pollack GH, Huntsman LL: Sarcomere length-active force relations in living mammalian cardiac muscle. *Am.J.Physiol.* 1974;227:383-389

53. Fabiato A, Fabiato F: Myofilament-generated tension oscillations during partial calcium activation and activation dependence of the sarcomere length-tension relation of skinned cardiac cells. *J.Gen.Physiol.* 1978;72:667-699

54. ter Keurs HEDJ, Rijnsburger WH, van Heuningen RV, Nagelsmit MJ: Tension development and sarcomere length in rat cardiac trabeculae. Evidence of length-dependent activation. *Circ.Res.* 1980;46:703-714

55. Kentish JC, ter Keurs HEDJ, Ricciardi L, Bucx JJJ, Noble MIM: Comparison between the sarcomere length-force relations of intact and skinned trabeculae from rat right ventricle. *Circ.Res.* 1986;58:755-768

56. Zhang YM: Sarcomplasmic reticulum and myofilament function in normal and failing heart. *phD Thesis* 1998, The University of Calgary

57. Hofmann PA, Fuchs F: Bound calcium and force development in skinned cardiac muscle bundles: effect of sarcomere length. *J.Mol.Cell.Cardiol.* 1988;20:667-677

58. Jewell BR: A reexamination of the influence of muscle length on myocardial performance. *Cir.Res.* 1977;40:221-230

59. Allen DG, Kentish JC: The cellular basis of the length-tension relation in cardiac muscle. *J.Mol.Cell.Cardiol.* 1985;17:821-840

60. Lakatta EG: Starling's law of the heart is explained by an intimate interaction of muscle length and myofilament calcium activation. [Review] [43 refs]. *J.Am.Coll.Cardiol.* 1987;10:1157-1164

61. Fabiato A, Fabiato F: Dependence of the contractile activation of skinned cardiac cells on the sarcomere lenght. *Nature* 1975;256:54-56

62. Lab MJ: Contraction-excitation feedback in myocardium; physiological basis and clinical relevance. *Circ.Res.* 1982;50:757-766

63. Allen DG, Kurihara S: The effects of muscle length on intracellular calcium transients in mammalian cardiac muscle. *J.Physiol.* 1982;327:79-94

64. Morgan JP, Blinks JR: Intracellular calcium transients in the cat papillary muscle. *Can.J.Physiol.Pharmacol.* 1982;60:524-528

65. Fabiato A: Sarcomere length dependence of calcium release from the sarcoplasmic reticulum of skinned cardiac cells demonstrated by differential microspectrophotometry with arsenazo II. *J.Gen.Physiol.* 1980;76:15A-15A

66. Lab M, Allen DG, Orchard CH: The effects of shortening on myoplasmic calcium concentration and on the potential in mammalian ventricular muscle. *Circ.Res.* 1984;55:825-829

67. Allen DG, Nichols CG, Smith GL: The effects of changes in muscle length during diastole on the calcium transient in ferret ventricular muscle. *J.Physiol.* 1988;406:359-370

68. Allen DG, Kentish JC: Calcium concentration in the myoplasm of skinned ferret ventricular muscle following changes in muscle length. *J.Physiol.* 1988;407:489-503

69. Hofmann PA, Fuchs F: Effect of length and cross-bridge attachment on Ca^{2+} binding to cardiac troponin C. *Am.J.Physiol.* 1987;253:90-96

70. Endo M: Stretch-induced increase in activation of skinned muscle fibres by calcium. *Nature New Biology* 1972;237:211-213

71. Bremel RD, Weber A: Cooperation within actin filament in vertebrate skeletal muscle. *Nature* 1972;238:97-101

72. Hofmann PA, Fuchs F: Evidence for a force-dependent component of calcium binding to cardiac troponin C. *Am.J.Physiol.* 1987;253:541-546

73. Wang YP and Fuchs F: Length, force, and Ca^{2+} -troponin C affinity in cardiac and slow skeletal muscle. *Am.J.Physiol.* 1994;266,C1077-C1082

74. Fuchs F and Wang YP: Force, length, and Ca^{2+}-troponin C affinity in skeletal muscle. *Am.J.Physiol.* 1991;261(30):C787-C792

75. Allen DG: Shortening of tetanized skeletal muscle causes a fall of intracellular calcium concentration [proceedings]. *J.Physiol.* 1978;275:63-63

76. D'Agnolo A, Luciani GB, Mazzucco A, Gallucci V, and Salviati G: Contractile properties and Ca^{2+} release activity of the sarcoplasmic reticulum in dilated cardiomyopathy. *Circulation* 1992;85:518-525

77. Perreault CL, Bing OH, Brooks WW, Ransil BJ, Morgan JP: Differential effects of cardiac hypertrophy and failure on right versus left ventricular calcium activation. *Circ.Res.* 1990;67:707-712

78. Vahl CF, Bonz A, Timek T, and Hagl S: Intracellular calcium transient of working human myocardium of seven patients transplanted for congestive heart failure. *Circ.Res.* 1994;74(5):952-958

79. Vahl CF, Timek T, Bonz A, Fuchs H, Dillman R, Hagl S: Length dependence of calcium- and force-transients in normal and failing human myocardium. *J.Mol.Cell.Cardiol.* 1998;30:957-966

80. Holubarsch CH, Ruf T, Goldstein DJ, Ashton RC, Nickl W, Pieske B, Pioch K, Ludemann J, Wiesner S, HasenfuB G, Posival H, Just H, Burkhoff D: Existence of the Frank-Starling mechanism in the failing human heart. *Circulation* 1996;94:683-689

81. Schwinger RHG, Bohm M, Koch A, Schmidt U, Morano I, Eissner HJ, Ueberfuhr P, Reichart B, Erdmann E: The failing human heart is unable to use Frank Starling's mechanism. *Circ.Res.* 1994;74(5):959-969

82. Huxley AF: Muscle structure and theories of contraction. *Prog.Biophys.Biophys.Chem.* 1957;7:255-318

83. Huxley HE: The mechanism of muscular contraction. [Review] [46 refs]. *Science* 1969;164:1356-1366

84. Huxley HE, Brown W: The low angle x-ray diagram of vertebrate striated muscle and its behaviour during contraction and rigor. *J.Mol.Biol.* 1967;30:383-434

85. Huxley AF, Simmons RM: Proposed mechanism of force generation in striated muscle. *Nature* 1971;233:533-538

86. Uyeda TQ, Abramson PD, Spudich JA: The neck region of the myosin motor domain acts as a lever arm to generate movement. *Proc.Natl.Acad.Sci.USA* 1996;93:4459-4464

87. Kawai M, Wray JS, Zhao Y: The effect of lattice spacing change on cross-bridge kinetics in chemically skinned rabbit psoas muscle fibers. I. Proportionality between the lattice spacing and the fiber width. *Biophys.J.* 1993;64:187-196

88. Adhikari BB, Fajer PG: Myosin head orientation and mobility during isometric contraction: effects of osmotic compression. *Biophys.J.* 1996;70:1872-1880

89. Rayment I, Rypniewski WR, Schmidt-Base K, Smith R, Timchick DR, Benning MM, Winkelmann DA, Wesenberg G, Holden HM: Three-Dimentional structure of myosin subfragment-1: A molecular motor. *Science* 1993;261:50-58

90. Cecchi G, Bagni MA, Griffiths PJ, Ashley CC, Maeda Y: Detection of radial crossbridge force by lattice spacing changes in intact single muscle fibers. *Science* 1990;250:1409-1411

91. Godt RE, Maughan DW: Swelling of skinned muscle fibres of the frog: experimental observations. *Biophys.J.* 1977;19:106-116

92. Ford LE, Nakagawa K, Desper J, Seow C, Effect of osmotic compression on the force-velocity properties of glycerinated rabbit skeletal muscle cells. *J.Gen.Physiol.* 1991;97:73-88

93. Godt RE, Maughan DW: Influence of osmotic compression on Calcium activation and tension in skinned muscle fibers of the rabbit. *Pfluegers Arch.* 1981;391:334-337

94. McDonald KS and Moss RL: Osmotic compression of single cardiac myocytes eliminates the reduction in Ca^{2+} sensitivity of tension at short sarcomere length. *Cir. Res.* 1995;77:199-205

95. Lamont C, Miller DJ: Hypertonic shrinkage of the lattice spacing of chemically skinned cardiac muscle increases Ca^{2+} sensitivity and peak force. *J.Physiol.* 1987;386:57A

96. Rome E: X-ray diffraction studies of the filament lattice of striated muscle in various bathing media. *J.Mol.Biol.* 1968;37:331-344

97. Harrison SM, Lamont C, Miller DJ: Hysteresis and the length dependence of calcium sensitivity in chemically skinned rat cardiac muscle. *J.Physiol.* 1988;401:115-143

98. Wang YP, Fuchs F: Osmotic compression of skinned cardiac and skeletal muscle bundles: effects on force generation, Ca^{2+} sensitivity and Ca^{2+} binding. *J.Mol.Cell.Cardiology* 1995;27:1235-1244

99. Matsubara I, Elliot GF: X-ray diffraction studies on skinned single fibres of frog skeletal muscle. *J.Mol.Biol.* 1972;72:657-669

100. Matsubara I, Millman BM: X-ray diffraction patterns from mammalian heart muscle. *J.Mol.Biol.* 1974;82:527-536

101. Magid A, Reedy MK: X-ray diffraction observations of chemically skinned frog skeletal muscle processed by in improved method. *Biophys.J.* 1980;30:27-40

102. April EW, Maughan DW: Active force as a function of filament spacing in crayfish skinned muscle fibers. *Pflugers Arch.* 1986;407:456-460

103. Allen JD, Moss RL: Factors influencing the ascending limb of the sarcomere length-tension relationship in rabbit skinned muscle fibres. *J.Physiol.* 1987;390:119-136

104. Goldman YE: Measurement of sarcomere shortening in skinned fibers from frog muscle by white light diffraction. *Biophys.J.* 1987;52:57-68

105. Metzger JM, Moss RL: Thin filament regulation of shortening velocity in rat skinned skeletal muscle: effect of osmotic compression. *J.Physiol.* 1988;398:165-175

106. Raucher D, Fajer PG: Orientation and dynamics of myosin heads in aluminum fluoride induced pre-power stroke states: an EPR study. *Biochemistry* 1994;33:11993-11999

107. Stienen GJM, Blange T: Tension responses to rapid length changes in skinned muscle fibres of the frog. *Pflugers Arch.* 1985;405:5-11

108. Pfeffer MA, Braunwald E: Ventricular remodeling after myocardial infarction; experimental observations and clinical implications. *Circulation* 1990;81:1161-1172

109. Sabbah HN and Sharov VG: Apoptosis in heart. *Prog.Cardiov.Dis.* 1998;40(6):549-562

110. Grajek S, Lesiak M, Pyda M, Zajac M, Paradowski S, and Kaczmarek E: Hypertrophy or hyperplasia in cardiac muscle. Post-mortem human morphometric study. *Eur.Heart J.* 1993;14(1):1-3

111. Weber KT, SUN Y, Katwa LC, Cleutjens JP, and Zhou G: Connective tissue and repair in the heart. Potential regulatory mechanisms. *Ann. N.Y. Acad. Sci.* 1995;452:286-299

112. Capasso JM, Fitzpatrick D, and Anversa P: Cellular mechanisms of ventricular failure: myocyte kintics and geometry with age. *Am.J.Physiol.* 1992;262(6):H1770-H1781

113. Lue WM, Boyden PA: Abnormal electrical properties of myocytes from chronically infarcted canine heart. Alteration in dVmax and the transient outward current. *Circulation* 1992;85:1175-1188

114. Nabauer M, Beuckelmann DJ, Erdmann E: Characteristics of transient outward current in human ventricular myocytes from patiens with terminal heart failure. *Circ.Res.* 1993;73:386-394

115. Takahashi T, Allen PD, Lacro RV, Marks AR, Dennis AR, Schoen FJ, Grossman W, Marsh JD, Izumo S: Expression of dihydropyridine receptor (Ca^{2+} channel) and calsequestrin genes in the myocardium of patients with end-stage heart failure. *J.Clin.Invest.* 1992;90:927-935

116. Rasmussen PR, Minobe W, Bristow MR: Calcium antagonist binding sites for failing and nonfailing human ventricular myocardium. *Biochem.Pharmacol.* 1990;39:691-696

117. Fabiato A: Simulated calcium current can both cause calcium loading in and trigger calcium release from the sarcoplasmic reticulum of skinned canine cardiac purkinje cell. *J.Gen.Physiol.* 1985;85:291-320

118. Bassani RA and Bers DM: Rate of diastolic Ca^{2+} release from the sarcomplasmic reticulum of intact rabbit and rat ventricular myocytes. *Biophys.J.* 1995;68:2015-2022

119. Go LO, Moschella MC, Watras J, Handa KK, Fyfe BS, and Marks AR: Differential regulation of two types of intracellular calcium release. *J.Clin.Invest.* 1995;95(2):888-894

120. Schillinger W, Meyer M, Kuwajima G, Mikoshiba K, Just H, and Hasenfuss G: Unaltered ryanodine receptor protein levels in ischemic cardiomyopathy. *Mol.Cell.Biochem.* 1996;106-161, 297-302

121. Nimer LR, Needleman DH, Hamilton SL, Krall J, Movsesian MA: Effect of ryanodine on sarcoplasmic reticulum Ca^{2+} accumulation in nonfailing and failing human myocardium. *Circulation* 1995;92:2504-2510

122. Stern MD: Theory of excitation-contraction coupling in cardiac muscle. *Biophys.J.* 1992;63:497-517

123. Flesch M, Schwinger RH, Schnabel P, Schiffer F, van Gelder I, Bavendiek U, Sudkamp M, Kuhn-Regnier F, Bohm M: Sarcoplasmic reticulum Ca^{2+} ATPase and phospholamban mRNA and protein levels in end-stage heart failure due to ischemic or dilated cardiomyopathy. *J.Mol.Med.* 1996;74:321-332

124. Schillinger W, Lehnart SE, Prestle J, Preuss M, Pieske B, Maier LS, Meyer M, Just H, Hasenfuss G: Influence of SR Ca^{2+}-ATPase and Na^{+}-Ca^{2+}-exchanger on the force-frequency relation. [Review] [38 refs]. *Basic.Res.Cardiol.* 1998;93 Suppl 1:38-45

125. Kiss E, Ball NA, Kranias EG, Walsh RA: Differential changes in cardiac phospholamban and sarcoplasmic reticular Ca^{2+}-ATPase protein levels. Effects on Ca^{2+} transport and mechanics in compensated pressure-overload hypertrophy and congestive heart failure. *Circ.Res.* 1995;77:759-764

126. Munch G, Bolck B, Hoischen S, Brixius K, Bloch W, Reuter H, Schwinger RH: Unchanged protein expression of sarcoplasmic reticulum Ca^{2+}-ATPase, phospholamban, and calsequestrin in terminally failing human myocardium. *J.Mol.Med.* 1998;76:434-441

127. Litwin SE, Bridge JHB: Enhanced Na^{+}-Ca^{2+} exchange in the infarcted heart. Implications for excitation-contraction coupling. *Circ.Res.* 1997;81:1083-1093

128. Lehnart SE, Schillinger W, Pieske B, Prestle J, Just H, Hasenfuss G: Sarcoplasmic reticulum proteins in heart failure. [Review] [52 refs]. *Ann. N.Y. Acad. Sci.* 1998;853:220-230

129. Solaro RJ: Myosin and why hearts fail [editorial; comment]. *Circulation* 1992;85:1945-1947

130. Anderson PAW, Greig A, Mark T, Malouf N, Oakley AE, Ungerleider R, Allen P, Kay B: Molecular basis of human cardiac troponin T isoforms expressed in the developing, adult, and failing heart. *Cic. Res.* 1995;76:681-686(abstract)

131. Pagani ED, Alousi A, Grant AM, Older TM, Dziuban SW, Jr., Allen PD: Changes in Myofibrillar Content and MgATPase activity in ventricular tissues from patients with heart failure caused by coronary artery disease, cardiomyopathy, or mitral valve insufficiency. *Circ.Res.* 1988;63:380-385

132. Geenen DL, Malhotra A, Scheuer J: Regional variation in rat cardiac myosin isoenzymes and ATPase activity after infarction. *Am.J.Physiol.* 1989;256/25:H745-H750

133. Pope B, Hoh JFY, Weeds A: The ATPase activities of rat cardiac myosin isoenzymes. *FEBS Lett.* 1980;118:205-208

134. Morano I, Ritter O, Bonz A, Timek T, Vahl CF, Michel G: Myosin light chain-actin interaction regulates cardiac contractility. *Circ.Res.* 1995;76:720-725

135. Moss RL: Ca^{2+} Regulation of Mechanical Properties of Striated Muscle. *Circ.Res.* 1992;70:865-884

136. Margossian SS, White HD, Caulfield JB, Norton P, Taylor S, Slayter HS: Light chain2 profile and activity of human ventricular myosin during dilated cardiomyopathy; identification of a causal agent for impaired myocardial function. *Circulation* 1992;85:1720-1733

137. Sutsch G, Brunner UT, Schulthess CV, Hirzel HO, Hess OM, Turina M, Krayenbühl HP, Schaub MC: Hemodynamic performance and myosin lihgt chain-1 expression of the hypertrophied left ventricle in aortic valve disease before and after calve replacemenmt. *Basic.Res.Cardiol.* 1992;87:285-290

138. Hunkeler NM, Kullman J, Murphy A: Troponin I isoform expression in human heart. *Circ.Res.* 1991;69:1409-1414

139. Steinert PM, Jones JC, Goldman RD: Intermediate filaments. [Review] [69 refs]. *J.Cell.Biol.* 1984;99:22s-27s

140. Schaper J, Froede R, Heiz S, Buck A, Hashizuma H, Speiser B, Friedl A, Bleese N: Impairment of myocardial ultrastructure and changes of the cytoskeleton in dilated cardiomyopathy. *Circulation* 1991;83:504-514

141. Tsutsui H, Ishihara K, Cooper IV G: Cytoskeletal role in the contractile dysfunction of hypertrophied myocardium. *Science* 1993;260:682-687

142. Hein S, Scholz D, Fujitani B, Rennollet H, Brand T, Friedl A, and Schaper J: Altered expression of titin and contractile proteins in failing human myocardium. *J.Mol.Cell. Cardiol.* 1994;26:1291-1306

143. Tagawa H, Wang N, Narishige T, Ingber DE, Zile MR, Cooper IV G: Cytoskeletal mechanics in pressure-overload cardiac hypertrophy. *Cir. Res.* 1997;80:281-289

144. Endo M, Kitazawa T: EC coupling studies in skinned cardiac fibres, in Morad M (ed): *Biophysical aspects of cardiac muscle*. New York, Academic Press, 1978, 307-327

145. McFarland BH, Inesi G: Solubilization of sarcoplasmic reticulum with Triton X-100. *Arch.Biochem.Biophys.* 1971;145:456-464

146. Kargacin GJ, Fay FS: Physiological and structural properties of saponin-skinned single smooth muscle cells. *J.Gen.Physiol.* 1987;90:49-73

147. Gardner JP, Stout MA, Harris SR: Calmodulin loss in vascular smooth muscle following Triton X-100 or saponin skinning. *Pflugers Arch.* 1989;414:484-491

148. ter Keurs HEDJ, de Tombe PP: determinants of velocity of sarcomere shortening in mammalian myocardium, in Sugi H, Pollack GH (eds): *mechanism of myofilament sliding in muscle contraction*. New York, plenum press, 1993, 649-664

149. Glantz SA: *Primer of Bio-Statiscs*, Fourth Edition, San Francisco, McGraw-Hill, 1997

150. Fabiato A: Calcium-induced release of calcium from the cardiac sarcoplasmic reticulum. *Am.J.Physiol.* 1983;245:C1-C14

151. Sipido K, Wier WG: Flux of Ca^{2+} across the sarcoplasmic reticulum of guinea-pig cardiac cells during exctitation-contraction coupling. *J.Physiol.* 1991;435:605-630

152. Harrison SM, Bers DM: Correction of proton and Ca^{2+} association constants of EGTA for temperature and ionic strength. *Am.J.Physiol.* 1989;256(25):C1250-C1256

153. Bers DM: *Excitation-contraction coupling and cardiac contractile force*, ed1, Boston/London, Kluwer Academic, 1991, 93-119

154. Isenberg G, Wendt-Gallitelli MF: Cellular mechanisms of excitation contraction coupling, in anonymous i*solated adult cardiomyocytes. Vol. II.* 1990, 213-248

155. Mitchell RD, Simmerman HKB, Jones LR: Ca^{2+} binding effects on protein conformation and protein interactions of canine cardiac calsequestrin. *J.Biol.Chem.* 1988;263:1376-1381

156. Lullmann H, Peters T, Preuner J: Role of the plasmalemma for calcium homeostasis and for excitation-contraction coupling in cardiac muscle, in Drake-Holland AJ, Noble MIM (eds): *Cardiac metabolism.* John Wiley & Sons Ltd., 1983, 1-18

157. Rich TL, Langer GA, Klassen MG: Two components of coupling calcium in single ventricular cell of rabbits and rats. *Am.J.Physiol.* 1988;254:H937-H946

158. Cassidy PS, Kerrick WG, Hoar PE, Malencik DA: Exogenous calmodulin increases Ca^{2+} sensitivity of isometric tension activation and myosin phosphorylation in skinned smooth muscle. *Pflugers Arch.* 1981;392:115-120

159. Sparrow MP, Mrwa U, Hofmann F, Ruegg JC: Calmodulin is essential for smooth muscle contraction. *FEBS Lett.* 1981;125:141-145

160. Gao WD, Backx PHM, Azan-Backx M, Marban E: Myofilament Ca^{2+} sensitivity in intact versus skinned rat ventricular muscle. *Circ.Res.* 1994;74:408-415

161. Blatter LA, McGuigan JA: Estimation of the upper limit of the free magnesium concentration measured with Mg-sensitive microelectrodes in ferret ventricular muscle: (1) use of the Nicolsky-Eisenman equation and (2) in calibrating solutions of the appropriate concentration. *Magnesium* 1988;7:154-165

162. Davidenko JM, Cohen L, Goodrow R, Antzelevitch C: Quinidine-induced action potential prolongation, early afterdepolarizations, and triggered activity in canine purkinje fibers: effects of stimulation rate, potassium, and magnesium. *Circulation* 1989;79:674-686

163. White RE, Hartzell HC: Effects of intracellular free magnesium on calcium current in isolated cardiac myocytes. *Science* 1988;239:778-780

164. White RE, Hartzell HC: Magnesium ions in cardiac function. Regulator of ion channels and second messengers. [Review] [109 refs]. *Biochem.Pharmacol.* 1989;38:859-867

165. Aomine M, Tatsukawa Y, Yamato T, Yamasaki S: Antiarrhythmic effects of magnesium on rat papillary muscle and guinea pig ventricular myocytes. *Gen.Pharmacology* 1999;32:107-114

166. Chiese M, Inesi G: Mg^{2+} and Mn^{2+} modulation of Ca^{2+} transport and ATPase activity in sarcoplasmic reticulum vesicles. *Arch.Biochem.Biophys.* 1981;208:586-592

167. Karaki H: Magnesium as a modifier of smooth muscle contractility. [Review] [53 refs]. *Microcirculation, Endothelium, & Lymphatics* 1989;5:77-97

168. Kawano S: Dual mechanisms of Mg^{2+} block of ryanodine receptor Ca^{2+} release channel from cardiac sarcoplasmic reticulum. *Receptors Channels* 1998;5:405-416

169. Valentin-Ranc C, Carlier MF: Evidence for the direct interaction between tightly bound divalent metal ion and ATP on actin. Binding of the lambda isomers of beta gamma-bidentate CrATP to actin. *J.Biol.Chemistry* 1989;264:20871-20880

170. Morimoto S: The effect of Mg^{2+} on the Ca^{2+} binding to troponin C in rabbit fast skeletal myofibrils. *Biochim.Biophys.Acta* 1991;1073:336-340

171. Potter JD: Magnessium and the regulation of muscle contraction. *Fed.Proc.* 1981;40:2653-2656

172. Endo M, Kitazawa T, Iino M, Kakuta Y: Effect of "viscosity" of the medium on mechanical properties of skinned skeletal muscle fibers, in Sugi H, Pollack GH (eds): *Cross-bridge mechanism in muscle contraction.* Baltimore, University Park Press, 1979, 365-376

173. Maughan DW, Godt RE: Inhibition of force production in compressed skinned muscle fibers of the frog. *Pflugers Arch.* 1981;390:161-163

174. Roos KP, Brady AJ: Osmotic compression and stiffness changes in relaxed skinned cardiac myocytes in PVP-40 and Dextran T-500 [published erratum

appears in Biophys J 1991 Jan;59(1):following 255-6]. *Biophys.J.* 1990;58:1273-1283

175. Miller DJ, Lamont C, O DJJ: Natural calcium-sensitizing compounds of the heart, in Lee JA, Allen DG (eds): *Modulation of Cardiac Calcium Sensitivity*. New York, Oxford University Press, 1993, 115-139

176. Steele DS, Smith GL, Miller DJ: The effects of taurine on Ca^{2+} uptake by the sarcoplasmic reticulum and Ca^{2+} sensitivity of chemically skinned rat heart. *J.Physiol. (Lond)* 1990;422:499-511

177. Morano I, Bachle-stolz C, Katus A, Ruegg JC: Increased calcium sensitivity of chemically skinned human atria by myosin light chain kinase. *Basic.Res.Cardiol.* 1988;83:350-359

178. Miller DJ, Smith GL: EGTA purity and the buffering of calcium ions in physiological solutions. *Am.J.Physiol.* 1984;246:C160-C166

179. Moisescu DG, Pusch H: A pH-metric method for the determination of the relative concentration of calcium to EGTA. *Pflugers Arch.* 1975;355:R122-R122

180. Illingworth JA: A common source of error in pH measurements. *Biochem.J.* 1981;195:259-262

181. Martell AE, Smith RM: *Critical stability constants*, New York & London, Plenum Press, 1974,

182. Good NE, Winget GD, Winter W, Connolly TN, Izawa S, Singh RMM: Hydrogen ions buffer for biological research. *Biochemistry* 1966;5:467-477

183. Hollander EH: Force Calcium relation in intact Rat Myocardium. *MSc thesis* 1995, the University of Calgary

184. Harrison SM, Bers DM: Influence of temperature on the calcium sensitivity of the myofilaments of skinned ventricular muscle from the rabbit. *J.Gen.Physiol.* 1989;93:411-428

185. de Tombe P: Myocardial sarcomere dynamics. *PhD thesis* 1989, the University of Calgary

186. Zhang YM, Davidoff AW, ter Keurs HEDJ: Force-sarcomere length relation in skinned rat cardiac trabeculae with heart failure. *Conference Proceeding* 1998

187. Godt RE, Maughan DW: Swelling of skinned muscle fibres of the frog: experimental observations. *Biophys.J.* 1977;19:106-116

188. Krasner B, Maughan DW: Dextran T500 decreases skinned fiber width, tension, and ATPase. *Biophys.J.* 1981;33:27a

189. Millman BM, Irving TC: Filament lattice of frog striated muscle; radial forces, lattice stability, and filament compression in the A-band of relaxed and rigor muscle. *Biophys.J.* 1988;54:437-447

190. Moss RL, Swinford AE, Greaser ML: Alteration in the Ca^{2+} sensitivity of tension development by single skeletal muscle fibers at stretched lengths. *Biophys.J.* 1983;43:115-119

191. Sweitzer NK, Moss RL: The effect of altered temperature on Ca^{2+} sensitive force in skinned single cardiac myocytes: Evidence for force dependence of thin filament actvation. *J.Gen.Physiol.* 1990;96:1221-1245

192. Forge V, Mintz E, Canet D and Guillain F: Lumenal Ca^{2+} dissociation from the phosphorylated Ca^{2+}-ATPase of the sarcoplasmic reticulum is sequential. *J.Biol.Chem.* 1995;270(31):18271-18276

193. Martonosi AN: Structure-function relationships in the Ca^{2+}-ATPase of sarcoplasmic reticulum: facts, speculations and questions for the future. *Biochim.et Biophys. Acta* 1996;1275(1-2): 111-117

194. Wictome M, Henderson I, Lee AG, and East JM: Mechanism of inhibition of the calcium pump of sarcoplasmic reticulum by thapsigargin. *Biochem.J.* 1992;283:525-529

195. Fujimori T and Jencks WP: Binding of two Sr^{2+} ions changes the chemical specificities for phosphorylation of the sarcoplasmic reticulum clacium ATPase through a stepwise mechanism. *J. Biol.Chem.* 1992;267(26):18475-18487

196. Wier WG, Yue DT: Intracellular calcium transients underlying the short-term force-interval relationship in ferret ventricular myocardium. *J.Physiol.* 1986;376:507-530